PNNL-11686
UC-721

Pacific Northwest
National Laboratory

Operated by Battelle for the
U.S. Department of Energy

Research on Jet Mixing of Settled Sludges in Nuclear Waste Tanks at Hanford and Other DOE Sites: A Historical Perspective

M. R. Powell
Y. Onishi
R. Shekarriz

RECEIVED
OCT 22 1997
OSTI

September 1997

PNNL-11686

Prepared for the U. S. Department of Energy
under Contract DE-AC06-76RLO 1830

DISCLAIMER

This report was prepared as an account of work sponsored by an agency of the United States Government. Neither the United States Government nor any agency thereof, nor Battelle Memorial Institute, nor any of their employees, makes **any warranty, expressed or implied, or assumes any legal liability or responsibility for the accuracy, completeness, or usefulness of any information, apparatus, product, or process disclosed, or represents that its use would not infringe privately owned rights**. Reference herein to any specific commercial product, process, or service by trade name, trademark, manufacturer, or otherwise does not necessarily constitute or imply its endorsement, recommendation, or favoring by the United States Government or any agency thereof, or Battelle Memorial Institute. The views and opinions of authors expressed herein do not necessarily state or reflect those of the United States Government or any agency thereof.

PACIFIC NORTHWEST NATIONAL LABORATORY
operated by
BATTELLE
for the
UNITED STATES DEPARTMENT OF ENERGY
under Contract DE-AC06-76RLO 1830

Printed in the United States of America

Available to DOE and DOE contractors from the Office of Scientific and Technical Information, P.O. Box 62, Oak Ridge, TN 37831; prices available from (615) 576-8401.

Available to the public from the National Technical Information Service, U.S. Department of Commerce, 5285 Port Royal Rd., Springfield, VA 22161


This document was printed on recycled paper.

PNNL-11686
UC-721

Research on Jet Mixing of Settled Sludges in Nuclear Waste Tanks at Hanford and Other DOE Sites: A Historical Perspective

M. R. Powell
Y. Onishi
R. Shekarriz

September 1997

DISTRIBUTION OF THIS DOCUMENT IS UNLIMITED

MASTER

Prepared for the U.S. Department of Energy
under Contract DE-AC06-76RLO 1830

Pacific Northwest National Laboratory
Richland, Washington 99352

DISCLAIMER

Portions of this document may be illegible in electronic image products. Images are produced from the best available original document.

Executive Summary

Jet mixer pumps will be used in the Hanford Site double-shell tanks to mobilize and mix the settled solids layer (sludge) with the tank supernatant liquid. Predicting the performance of the jet mixer pumps has been the subject of analysis and testing at Hanford and other U.S. Department of Energy (DOE) waste sites. One important aspect of mixer pump performance is sludge mobilization. The research that correlates mixer pump design and operation with the extent of sludge mobilization is the subject of this report.

Sludge mobilization tests have been conducted in tanks ranging from 1/25-scale (3 ft-diameter) to full scale have been conducted at Hanford and other DOE sites over the past 20 years. These tests are described in Sections 3.0 and 4.0 of this report. The computational modeling of sludge mobilization and mixing that has been performed at Hanford is discussed in Section 5.0.

Much has been learned from testing and modeling. The bulleted items below summarize the present ability to predict sludge mobilization and identify the remaining issues and areas of uncertainty.

- The most accurate correlation of effective cleaning radius (ECR) with mixer pump design and sludge properties yet developed from scaled testing is:

$$\text{ECR (cm)} = 4.0\, U_o D\, \tau_s^{-0.46} \qquad \text{(S.1)}$$

  where U_o is the nozzle exit velocity (cm/s), D is the nozzle diameter (cm), and τ_s is the undisturbed sludge shear strength (dyne/cm^2) at the waste temperature expected during mixer pump operation. Based on the uncertainties in ECR measurement at 1/25-scale, which is where this correlation was developed, it is recommended that a proportionality constant of 3.0 be used instead of 4.0 as an added degree of conservatism. Equation S.1 is valid for cohesive tank sludge. Sludge that has less cohesion than is implied by its shear strength is expected to yield a larger ECR than is predicted.

- A series of 1/12-scale sludge mobilization tests using a single simulant type was conducted in fiscal year 1987 to predict the expected ECR in Hanford double-shell tank 101-AZ. The ECRs from this testing were correlated with simulant shear strength by the equation:

$$\text{ECR (cm)} = 17.3\, U_o D\, \tau_s^{-0.67} \qquad \text{(S.2)}$$

  Because only a relatively narrow range of sludge properties was tested, this correlation should be used only to predict ECRs for sludge with a shear strength of approximately 10,000 dyne/cm^2. In this range, the predicted ECRs are consistent with, but somewhat more conservative than, the ECRs predicted by the 1/25-scale correlation (Equation S.1).

- Computational modeling of the sludge mobilization and mixing process has been conducted at Hanford. Currently, the accuracy of the ECR and ECR growth rate predictions made from computer modeling is constrained by the accuracy of the existing waste characterization data and an incomplete

understanding of the mechanisms of sludge mobilization. Despite these problems, numerical modeling of mobilization and mixing is useful for predicting more thoroughly understood phenomena (e.g., chemical equilibria, particle settling, and jet impact forces).

- The ECR growth rates observed during scaled and full-scale sludge mobilization testing can be used to estimate how much time will be required to reach the final ECR in the full-scale tanks at Hanford. Between 50 and 500 hours of mixer pump operation likely will be required before the ECR growth rate is reduced to an insignificant level (see Section 4.5.2).

- Scale-up of the ECR correlation given above has not been demonstrated conclusively, but comparison of the 1/25-scale results with results of full-scale tests using similar, but not identical, waste simulants is consistent with the expected linear scaling relationship (see description of scaling methodology in Section 2.2).

- Sludge mobilization testing has not been conducted using fluids that are strongly non-Newtonian. Thus, Non-Newtonian slurry effects are not explicitly addressed by the ECR correlations developed from scaled tests. Computational modeling may be a valuable tool for evaluating the effects of non-Newtonian rheology on sludge mobilization. Whether non-Newtonian rheology effects will significantly affect the ECR is the subject of on-going research.

- Given an accurate sludge shear strength measurement, the ECR predicted using Equation S.1 is expected to be accurate to within about 20%.[a] In practice, however, the accuracy of the shear strength measurement is not known. Sample disruption, variations in waste composition within each tank, and changes in sample properties with temperature all can significantly affect the shear strength. The uncertainty in the shear strength data can be reduced through a series of tests designed to quantify the potential sampling disruption effects on shear strength measurements. Additional data may be obtained by observing the dynamics of core sample extrusions in the hot cell. Section 6.0 describes several activities that will improve the accuracy of sludge shear strength data.

---

[a]This assumes that the slurry rheology is not strongly non-Newtonian. The predicted ECR will be larger than the actual ECR if the sludge strength is not entirely due to cohesion.

Contents

Figures

Tables

Nomenclature

A	empirical constant
c	solid concentration
C_D	drag coefficient
D	nozzle diameter, cm
d_s	solid diameter
DOE	U.S. Department of Energy
DST	double-shell tank
E	erodibility coefficient
ECR	effective cleaning radius, cm
g	gravitational acceleration, 980 cm^2/s
INEEL	Idaho National Environmental Engineering Laboratory
I_p	plasticity index
k	empirical constant
n	nozzle oscillation frequency in Equation 2.3, rad/s
n	empirical constant in Equation 5.5
ORNL	Oak Ridge National Laboratory
PNNL	Pacific Northwest National Laboratory
Re_p	particle Reynolds number
SRS	Savannah River Site
S_d	amount of solid deposited per unit bottom surface area per unit time
S_e	amount of solid eroded per unit bottom surface area per unit time
U, u	fluid velocity, m/s
u_*	shear velocity
U_o	nozzle exit velocity, cm/s
w_o	non-hindered fall velocity
w_s	apparent particle fall velocity
WVDP	West Valley Demonstration Project
γ	specific weight of fluid
γ_s	specific weight of solid
μ, ν	viscosity, Pa-s
ρ	slurry density, kg/m^3
τ_*	dimensionless shear stress
τ_o	bed shear stress
τ_{cd}	critical shear stress for deposition
τ_{ce}	critical shear stress for erosion
τ_s	shear strength, $dyne/cm^2$

1.0 Introduction

There are 28 one-million-gallon double-shell radioactive waste tanks on the Hanford Site in southeastern Washington State. The waste in these tanks was generated during processing of nuclear materials. Solids-laden slurries were placed into many of the tanks. Over time, the waste solids have settled to form a layer of sludge in the bottom of these tanks. The thickness of the sludge layer varies from tank to tank, from a few centimeters or no sludge to about 4.5 m (15 ft) of sludge.

It is planned that the waste will be removed from these tanks as part of the overall Hanford Site cleanup efforts. Jet mixer pumps will be placed into the tanks to stir up (mobilize) the sludge and form a uniform slurry suitable for pumping to downstream processing facilities. These mixer pumps use powerful jets of tank fluid directed horizontally out of two diametrically opposed nozzles near the tank bottom. These fluid jets impinge upon the sludge and suspend the solid particles. The amount of sludge mobilized by the mixer pump jets depends not only on the jet properties, but on the ability of the sludge to resist the stresses imposed by the jets. The goal of the sludge mobilization work described in this document is to develop a methodology to predict how much sludge will be mobilized by the mixer pumps based on the size and velocity of the mixer pump jets and the physical and chemical properties of the tank sludge.

Mixer pump tests using simulated tank sludge have been conducted at several U.S. Department of Energy (DOE) sites over the past 20 years. Tests have been conducted ranging in scale from a 3-ft-diameter tank to a full-scale (85-ft diameter at the Savannah River Site) tank. Although much progress has been made in the ability to predict sludge mobilization by mixer pumps, some issues remain open. These issues will be discussed in this report.

The primary purpose of this document is to consolidate the existing sludge mobilization prediction information. Currently, the relevant data are contained in several lengthy reports. This document draws heavily from the larger reports, but includes only the key findings. Complete descriptions of all relevant experimental details are given in the reports referenced throughout this document. This document also identifies the areas of greatest uncertainty and provides suggestions for further research.

Section 2.0 discusses the some of the key terms used in sludge mobilization research as well as the scaling methodology used to design experiments. Scaled mixer pump testing at other DOE sites and at Hanford are described in Sections 3.0 and 4.0 of this report, respectively. The computational modeling of sludge mobilization and mixing that has been performed at Hanford is discussed in Section 5.0. Conclusions and recommendations are given in Section 6.0.

2.0 Background

The terms and variables used to model the tank sludge mobilization process are introduced in this section. Following a definition of relevant terms, the expected scaling methodology is described.

2.1 Definition of Terms and Variables

A mixer pump installed in the central riser of a Hanford double-shell tank (DST) is shown in Figure 2.1.[a] For several tanks, the pump intake, which is designed to be approximately 7 inches from the tank bottom, will be located within the sludge layer. The pump will draw the slurry at the intake point and will deliver two opposing high-momentum jets at the exits, as shown in Figure 2.1. It is the momentum of these jets that is thought to promote dislodging of the sludge and settled solids and to create homogeneity via turbulent mixing in the tank.

The effectiveness of the fluid jets for dislodging the sludge depends on several mechanisms. The most important mechanisms are: 1) the loss of jet velocity with distance, 2) the interaction of the jets with the sludge banks, and 3) the failure mechanism of the sludge bank.

The rate of growth and velocity decay of a jet is dominated by the turbulence in the jet. If the fluid in the jet is Newtonian with low solids loading, its rate of growth and velocity decay become independent of nozzle exit velocity, fluid viscosity and density, and nozzle diameter, as long as the jet Reynolds number is sufficiently large and well into the turbulent regime (Rajaratnam 1976).[b] The effect of non-Newtonian rheology and solids loading is expected to have an impact on the rate of growth even in the fully-turbulent regime. However, only limited information is available on this topic (Shekarriz et al. 1994, 1995, 1996).

Jet interaction with the sludge bank is a more complex problem. Theoretically, if the geometry of this interaction is well-defined, the problem can be modeled with little difficulty. For example, if the jet impinges perpendicularly on a flat sludge bank, the flow can be modeled as stagnation flow. Theoretical treatment of this problem with closed-form solutions are available, from which the stress field acting on the sludge bank can be computed. However, during the mobilization process, the angle of impact of the jet on the sludge bank may vary depending on the buoyancy force acting on the jet, the nozzle exit velocity, and the predominant recirculation pattern in the tank, among other variables. Further, the jet-sludge interaction is strongly influenced by the relative position of the jet elevation versus the height of the sludge layer. Considering that the jet forces are primarily due to their axial momentum, their shear stress forces at each axial location are much smaller than the pressure forces.

No less important is the mechanism of the sludge bank failure upon interaction with the jet. A large body of literature exists on mechanisms of erosion of riverbeds and estuaries (e.g., Young 1991, Perigaud 1984, Cleaver and Yates 1973, and Haji et al. 1988). Some similarity exists between the erosion of tank

---

[a] An alternative configuration is installation of two mixer pumps in a DST at two opposite locations, but equal distance from the center of the tank.

[b] It is also assumed that the jet is without significant angular momentum (swirl) at the nozzle exit.

waste sludge and sediment beds in rivers. However, there are several fundamental differences that make the current sludge mobilization problems unique.

The DST sludges have been shown to have very small primary particle sizes (Onishi et al. 1996a; Brooks et al. 1997). These sludges tend to by highly cohesive which translates to high yield stresses in both shear and compressive modes. In general, the compressive yield stress is several times larger than the shear yield (Onishi et al. 1996a). From a purely rheological stand-point, where the sludge is treated as a continuum, the failure mode depends on the jet-sludge bank interaction geometry. The failure will take place along the plane of principal stresses (according to maximum stress failure theory). Obviously, under pure shear (when the jet is moving parallel to the sludge-liquid interface) the failure mode will be in pure shear.

From a more microscopic perspective, erosion of the particles near the interface depends on the nature of particle-particle interaction potential and the local external forces acting on the particles. Recent studies by Scales et al. (1997) based on scaling arguments reveal that the yield stress of a colloidal dispersion can be linked to the separation of particles in a tensile mode. Of course, at the limit where primary particles are larger (>10 μm) or colloidal attractions are small (stable suspensions), only the hydrodynamic lubrication and Coulombic forces keep the particles together, as is the case for many of estuaries and riverbed erosion problems.

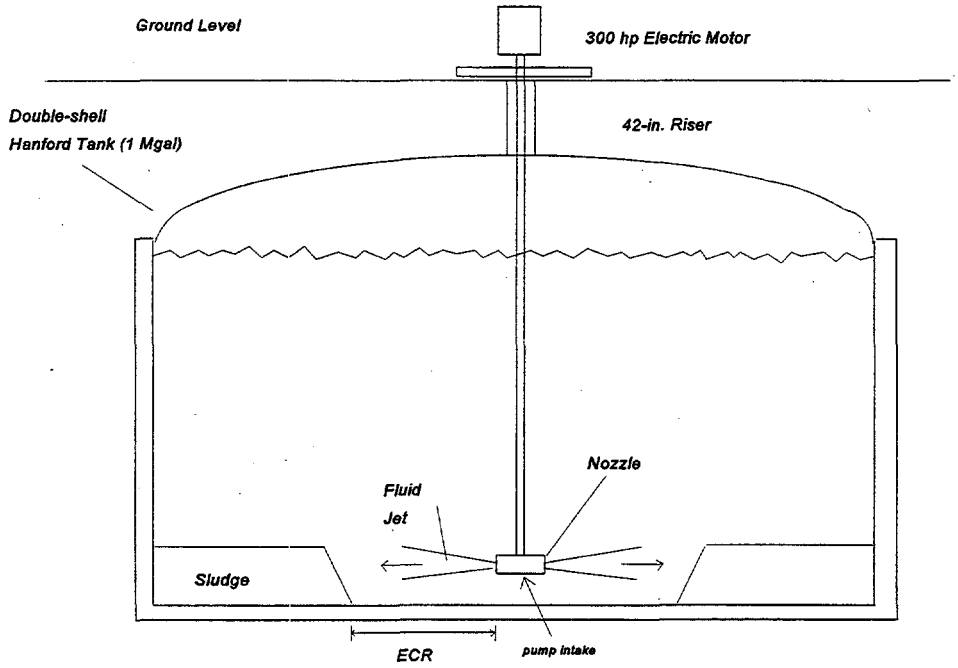

Figure 2.1. Sketch of Mixer Pump Installed in Double-Shell Tank

Given the complexity of this problem, it is appropriate to develop a more empirical approach as a solution methodology. The empirical approach relies on an extensive experimental database to capture the physicochemical process in mathematical correlations. These correlations, if properly developed, are scale-invariant. That is, the correlations will work at any scale of the system. The disadvantage of an empirical approach, however, is the risk that some of the fine details of the flow physics, rheology, and chemical interactions are lost during the consolidation of all the mechanisms in a single empirical correlation. Thus, it is extremely important to recognize the limitations of an empirical approach and to emphasize the need for careful validation of the empirical correlations throughout the spectrum of the parameter domain of interest.

In this section, we will review the approach used so far for developing some of the existing empirical correlations. Several key terms and variables are identified in Figure 2.1. Key terms and variables are:

1) The effective cleaning radius (ECR) is the distance between the mixer pump nozzle exit and the base of the distant sludge bank. Thus a mixer pump mobilizes the sludge within a circular area with a radius equal to the ECR plus the distance between the nozzle tip and the pump column centerline.

2) U_o is the bulk velocity with which the fluid exits the mixer pump nozzles. U_o is called the nozzle exit velocity and is equal to the volumetric flow rate of fluid issuing from each nozzle divided by the nozzle cross-sectional area.

3) D is the inside diameter of the nozzles.

Another important variable is the sludge shear strength, τ_s, which quantifies the shearing stress required to induce mechanical failure in the sludge. The shear strength of sludge-like materials is usually measured using a shear vane. The vane is inserted into the sludge and slowly twisted until failure is observed. The torque required to induce failure is directly proportional to the sludge shear strength. See ASTM D4648-94 for a complete description of the vane shear strength measurement procedure for shear strength measurement in soils.

2.2 Scaling Methodology

The scaling methodology used to design and conduct the scaled sludge mobilization experiments is described in this section. This same scaling methodology was used to design sludge mobilization tests conducted at Hanford, Savannah River, and West Valley (see Sections 3.0 and 4.0).

Testing of a process in a scale model will yield results identical (but scaled) to full-scale results only if all properties, forces, and transport mechanisms can be exactly scaled. This is generally not possible because some phenomena scale in different ways that are incompatible. Even so, the results obtained from tests that are not exactly scaled can be interpreted using appropriate scaling relationships. The processes of sludge mobilization and mixing are controlled by the geometric, kinematic, and dynamic factors of the process. Hence, tests are conducted in a geometrically similar model in a manner that is as kinematically and dynamically similar as practical.

The 1/12-scale and 1/25-scale test facilities used for sludge mobilization testing at Pacific Northwest National Laboratory (PNNL) are geometrically scaled models of a Hanford DST. The arrangement of

possible pump positions and air-lift circulators in the 1/12-scale tank is exactly the same as in the full-scale tanks with all dimensions being linearly scaled. The 1/25-scale tank includes only a central riser position and no air-lift circulators.

Kinematic similarity is concerned with solid or fluid systems in motion and, therefore, is related to velocity and time. Times are measured from an arbitrary zero for similarly moving systems, and corresponding times will have a constant ratio. Geometrically similar moving systems are kinematically similar when corresponding particles trace out geometrically similar paths in corresponding (scaled) times (Johnstone and Thring 1957).

Dynamic similarity is concerned with the forces that act on masses in the system (Sabersky et al. 1971). In dynamically similar systems, the same kinds of forces (gravity, viscosity, etc.) act on corresponding particles at corresponding times. If all applied forces affect motion (as opposed to static stresses), a dynamically similar system will also be kinematically similar because motions are functions of the applied forces. In fluid systems, the pressure, inertial, gravitational, viscous, and interfacial (e.g., surface tension) forces are the most important. Of these, inertial, gravitational, and viscous forces are expected to control the slurry flow aspects of sludge mobilization. The relative magnitudes of these forces can be represented by the following dimensionless groups:

$$\text{Reynolds Number} = \text{Re} = \frac{\rho U d}{\mu} = \frac{\text{inertial forces}}{\text{viscous forces}} \tag{2.1}$$

$$\text{Froude Number} = \frac{U^2}{Lg} = \frac{\text{inertial forces}}{\text{gravitational forces}} \tag{2.2}$$

$$\text{Strouhal number} = \frac{D/U_o}{1/n} = \frac{\text{time scale of steady flow}}{\text{time scale of unsteady flow}} \tag{2.3}$$

where ρ = fluid density, kg/m^3
U = fluid velocity, m/s
L = characteristic length, m
n = nozzle oscillation frequency, rad/s
μ = viscosity, Pa-s
g = acceleration of gravity, 9.8 m/s^2
D = nozzle diameter, m

For dynamic similarity, the values of the Froude, Strouhal, and Reynolds numbers should be the same in the model and in the full-scale system. The Froude number embodies the ratio of the inertial to gravitational forces. The modeling of sludge mobilization operations is not directly concerned with the rate at which the suspended particles settle. It is assumed that if the momentum of the mixer pump jet is powerful enough to mobilize the sludge then it will also be powerful enough to prevent particle settling at

distances within the ECR. However, accumulation of larger-size particles in regions outside of the influence of the jets may be of concern when mixing uniformity is considered.

In homogeneous systems that have little surface disturbance, such as fully-baffled agitated tanks, the gravitational effects (given by the Froude number) can be neglected (Dickey, 1976). If particle settling (hence the Froude number effect) is ignored, then this will be the case in the DSTs until the final stages of retrieval when the fluid surface has been lowered near the elevation of the jet. Therefore, dynamic similarity for the 1/12-scale and 1/25-scale tests requires that only the Reynolds and Strouhal numbers be the same in the scaled tests as they will be in the DSTs.

It is theoretically possible to substitute a liquid with physical properties that would produce the same Reynolds and Strouhal numbers, thereby maintaining dynamic similarity. But that approach is not practical because the substitution would probably require the use of hazardous fluids and introduce much higher costs.

An alternative approach to explicit system similarity (i.e., matching Reynolds number and Froude number at both scales) is to use identical fluid and sludge properties and employ known mathematical relationships to extend the test results to full-scale. This is the approach that is used to design scaled sludge mobilization tests. The approach is described in more detail throughout the following sections.

Mobilization of sludge is thought to be caused by the impact of the jet on the sludge and/or the shearing force of the jet at the sludge surface, which induces erosion, as described previously. Both of these mechanisms are functions of the jet velocity. If identical fluid properties (assumed Newtonian) are used in the scale model and the full-scale tank, the centerline jet velocities at geometrically similar points between the model and the full-scale tank can be made equal by maintaining the same nozzle velocity and scaling the nozzle diameter linearly. The maximum downstream fluid velocity in a submerged turbulent Newtonian jet issuing into the same Newtonian stagnant fluid is given by the equation (Rajaratnam 1976):

$$U_{max} = C \frac{U_o D}{x} \tag{2.4}$$

where C is a constant equal to about 6.2 and x is the downstream distance from the nozzle exit. It is apparent from this equation that fluid jets with equal exit velocities and scaled nozzle diameters will be kinematically similar. It is important to emphasize that the effect of free stream turbulence is not included in Equation 2.4.

Since the fluid velocities are the same at both scales (assuming D is linearly scaled), the time required for an element of fluid to be transported between corresponding points will be reduced by a factor of 12 in the 1/12-scale facility and a factor of 25 in the 1/25-scale facility.

To maintain kinematic similarity, each rotation of the scale-model mixer pump must mobilize a scaled quantity of sludge that corresponds to the quantity that will be mobilized per pump rotation in the full-scale tank. Further, the scale model fluid jets should entrain a scaled amount of fluid due to pump column rotation. Both these requirements can be met by rotating the scale model mixer pump column at

a faster rate. In the 1/25-scale experiments, for example, the mixer pump is rotated 25 times faster than the rate expected at full-scale. As a result, mixing rate is scaled linearly with tank size. One hour of mixer pump operation at 1/25-scale produces an amount of sludge mobilization that corresponds to that obtained from 25 hours of mixer pump operation at full scale.

Thus, sludge mobilization tests are conducted such that the nozzle exit velocity (U_o) is identical to that at full-scale and all dimensions (nozzle size, tank size, etc.) are scaled linearly. The mixer pump column rotation rate is also scaled such that in a 1/N-scale test the mixer pump is rotated (or oscillated) N times faster. Finally, the sludge and supernate simulants are designed to have properties approximating those of the tank waste.

More difficult to scale are the scales of turbulence in the tank. In general, the turbulent kinetic energy, which is in large part responsible for mixing in the tanks, is generated from mean flow kinetic energy. The total kinetic energy is distributed over different scales of turbulence (or eddies) all the way from the characteristic length (integral lengths scale at which turbulence is generated) to the microscales of turbulence. It has been shown that the integral length scale grows linearly in the downstream direction in a turbulent Newtonian jet (Wyganski and Fiedler 1969). It is thus clear that the integral length scales are directly tied to the size of the system (full scale, 1/12, 1/25, etc.). Thus, the spectral distribution of the turbulent kinetic energy becomes dependent on the geometry. It is currently not clear what the most effective turbulent length scales are for dislodging and mobilization of the sludges. As a result of this uncertainty, this aspect of jet mixing is ignored in the scaling methodology. Further tests are being performed to address the significance of turbulence scaling issues.

2.3 Justification for Scaled Sludge Mobilization Testing

Historically, sludge mobilization tests have been conducted in an effort to determine the mixer pump design and number of mixer pumps required to achieve the desired amount of sludge mobilized. One-sixth scale tests at West Valley Nuclear Services (West Valley, New York), for example, were used to determine that five mixer pumps of a given design would be needed to mobilize the sludge in Tank 8D-2.

Sludge mobilization research at Hanford was conducted with the goal of developing a suitably accurate correlation between mixer pump design, waste properties, and the fraction of sludge mobilized (as quantified by the ECR). Unfortunately, the complexity of the problem, coupled with the great difficulty associated with obtaining accurate waste characterization data, has limited the usefulness of the ECR correlations developed thus far. The baseline DST retrieval system currently consists of two mixer pumps, each with the maximum U_oD that is practical. It is unlikely that more than two pumps will be installed in any given tank because of the costs involved. To be useful for predicting the number of pumps required, the ECR correlations must be able to accurately predict whether one mixer pump or two are required. The existing correlations may provide sufficient accuracy for this determination, but only if accurate waste property data are available, and currently they are not. The difficulties associated with waste property measurements are discussed in Section 4.5.3.

Despite the limitations imposed by waste characterization difficulties, sludge mobilization research still is useful. Some retrieval system questions can be addressed without the need for accurate waste characterization. The effects of mixer pump nozzle design on the ECR, for example, have been studied and found to be significant (Powell et al. 1994a). Operational questions can also be addressed through a combination of analysis, numerical modeling, and scaled testing. Whether the mixer pump column

should be continuously rotated or indexed is one such question that can be answered without the need for specific waste characterization data. A pre-existing understanding of the sludge mobilization and mixing process is also needed to help address unforeseen problems which may become apparent once full-scale retrieval is begun.

3.0 ECR Testing at Other DOE Sites

Mixer pumps are part of the baseline sludge retrieval approach at several DOE waste sites. Over the past two decades, various sludge mobilization tests have been conducted at these sites in an effort to predict full-scale mixer pump performance. The tests conducted at the Savannah River Site (SRS), the West Valley Demonstration Project (WVDP), the Oak Ridge National Laboratory (ORNL), and the Idaho National Engineering and Environmental Laboratory (INEEL) are described in this section. The details of sludge mobilization tests conducted at Hanford are provided in Section 4.0.

3.1 Savannah River Site (SRS)

Sludge mobilization testing conducted at the SRS in South Carolina is described in this section. More detailed descriptions of these test programs are available in the reports referenced in the text.

3.1.1 Half-Tank Mockup Tests

In the mid-1970s mixer pumps were first tested at the SRS. A half-tank mockup was used to evaluate sludge mobilization using a 150-hp mixer pump equipped with 3.8-cm (1.5-in.) diameter nozzles (Bradley et al. 1977). This mixer pump was capable of producing a nozzle exit condition of $U_oD = 1.3$ m^2/s (14 ft^2/s) under full power and was rotated at 1/3 rpm during all the tests.[a] The half-tank mockup was a semi-circular section (one-half of a circle) with a diameter of 75 ft and a height of about 5 ft.

According to Bradley et al. (1977), several sludge mobilization tests were conducted in the half-tank mockup. To simulate the sludge, 36,300 kg (40 tons) of dry kaolin clay was placed in the tank bottom and then water added to bring the total depth of simulant to 0.9 m (3 ft). The dry kaolin absorbed some unquantified fraction of the water to form a paste-like sludge layer on the bottom of the tank. The simulated sludge layer was roughly 0.46 m (1.5 ft) thick. Assuming a 0.46-m sludge depth of uniform consistency, the solids concentration is estimated to have been 25 wt%. Churnetski (1982) reports that the sludge concentration in the half-tank mockup tests was 30 wt% but it is not clear how this value was determined. No physical property characterization data for the sludge layer were reported. Selby (1981) reports yield stresses of 50 and 110 Pa for 25 wt% and 30 wt% SRS kaolin slurries, respectively.

The mixer pump was then operated for a specified period of time at a specified pump speed to mobilize the sludge. It was observed that essentially all of the sludge mobilization occurred during the first 50 hours of mixer pump operation. Once the specified pump operation time had passed, the kaolin slurry was pumped away to reveal the remaining sludge layer. The ECR was quantified by measuring the distance between the mixer pump nozzle exits and the base of the sludge bank.

Half-tank mockup testing verified that the ECR is directly proportional to U_oD. The proportionality constant, ECR/U_oD, for these test conditions was 0.045 ± 0.005 s/cm. This value may have been biased

---

[a] U_oD will be used from here on as a characteristic parameter representing the initial condition of the jet. It is assumed that the conditions farther downstream, at which point dislodging and mixing of the sludge takes place, are relatively insensitive to the exact velocity profile at the nozzle exit for a turbulent, non-swirling, Newtonian jet.

low by slurry yield stress effects compared to what would have been obtained if the tank slurry had no significant yield stress. The kaolin concentration in the slurry (mobilized sludge mixed with supernate) reached as high as 7 wt%, and the yield stress for a 7 wt% slurry of the SRS kaolin is approximately 1.5 Pa (Selby 1981). As is discussed in Section 4.5.4, increases in slurry yield stress are expected to decrease the apparent mobilization susceptibility of the sludge. Powell et al. (1995) report that the ECR/U_oD for a relatively weak (τ_s = 640 Pa) kaolin clay sludge simulant was 0.059 ± 0.007 s/cm when the slurry yield stress was less than 0.1 Pa. However, when the slurry yield stress was increased to 1.2 Pa by adding additional kaolin clay to the slurry, the ECR/U_oD decreased to 0.042 ± 0.004 s/cm.

Based on this testing, it was concluded that these 150-hp mixer pumps will produce an ECR of about 6.1 m (20 ft) in the waste tanks at the SRS. This implicitly assumes that the kaolin clay used for the half-tank mockup tests is a reasonable simulant for the SRS tank sludge. Validation or justification of the sludge simulant is not addressed in reports describing this work.

3.1.2 Full-Tank Mockup Testing

After the half-tank tests were completed, an effort was launched to design and build higher capacity mixer pumps that would produce larger ECRs. The half-tank geometry was not suitable for testing these higher capacity mixer pumps, so a full-tank mockup was constructed. The full-tank mockup was similar to the half-tank facility except that the tank was a complete circular tank with a diameter of 25.9 m (85 ft) and a height of 2.4 m (8 ft) as described by Churnetski (1982).

Sludge simulant preparation was similar to that described for the half-tank mockup testing with the exception that a fresh batch of sludge simulant was not prepared between each test. Instead, the kaolin clay was mixed with all the tank supernate and then allowed to settle to the desired average concentration. The amount of kaolin in the tank was held constant at about 118,000 kg (130 tons), and the settling times were varied such that the average kaolin concentration in the sludge was reported to have varied between 17 wt% and 22 wt% (Churnetski 1982). No significant dependence of the ECR on the sludge simulant kaolin concentration was observed over this range.

Both the standard mixer pump, which was used in the half-tank facility, and an increased capacity mixer pump were tested in the full-tank mockup. The increased-capacity pump had 3-in. nozzles and was capable of producing a U_oD of up to 2.1 m^2/s (22.7 ft^2/s). Again, the direct proportionality between ECR and U_oD was observed. The proportionality constant was found to be 0.064 ± 0.006 s/cm for these test conditions. This is larger than that found in the half-tank mockup tests. This difference is likely due to the lower kaolin concentration in the sludge simulant (roughly 20 wt% versus the 30 wt% used for the half-tank mockup tests). According to Selby (1981), the yield stresses of 17 wt% and 22 wt% kaolin slurries are approximately 14 and 30 Pa, respectively. These yield stresses are low enough that the sludge bank probably flowed under its own weight. The stronger simulant used for the half-tank mockup testing (Section 3.1.1) probably flowed much less.

The kaolin concentration in the slurry during the full-tank mockup tests was similar to that of the half-tank tests. As is described in Section 3.1.1, the high slurry yield stress may have resulted in the ECRs being smaller than what would have been obtained had a low yield stress slurry been used.

3.1.3 1/12-Scale Testing

All of the full-scale mixer pump sludge mobilization tests at SRS used essentially the same sludge simulant. The consistency of the sludge was determined by the extent to which the kaolin clay absorbed water and, in the case of the full-tank mockup tests, by how long the clay slurries were allowed to settle. No direct rheological measurements of the sludge simulant were reported. In a series of 1/12-scale tests, however, the rheological properties of the sludge simulant were varied.[a]

Three sets of sludge mobilization tests were conducted in which the weight fraction of solid particles (kaolin) was changed. The kaolin concentrations were 44 wt%, 49 wt%, and 56 wt%. The consistency ranged from "barely pourable" at 44 wt% to "not pourable" at 56 wt%. No quantitative rheological measurements were performed. However, the yield stress for all three sludge simulants was speculated to be in excess of 100 Pa. The same U_oD was used for all the tests (0.177 m^2/s = 1.9 ft^2/s) and each test was conducted for 30 minutes.

In all the tests, an ECR of about 76 cm (30 in.) was observed (ECR/U_oD about 0.043 s/cm). Based on this result, it was concluded that the ECR is independent of the yield stress of the sludge over the range of yield strengths tested. More recent testing at PNNL (described in Section 4.0) has confirmed that the ECR of kaolin clay sludge simulants is essentially independent of shear strength over the range of interest, but this is not true for sludge simulants prepared from different materials.

3.1.4 Experiences in Full-Scale Waste Tanks

Mixer pumps have been successfully used to mobilize and mix the waste contained in several of the waste tanks at the SRS (Poirier 1995; Hamm et al. 1989). Unfortunately, no physical property measurements have been made on samples of undisturbed, undiluted sludge. Thus, the observed ECRs cannot be quantitatively correlated with sludge properties. However, some qualitative observations may be provided, as discussed below.

In one instance, some ECR versus time data were collected. The retrieval of waste from Savannah River Tank 16 yielded ECR estimates following cumulative mixer pump operation times of about 86 hours, 150 hours, 310 hours, and 510 hours.[b] Hamm et al. (1989) plot the ECR versus time data on a log-log scale and found that the data were reasonably well fit by a straight line. From this curve it was concluded that the ECR grows in direct proportion to time raised to a power.

Hamm et al. (1989) developed a phenomenological model for the sludge suspension process in which the sludge is weakened by penetration of the tank liquid into the sludge surface and then the weakened material is swept away by the mixer pump jet. It follows from this assumption that the ECR is not

---

[a]T. Motyka, July 22, 1981, memorandum to J. F. Ortaldo entitled *Slurry pump efficiency on very thick slurries.* Savannah River Site, Aiken, SC.

[b]These time values are taken from Figure 2 in Hamm et al. (1989). The values in Hamm differ slightly from those reported in Elder (1979).

directly a function of the sludge yield stress or shear strength.[a] Hamm et al. (1989) used this model to derive an equation where ECR is directly proportional to time raised to a power, which they estimate to be between 0.33 and 0.5. The power estimated from a linear fit of the Tank 16 ECR versus time data was 0.28.

This model, along with the 1/12-scale tests that showed no dependence of ECR on kaolin yield stress (Section 3.1.3), apparently led some SRS personnel to conclude that the ECR does not depend on sludge properties. More recent testing at PNNL (described in Section 4.0) has demonstrated that in many cases the sludge properties must be known to predict the ECR.

Mixer pump testing at SRS, both at full-scale and at 1/12-scale, implied that an ECR of about 7.6 m (25 ft) or more should be obtained when a mixer pump with U_oD equal to 1.26 m^2/s (13.6 ft^2/s) is used. Four mixer pumps of this capacity were installed in SRS Tank 42 in the early 1990s. When the pumps were activated in 1994, much smaller-than-expected ECRs were obtained (Poirier 1995). Two of the pumps were apparently cavitating because no sludge mobilization was apparent near these pumps. The remaining two pumps resulted in ECRs between 4.9 m (16 ft) and 5.8 m (19 ft) as determined by sludge depth readings taken through tank risers. These unexpectedly small ECRs imply that the Tank 42 sludge resists mobilization more effectively than the kaolin clay used in the mock-up tests. Thus, it is apparent that sludge properties affect the ECR.

3.2 West Valley Demonstration Project (WVDP)

Only a single storage tank contained sludge at the WVDP. This tank, 8D-2, once contained roughly 170 m^3 of sludge but this waste has since been successfully mixed using mixer pumps.[b]

Scaled mixer pump tests in a 1/6-scale tank were conducted in the mid-1980s in an effort to determine the number of mixer pumps needed to mobilize the sludge in Tank 8D-2. The sludge in Tank 8D-2 was characterized using an in situ shear vane, which measured the shear strength of the sludge at four different depths. Sludge shear strength reportedly ranged from 0.4 kPa near the sludge surface to 34.2 kPa near the tank floor (Abdelhamid et al. 1984). A kaolin clay sludge simulant was formulated with a shear strength reported to be about 35 kPa for testing in the 1/6-scale tank. Scaled mobilization test results implied that as many as five mixer pumps would be required to ensure adequate sludge mobilization (Schiffauer et al. 1985). In these tests, the effect of sludge simulant properties on sludge mobilization was not investigated. Instead, the tests were run with a simulant supposedly similar to the Tank 8D-2 waste and the scaling methodology described in Section 2.2 was employed.

Because ECR and U_oD data are not provided in the reports describing the West Valley mobilization tests, it is not possible to compare the ECR/U_oD for this simulant to those for simulants used at SRS and PNNL. It is likely that ECR data are not reported simply because sludge mobilization was limited more by the presence of in-tank obstructions than by the mobilization resistance of the sludge. Inside Tank 8D-2 there are six 1.2-m diameter support columns that span from the tank floor to the ceiling. These

---

[a]This model is also described in Tatterson (1994), who notes that cohesive solids with a true yield point are not expected to follow this model.

[b]personal communication from John Fazio at WVDP to M. R. Powell on April 24, 1997.

columns and the steel gridwork on the tank floor reduce the effectiveness of the mixer pumps by preventing the jets from reaching sludge in some parts of the tank. Five mixer pumps must be used to ensure that essentially all of the sludge can be reached by the mixer pump jets. Five pumps were eventually installed into Tank 8D-2 (McMahon 1990).

The shear strengths reported for the kaolin clay simulant appear to be unrealistically high. It is claimed by Schiffhauer et al. (1985) and by Schiffauer and Inzana (1987) that the sludge simulant was prepared by mixing the clay slurry until the target shear strength of about 30 to 35 kPa was obtained, then the sludge simulant was pumped into the 1/6-scale tank. Pumping a 35 kPa slurry would be very difficult. Consider a 2-in. diameter pipe, 1-m long, filled with 35 kPa sludge. To initiate flow, a pressure of about 2.8 MPa (400 psi) is required. Further, a clay paste with 35 kPa shear strength will hold its shape when molded. This is inconsistent with the reports that the WVDP simulant spread out to cover the floor of the 1/6-scale tank. It seems probable that the shear strength of the kaolin clay simulant was incorrectly reported. Based on the qualitative descriptions of the sludge simulant given in Schiffhauer et al. (1985) and Abdelhamid et al. (1984), a shear strength of 0.35 kPa or less seems much more likely.

3.3 Oak Ridge National Laboratory (ORNL)

The authors are aware of only one study at ORNL that examined sludge mobilization. Tests were conducted in scale-models of the Melton Valley Storage Tanks (MVSTs), which are horizontal, cylindrical tanks 18.3 m (60 ft) long and 3.7 m (12 ft) in diameter. Submerged fluid jets were used to resuspend and mix simulated MVST waste (Hylton et al. 1995).

The sludge was simulated by a kaolin clay slurry with a yield stress of about 10 Pa. This is considerably smaller than the yield stresses for sludge in tanks at Hanford. For this reason, the ORNL sludge mobilization test results cannot be meaningfully compared to the mixer pump tests conducted at Hanford, SRS, and WVDP.

3.4 Idaho National Engineering and Environmental Laboratory (INEEL)

No sludge mobilization studies using mixer pumps or similar submerged-jet-based technologies have been conducted at INEEL. Mixer pumps were once considered for use in some of the tanks at INEEL, and a computer modeling study was performed (Meyer 1994). Sludge mobilization modeling work is described in Section 5.0.

4.0 Sludge Mobilization Testing at Hanford

Sludge mobilization testing at Hanford began in fiscal year 1987 with a series of 1/12-scale mixing tests, which resulted in a correlation between the ECR, the mixer pump U_oD, and the shear strength of the sludge simulant (τ_s). Later studies in smaller tanks refined this correlation and provided additional insight into the effects of mixer pump nozzle design, pump column rotation rate, and sludge dissolution effects.

Each series of Hanford sludge mobilization tests is briefly described in this section. More in-depth descriptions of the test programs can be found in the reports referenced in the text.

4.1 Fiscal Year 1987 Silica/Soda Ash Tests at 1/12-Scale[a]

In fiscal year 1987, plans were being made for the Tank 101-AZ mixer pump test. To support this test, PNNL conducted a series of ten 1/12-scale sludge mobilization tests. Two scale model mixer pumps were installed in the 1/12-scale tank at positions corresponding to the riser locations planned for mixer pump installation in Tank 101-AZ. A scale model of the 22 air-lift circulators was also used.

The sludge and supernatant liquid simulant properties were selected to approximate the best available estimates for the Tank 101-AZ waste properties. No physical property measurements had yet been made on core samples taken from Tank 101-AZ, so the waste properties were estimated based on qualitative descriptions of the waste (e.g., "consistency of cookie dough") and on measurements made using chemically based simulants. The sludge simulant was a mixture of silica powder and concentrated soda ash (sodium carbonate) solution. A reaction between the silica and the soda ash solution resulted in an increase in shear strength with time. By varying the amount of time elapsed from when the simulant was prepared, the desired shear strength could be achieved for each test.

Most tests were conducted when the shear strength was approximately 1000 Pa because the Tank 101-AZ sludge shear strength was estimated at 1000 Pa based on qualitative descriptions of the sludge.[b] Only three of the ten tests were run using shear strengths significantly different from 1000 Pa.

The ECRs were monitored during the tests by locating the sludge bank with the aid of a steel rod held vertically and pulled radially outward from each pump until resistance was encountered. Pump operation continued until the ECR growth rate was judged to be insignificant. The final test run, however, revealed that ECR growth for this simulant continues at a slow rate for at least 14 hours. Many of the early tests were stopped after only about 4 hours. Consequently, some of the end-of-test ECRs were likely smaller than the ECR at the asymptotic limit.

---

[a]A detailed description of these tests is given in C. L. Fow, P. A. Scott, G. A. Whyatt, and C. M. Ruecker. 1987. *Pilot-Scale Retrieval Tests Using Simulated NCAW.* 7W21-87-15. Pacific Northwest Laboratory, Richland, Washington. Technical Report for Westinghouse Hanford Company.

[b]Some DST sludge samples were described as having the consistency of cookie dough. Shear strength measurements of cookie dough established the 1000 Pa target shear strength.

The purpose of this test program was to investigate mixer pump performance for a sludge with a shear strength of about 1000 Pa. It was *not* the purpose of this work to develop a correlation between ECR and sludge shear strength. However, the data were used to develop a preliminary correlation between ECR and shear strength. The ECR versus shear strength data are plotted in Figure 4.1, and the correlation resulting from a linear fit of the data was reported as:

$$ECR = 17.3 U_o D \tau_s^{-0.67} \quad (4.1)$$

where ECR and D are in centimeters, U_o is in centimeters per second, and τ_s is in dynes per square centimeter (1 Pa = 10 dyne/cm^2). Note that more than 10 points are shown on the plot because every test involved at least two mixer pumps and, in some cases, multiple mixer pump flow rates were used.

The ECR predictions for the correlation given in Equation 4.1 are most applicable for tank sludge with a shear strength of about 1000 Pa (10,000 dyn/cm^2). Using this correlation to predict ECR for shear strengths significantly different from 1000 Pa is risky because so few data points were collected away from 1000 Pa. It should also be noted that the ECRs predicted by Equation 4.1 are probably biased low because the tests were not continued until ECR growth had completely ceased.

4.2 Fiscal Year 1988 Kaolin/Ludox Tests at 1/12-Scale[a]

Because of the considerable uncertainty in the shear strength dependence of the ECR correlation developed in fiscal year 1987 (Equation 4.1), another series of 1/12-scale tests was conducted. For these tests, a different type of sludge simulant was used. The previously used silica/soda ash simulant was impractical for tests of high shear strength simulants because too much time was required for the silica/soda ash to reach the high shear strength range. A new type of simulant was formulated. The shear strength of this simulant, composed of kaolin clay, water, salt, and colloidal silica (under the trade name Ludox), could be adjusted by varying the relative fractions of colloidal silica and kaolin in the initial mix. After only 24 hours of curing, the simulant was ready to test.

Seven 1/12-scale tests were performed using the same approach as was described in Section 4.1. Sludge shear strengths were varied from 1500 to 6000 Pa. The first six tests used the kaolin/Ludox simulant, and the seventh test used the silica/soda ash simulant.

The ECR data for these tests are shown in Figure 4.2. Unexpectedly, the ECRs for the kaolin/Ludox simulant did not follow the correlation given by Equation 4.1. Further, the kaolin/Ludox ECRs did not exhibit any discernable relationship to vane shear strength. This lack of a correlation is now attributed to a combination of tank vibration and sludge bank lifting effects, but this was not discovered until fiscal year 1994 when tests were conducted using this same simulant in a clear-bottomed tank (see Section 4.4 for a more complete description of these effects).

---

[a]A detailed description of these tests is given in C. L. Fow, G. A. Whyatt, and T. D. Powell. *Evaluation of a Triangular Arrangement of Mixing Pumps for Waste Retrieval from Double-Shell Tanks.* 7W21-88-1. Pacific Northwest Laboratory, Richland, Washington. Technical report for Westinghouse Hanford Company.

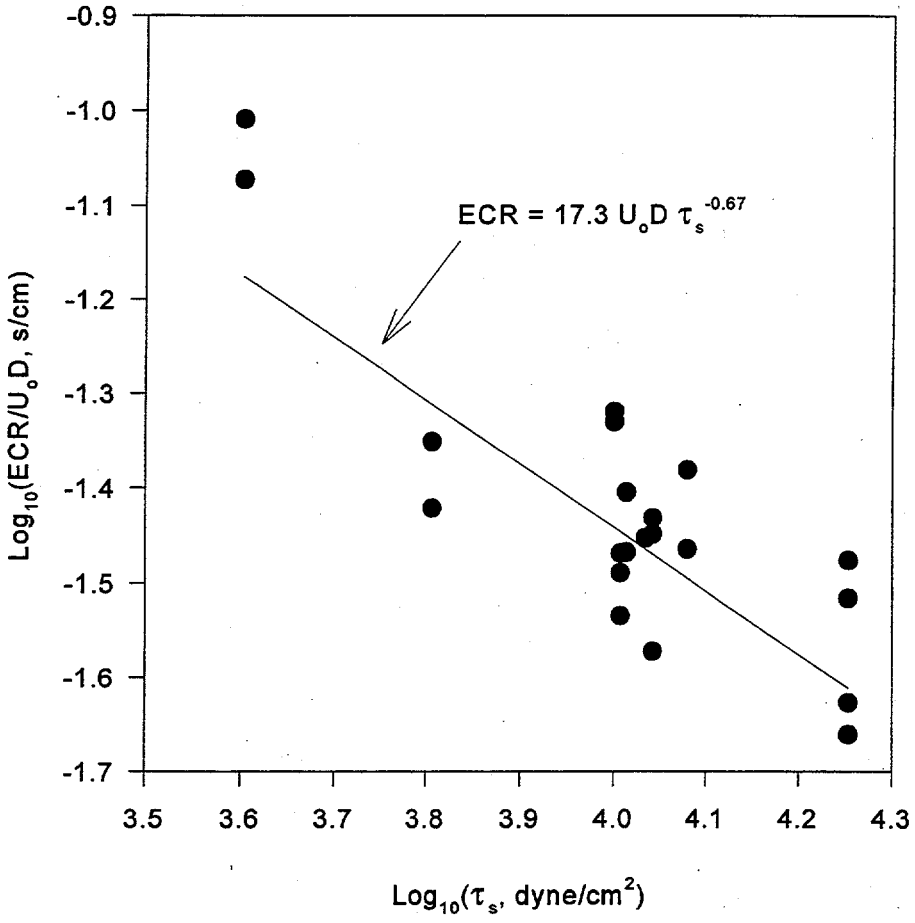

Figure 4.1. ECR Data from Fiscal Year 1987 1/12-Scale Testing (silica/soda ash simulant)

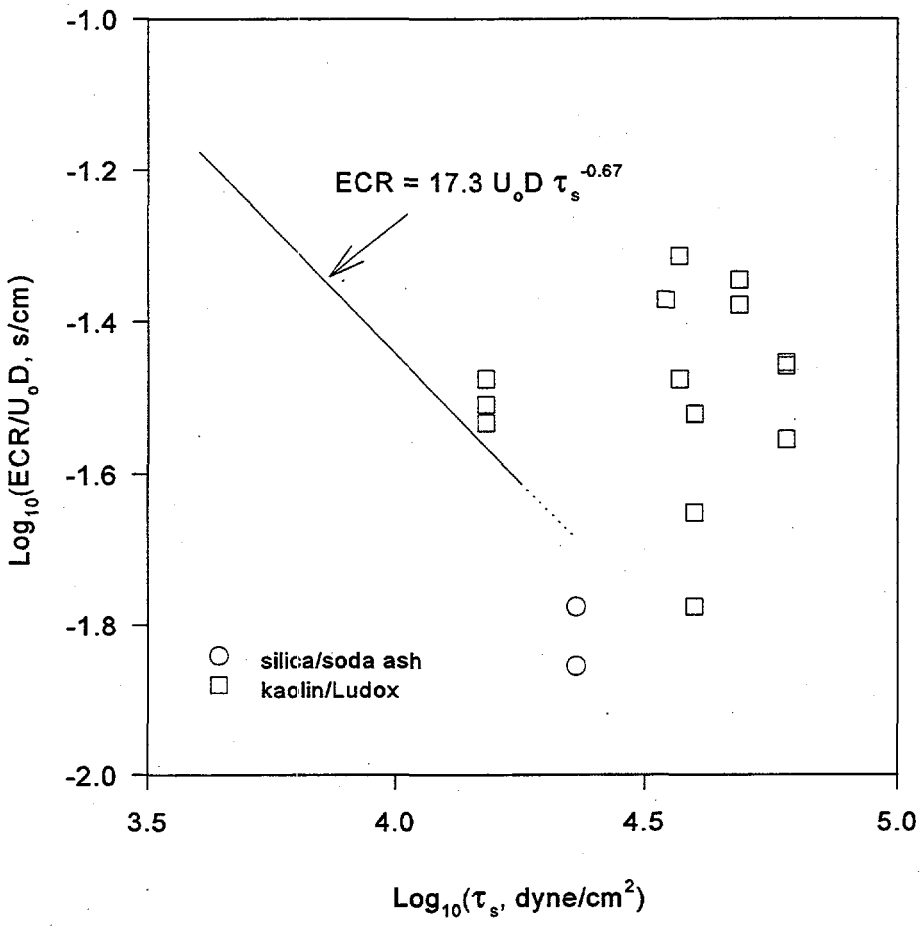

Figure 4.2. 1/12-Scale ECR Test Results for Fiscal Year 1988 Testing

4.3 Bench-Scale Sludge Mobilization Tests[a]

To determine why the anticipated correlation between shear strength and ECR was not observed for the kaolin/Ludox sludge simulant, a series of small-scale mobilization tests was conducted using three different types of sludge simulants: kaolin clay, bentonite clay, and silica/soda ash. Kaolin/Ludox was not used in these tests.

These tests were conducted at bench-scale; sludge in the bottom of a 100-gallon plastic drum was mobilized using a stationary waterjet mounted in the tank wall near the floor. Because the fluid jet was water (instead of slurry) and the nozzle was stationary (instead of rotating at a slow rate like a mixer pump), these tests are not actually scaled sludge mobilization tests. This simplified test design was selected to allow a large number of simulants to be tested for low cost. The goal of the bench-scale testing was to determine whether shear strength correlates with the mobilization resistance of sludge simulants. Development of a correlation between the ECR and shear strength was not the goal of these tests.

A total of 17 bench-scale tests was conducted. A single simulant subjected to three different jet flow rates was used for each test. The ECR for these tests was defined as the distance between the nozzle tip and the eroded sludge bank. The mobilizing waterjet flow rate was slowly increased until sludge mobilization was detected. Then the flow rate was maintained for at least 20 minutes before the tank was drained and the ECR measured. Using this procedure, the true, final ECR (asymptotic limit) is not necessarily obtained. Simulants with a slow ECR growth rate will yield smaller ECRs when measured in this way. Budget constraints did not allow for extended testing at each flow rate.

The bench-scale mobilization test data showed a correlation between ECR/U_oD and shear strength similar to the correlation found in the fiscal year 1987 1/12-scale tests. The ECR/U_oD values found in the bench-scale testing were larger than those found in the fiscal year 1987 tests, but the trend was similar (see Figure 4.3). A linear fit of the bench-scale ECR data for kaolin clay and bentonite clay yielded a correlation of the form:

$$\text{ECR} = 6.1 U_o D \tau_s^{-0.49} \qquad (4.2)$$

The silica/soda ash data were not included in this correlation because the silica/soda ash appeared to mobilize more easily than the clay simulants.

---

[a]A detailed description of these tests is given in G. A. Whyatt, C. L. Fow, T. D. Powell, and P. A. Scott. 1988. *FY 1988 Bench-Scale Sludge Mobilization Testing.* 7W21-88-05. Pacific Northwest Laboratory, Richland, Washington 99352. A Technical Report for Westinghouse Hanford Company.

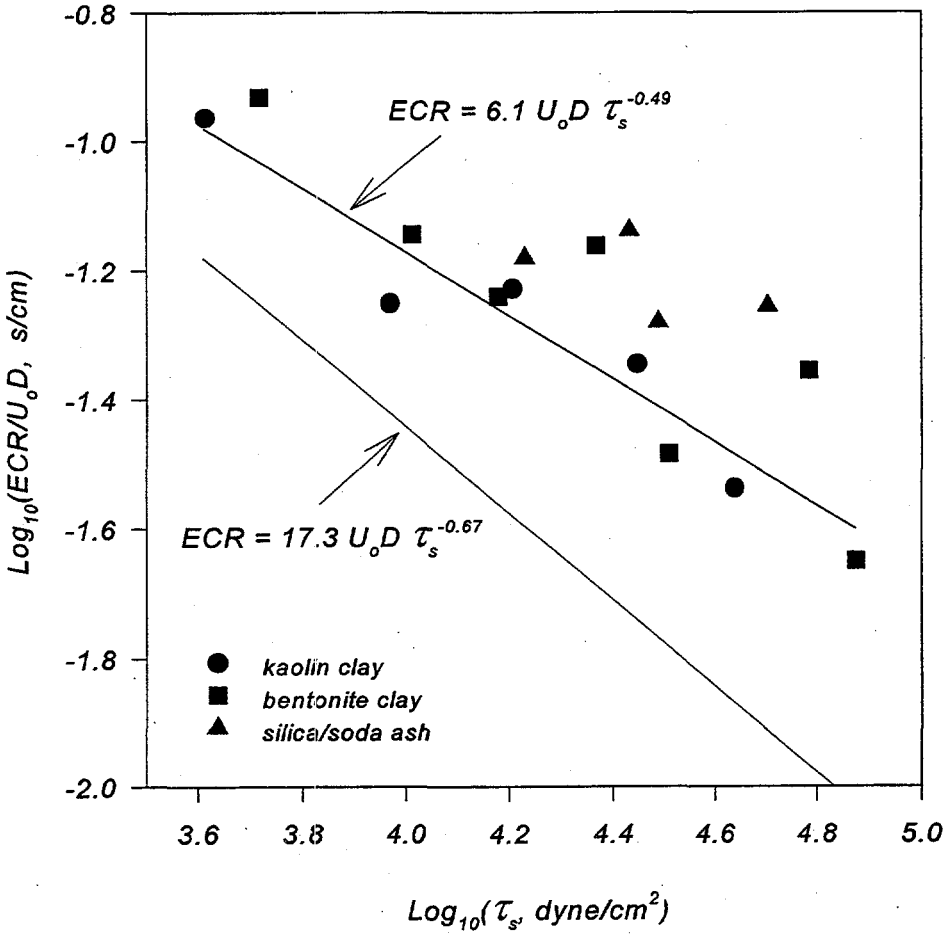

Figure 4.3. Bench-Scale Mobilization Test Results

4.4 1/25-Scale Sludge Mobilization Tests

The bench-scale test results indicated that ECR is a function of sludge shear strength even though the previous 1/12-scale kaolin/Ludox tests implied no such relationship. Clearly, whether a correlation between ECR and shear strength could be expected depended on the nature of the sludge simulant. In an effort to identify what types of simulants follow the ECR versus shear strength correlation, a series of tests in a 1/25-scale tank was conducted in fiscal years 1993 and 1994. Complete descriptions of the 1/25-scale tests are given in Powell et al. (1995a; 1995b).

The 1/25-scale tank is 0.91-m (3-ft) in diameter and constructed of Plexiglass. A scale-model mixer pump was positioned in the center of the tank and surrounded with a 7.6-cm (3-in.)-thick layer of simulated sludge. After adding supernate simulant (usually water), the mixer pump was operated and the ECR growth monitored. The ECR was measured by viewing the location of the sludge/slurry interface through the clear tank bottom. Mixer pump operation continued until the ECR growth stopped or until it reached a constant growth rate.[a] The flow rate was then either increased or the test was stopped. A sketch of the 1/25-scale facility is shown in Figure 4.4.

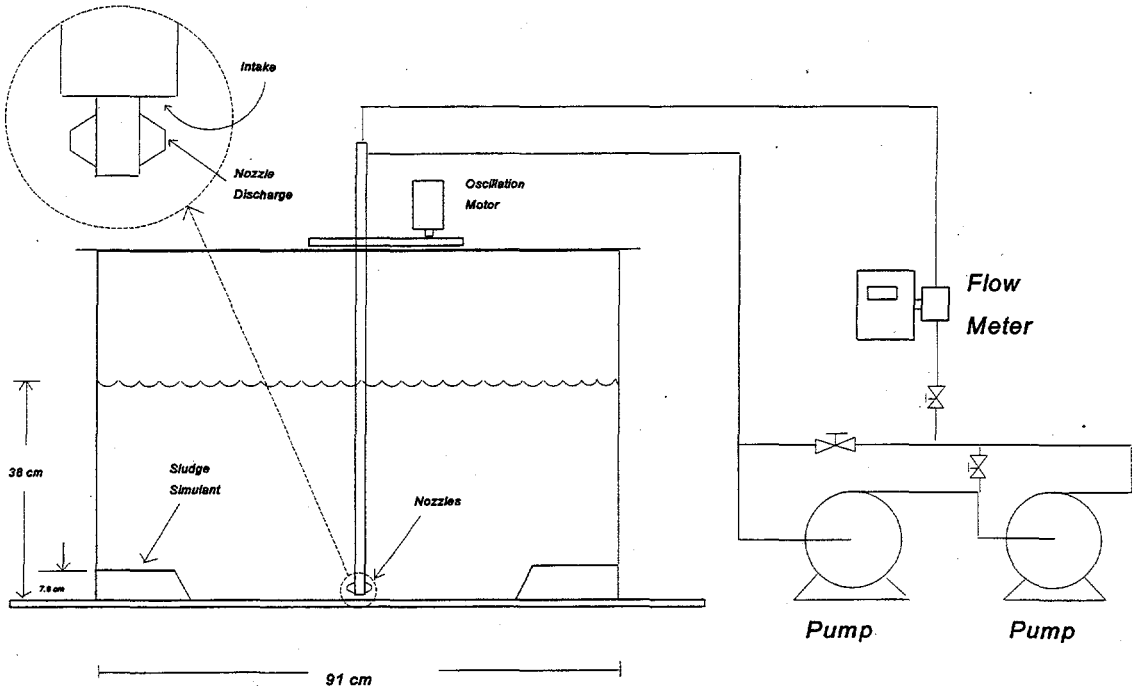

Figure 4.4. Sketch of 1/25-Scale Test Facility

[a]Some simulants, notably bentonite and mixtures of kaolin and bentonite, absorb water from the slurry, which results in a weakening of the sludge surface. The ECR growth rate for these simulants never reached zero because of this effect. Efforts were made to remove this effect from the data.

A total of 45 1/25-scale sludge mobilization tests was conducted during fiscal years 1993 and 1994. A variety of sludge simulant types covering a wide range of shear strengths was tested. Because the exact nature of the mobilization resistance of tank sludge is not known, testing of many different simulant types was performed in an effort to bracket the waste properties. The sludge simulant types used for testing were kaolin clay, bentonite clay, various mixtures of kaolin and bentonite, kaolin/Ludox, silica/soda ash, kaolin clay mixed with plaster of Paris, and kaolin clay mixed with concentrated salt solution. Powell et al. (1995a) addresses the mechanisms for strength development in each of these sludge simulants.

The primary goal of the 1/25-scale testing was to identify the sludge properties that correlate with ECR. Sludge simulants were tested for yield stress, tensile strength, and shear strength (both undisturbed and remixed). Soil erosion literature indicates that tensile strength should correlate most directly to the erosion resistance of cohesive soils (e.g., saturated clays), but tensile strength measurement is problematic.

The use of tensile strength as a direct measure of cohesion has been suggested by others in the literature (Nearing et al. 1991; Leavell and Peters 1987; Smalley 1970; Searle and Grimshaw 1959). That tensile strength might correlate with cohesive soil erosion resistance to turbulent flow was perhaps first suggested by Martin (1962) in his review of the paper by Moore and Masch (1962), which was one of the first attempts to correlate the erosion resistance of soils with physical properties. The use of tensile strength as an erosion predictor, however, has only recently received renewed attention (Nearing et al. 1991). This apparent oversight is likely an implicit recognition of the difficulty associated with obtaining tensile strength measurements on saturated soils. Currently no standard tensile strength measurement technique exists for soils with shear strengths in the range expected for tank sludge.

The 1/25-scale testing confirmed the bench-scale result that sludge shear strength can be correlated to the ECR provided that the shear strength is due to cohesive forces within the sludge rather than frictional forces. A sludge with a significant frictional component to its shear strength will mobilize more easily than a purely cohesive sludge with the same shear strength. Therefore, a correlation developed with cohesive sludge simulants can be used to make lower-bound estimates of the ECR. Given a shear strength measurement from tank sludge, the ECR expected from mixer pump operation can be estimated using the correlation developed for cohesive sludge. The actual ECR is expected to be equal to or greater than the predicted ECR.

The ECR data from the 1/25-scale tests are plotted in Figure 4.5. The correlation shown on the plot applies only to the cohesive sludge simulants (i.e., not to kaolin clay). Figure 4.6 includes the data points used in the development of the correlation. Along with the kaolin clay data points, several of the data points for the cohesive sludge simulants were not included in the correlation. Experimental difficulties were encountered during some tests and the ECR data for these tests were judged to be unreliable, so they were not included in the correlation. This is described further in Powell et al. (1995a) and Powell (1996).

The data in Figure 4.6 are reasonably well fit by the solid-line correlation included on the plot, which is:

$$ECR = 4.0\ U_o D\ \tau_s^{-0.46} \qquad (4.3)$$

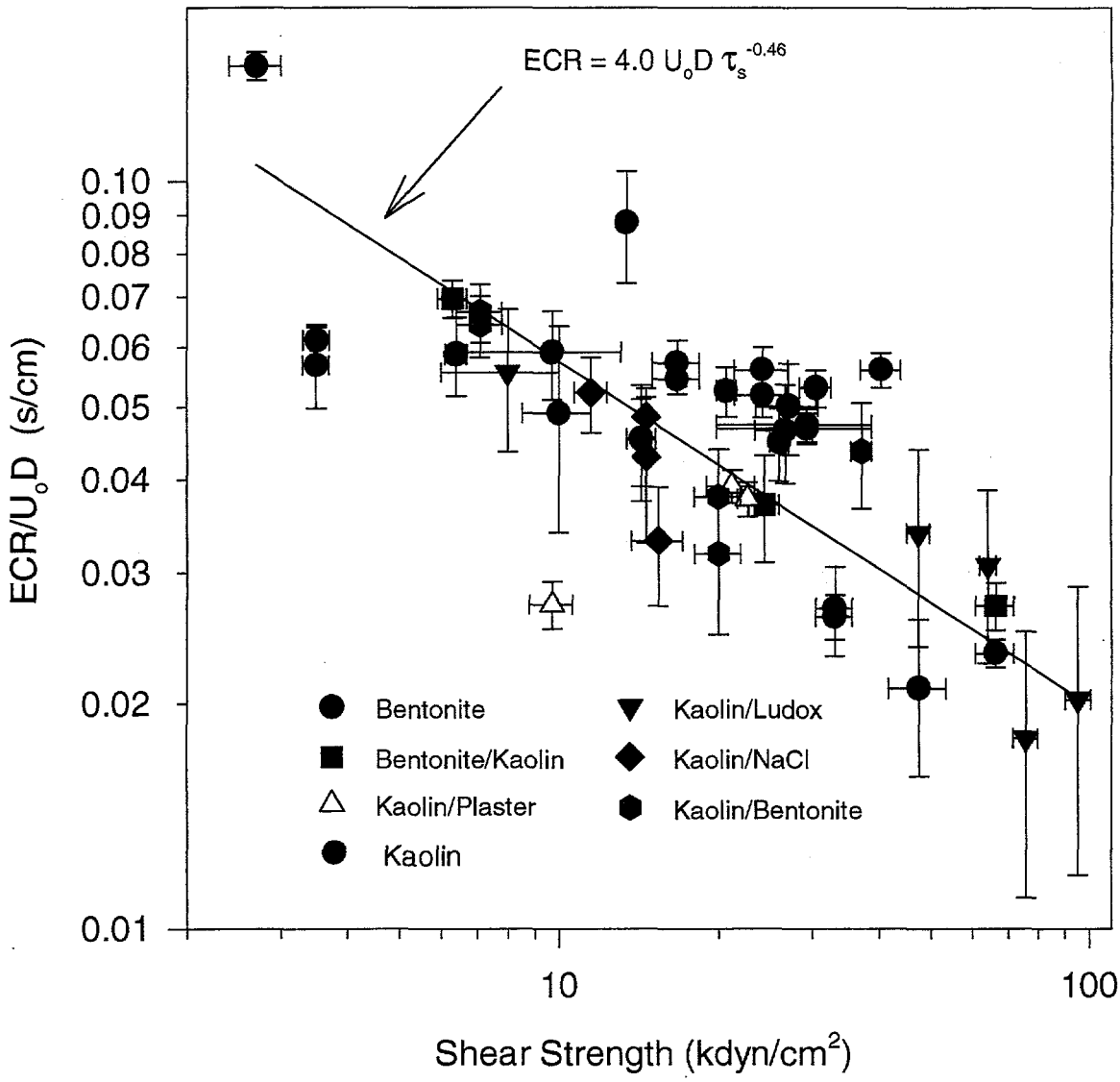

Figure 4.5. 1/25-Scale Sludge Mobilization Data

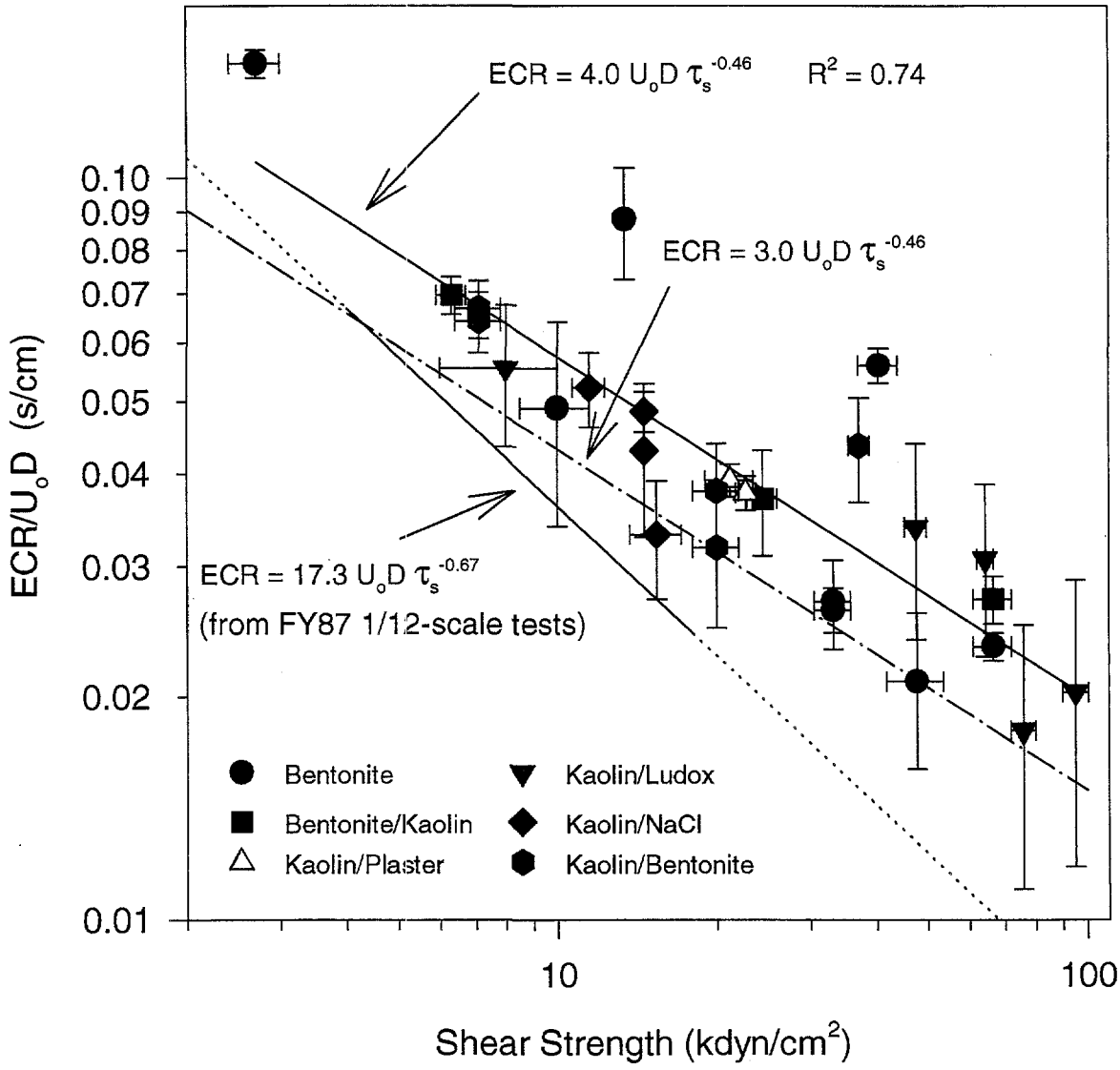

Figure 4.6. 1/25-Scale Cohesive Sludge Mobilization Data

For the purposes of predicting full-scale ECRs, however, a somewhat more conservative correlation is recommended. The ECR data in Figure 4.6 are biased high by several bentonite clay data points that appear to be outliers. Experimental difficulties were encountered during some bentonite clay tests that tended to increase the ECRs. The problem was that the bentonite sludge simulant density is relatively low. This permitted the mixer pump jets to occasionally lift the sludge bank and force slurry under the sludge bank. This reduced the sludge bank adhesion to the tank floor and resulted in larger ECRs. This may have occurred during the tests that appear to be outliers.

The dashed-line correlation shown in Figure 4.6 should be used to make full-scale ECR predictions. This correlation (ECR = 3.0 $U_o D\ \tau_s^{-0.46}$) is representative of the lower range of ECRs on the ECR/$U_o D$ versus shear strength plot. Reducing the empirical proportionality constant in Equation 4.3 from 4.0 to 3.0 is expected to reasonably account for the observed variability in the ECR measurements. It is worth noting that the fiscal year 1987 ECR correlation (also shown on Figure 4.6) is even more conservative than the dashed-line correlation, but the fiscal year 1987 correlation falls not too far below the lower edge of the error bars on the 1/25-scale data.

In addition to studying the effects of sludge properties on the ECR, some 1/25-scale tests were used to evaluate several possible modes of mixer pump operation and/or other sludge mixing enhancements. The findings from these tests were:

- Mixer pump nozzle design can significantly influence the ECR. In some tests using a poorly designed nozzle, the ECR was reduced by approximately 50% when compared to tests using a well-designed nozzle. Poor nozzle designs allow a significant fraction of the jet momentum to be non-axial (i.e., jet swirl or jet direction not aligned with nozzle axis).

- No significant difference in ECRs produced by rotating and non-rotating mixer pumps was observed during testing at 1/25-scale. This does not necessarily mean that no such difference would be observed at full-scale, but the implication is that mixer pump column rotation will not adversely affect ECR growth provided the rotation speed is low.

- A commercial dispersant was added to the tank supernatant liquid in one test in an attempt to increase the ECR of a kaolin simulant via chemical means. The dispersant had no effect. Dispersants are unlikely to improve mixer pump ECRs because the dispersant must be present within the sludge for it to be effective.

- ECR growth rate and the final ECR will be increased if the sludge contains a significant fraction of soluble solid material and the supernate is not saturated with that material. Just the presence of a salt concentration difference between the sludge and the supernate does not, however, appear to affect sludge mobilization. The permeability of the sludge is probably too low for this osmotic effect to result in significant ECR growth (Section 4.1.3 in Powell et al. 1994a).

- The mixing time required to reach the ECR varies considerably depending on the sludge simulant type and solids concentration. In some tests, the ECR was reached after less than 1 hour of mixing while in others more than 40 hours of mixing was required. The sludge properties that control the required mixing time are not well understood. This topic is explored further in Section 4.5.

4.5 Current State of ECR Correlation Prediction Capabilities

Over the past two decades, efforts have been made to develop accurate correlations between the ECR and tank waste properties. The experimental work has yielded a correlation between ECR and shear strength that is applicable to cohesive sludge simulants in the 1/25-scale tank. Based on the self-similar properties of submerged jets of Newtonian fluids, the 1/25-scale ECR predictions are expected to scale linearly to full-scale. Further, the SRS full-scale mixer pump test ECR data are consistent with linear scaling of the 1/25-scale data. However, accurate prediction of ECRs in full-scale radioactive waste tanks is still problematic.

The applicability and limitations of the existing ECR prediction correlation are discussed in this section.

4.5.1 Estimated Accuracy of ECR Correlations

Considerable data scatter is observed in the 1/25-scale test results. Non-homogeneous simulant compositions as well as variations in adhesion of the simulant to the tank floor are thought to be causes of the scatter. More accurate ECR correlations likely could be developed through larger-scale testing. Not only would errors due to possible non-linear scaling be reduced, but the effects of sludge adhesion and homogeneity would also likely become less important.

The uncertainty in the ECR predictions made based on the 1/25-scale testing for cohesive sludges is on the order of 20%. If the 1/25-scale correlation is used to make sludge mobilization predictions for the purpose of retrieval system design, the predicted ECR should be adjusted accordingly to account for this uncertainty.

This estimated ECR prediction uncertainty does *not* include the non-random effects of scale-up, non-Newtonian slurry rheology, and systematic errors in sludge shear strength measurements. The true accuracy of ECR predictions made using the 1/25-scale correlation will be worse than the ± 20% observed at 1/25-scale because of these effects, each of which is discussed in the sections below.

4.5.2 Scale Up of ECR Correlations

The ECR is expected to scale linearly provided that the test scaling methodology described in Section 2.2 is used. Thus, a 30-cm ECR observed in a 1/25-scale test should correspond to a full-scale ECR of 25*(0.30 m) = 7.50 m. Linear scaling is expected based on the self-similar properties of submerged, turbulent jets of Newtonian fluids. Linear scaling might not hold for jets of non-Newtonian fluids; this is addressed in Section 4.5.4.

There is some experimental evidence for the linear scaling of ECR. The full-scale mixer pump tests conducted at SRS used a kaolin clay sludge simulant. The ECR/U_oD values for the tests described in Section 3.1 were 0.045 ± 0.005 s/cm (half-tank mockup), 0.064 ± 0.006 s/cm (full-tank mock-up), and 0.072 s/cm (1/12-scale). The uncertainty on the ECR/U_oD for the 1/12-scale SRS test results cannot be estimated from the data provided in Motyka's memorandum (see Section 3.1). Based on PNNL's experience with tests at 1/12-scale, however, an uncertainty on the order of 10% or more (0.007 s/cm) is reasonable. Thus, both the 1/12-scale and full-tank mock-up results at SRS agree. This supports the

claimed linear scaling of ECR. The half-tank mock-up results may have been biased low by the restrictive tank geometry.

Further evidence for linear ECR scaling is the agreement of the PNNL 1/25-scale results with the SRS kaolin clay tests. Testing at PNNL using kaolin clay at 1/25-scale has found ECR/U_0D values that range from about 0.045 to 0.062 s/cm (Powell et al. 1995a). This is clearly consistent with the range of values found at SRS.

Once mobilized, kaolin clay forms a slurry with the supernate that is very nearly Newtonian at the concentrations encountered. Thus, the experimental validation of linear ECR scale-up can be applied only when the waste slurry is approximately Newtonian.

An attempt was made in fiscal year 1993 by PNNL to run a 1/25-scale test using the silica/soda ash sludge simulant. Comparison of the 1/25-scale results with the previously gathered 1/12-scale silica/soda ash data was inconclusive with respect to ECR Scale up. Interpretation of the results was complicated by the poor reproducibility of the silica/soda ash. This testing is detailed in Section 4.2 of Powell et al. (1995b).

Another important aspect of mixer pump testing scale-up is mixing time. Mixer pumps add heat to tank waste. If the pumps are run long enough, the waste temperature may become high enough to result in significant waste evaporation. The waste evaporation rate influences the ventilation system design. Thus, it is important to accurately predict (or bound) the required mixer pump operation time so that a sufficiently robust vent system is installed before tank mixing begins.

Whether the expected mobilization time scaling occurs has not been established. As discussed in Section 2.2, the time required to mobilize a given fraction of waste is expected to scale linearly with tank dimension. If the ECR is reached after 10 hours of mixing at 1/25-scale, then about 250 hours of mixing should be required at full-scale. No experiments have yet verified time scaling for sludge mobilization, but there is some evidence that supports it.

The full-scale mixer pump tests at SRS (both half-tank and full-tank mock-ups) were conducted for periods in excess of 75 hours. The experimenters noted, however, that no significant ECR growth was observed after about 50 hours of pump operation. It appears, then, that the final ECR is reached after about 50 hours in a full-scale test using kaolin clay. The 1/12-scale kaolin clay tests at SRS were conducted by placing a pile of simulant in one portion of the tank rather than covering the tank floor with sludge simulant, so the 1/12-scale data cannot be used to estimate the 1/12-scale mixing time.

Tests at PNNL in the 1/25-scale tank also used kaolin clay, albeit possibly not the same type of kaolin as was used at SRS (the SRS reports do not provide information about the type of kaolin used). Because the type of kaolin used at SRS is not known, a direct comparison between the PNNL and SRS results cannot be made. However, it is worth noting that the results are consistent with linear time scaling.

The characteristics of the kaolin sludge simulant are not specified in the SRS reports. Dry kaolin clay was placed in the test tank, and then it was covered by water. The clay imbibed some amount of the water to form a kaolin clay paste. The rheological characteristics of this paste are unknown. This is unfortunate because the kaolin ECR growth rate depends on shear strength. This is despite the fact that the kaolin ECR is relatively independent of shear strength (see Powell et al. 1995a). Without knowledge

of the full-scale SRS kaolin characteristics, it is difficult to determine which 1/25-scale PNNL kaolin test should be selected for comparison.

If it is assumed that the EPK Pulverized kaolin clay (from Feldspar Corporation, Edgar, Florida) used at PNNL will imbibe water to reach the same strength as the SRS sludge, then a comparison can be made. When dry, the PNNL kaolin imbibes water until its shear strength reaches about 150 Pa. Assuming this is representative of the SRS clay, a comparison can be made to fiscal year 1994 1/25-scale Test 2-K in which the kaolin shear strength was 350 Pa. No 1/25-scale tests were conducted using a lower shear strength. The ECR was reached in Test 2-K after about 1 hour of testing. Thus, a full-scale mobilization time of 25 hours would be expected. As stated earlier, full-scale mobilization times of about 50 hours were noted at SRS. Considering the uncertainty involved because of the probable difference in kaolin properties, the factor of two difference in mobilization times is not unreasonable. The 1/25-scale kaolin clay mobilization times ranged from 1 hour to just over 10 hours. The range of full-scale kaolin mobilization times predicted by these results is from 25 to 250 hours. For some simulants, over 40 hours was required to reach the ECR at 1/25-scale. This would predict a full-scale mobilization time of more than 40 days.

SRS personnel gathered full-scale ECR versus time data during the retrieval of waste from Tank 16 (Hamm et al. 1989). The ECR growth was noted even after more than 500 hours of mixer pump operation. No sludge characterization was performed, so it is unknown whether the Tank 16 sludge could be compared to the simulants used in any of the scaled tests. This result, however, confirms that mixer pump operation times can be quite long. Further, the difference in mobilization times between the Tank 16 sludge and the full-scale kaolin tests demonstrates that the mobilization time depends on sludge properties.

To summarize, there is reasonable assurance the ECR scales linearly provided that the waste slurry rheology is near Newtonian. It is not clear, however, whether the mobilization rates observed during scaled testing can be used to predict full-scale mobilization rates. Further, because the waste properties that govern mobilization rate have not yet been identified and experimentally confirmed, it is not clear whether the sludge simulants used previously are even appropriate for the prediction of mobilization rate. Unless further study into mobilization rate is performed, it seems the best estimate for full-scale mobilization times must be taken from full-scale experience at SRS. This puts the current best estimate for the time required to reach the ECR at somewhere between about 50 and 500 hours (perhaps more).

4.5.3 Shear Strength Measurement Uncertainties

Probably the single greatest obstacle to making accurate ECR predictions is sludge characterization. A correlation has been developed to allow the prediction of ECR based on the sludge shear strength. Given an accurate estimate of shear strength in a tank containing homogeneous waste, the ECR can be predicted to probably within 20% (assuming linear ECR scaling occurs and non-Newtonian slurry effects are not significant). However, tank waste is not homogeneous, and even if it was, obtaining accurate shear strength data is difficult.

Variations in the tank waste properties are known to exist. Thus, it is expected that the shear strength varies to some extent within each tank. Whether this variation is significant has not been determined for any of the DSTs, but even if it had, the variability of waste properties in one tank does not necessarily reflect the variability in a different tank unless the wastes and waste histories are similar. To overcome

the problem of waste property variability, multiple shear strength measurements in different parts of the tank are required. The exact number of samples required to obtain a desired degree of accuracy in the shear strength estimate cannot be determined *a priori* as it is a function of the shear strength variability. A minimum of four independent shear strength measurements likely would be required to meet any reasonable shear strength accuracy criterion.

The shear strength of sludge depends not only on the chemistry, morphology, and solids concentration of the sludge, but on the amount of disruption that occurs during shear strength measurement and on the conditions under which the measurement is made.

Disruption can break down bonds between sludge particles, and this results in a decrease in the measured shear strength. Whether disruption effects are significant depends on the nature of the interparticle bonds. Some sludge-like materials, such as kaolin clay, reform the interparticle bonds very quickly so that disruption does not appreciably affect their shear strengths. Other sludge simulants are much more significantly affected by disruption. The silica/soda ash, kaolin/Ludox, and kaolin/plaster simulants used for 1/25-scale testing at PNNL can be changed from a stiff paste (shear strength in excess of 1000 Pa) to an easily pourable slurry (shear strength less than 100 Pa) simply by mixing. This behavior has also been noted in some tank waste samples. The first core sample from Hanford DST 101-AZ, for example, was subjected to mixing before the a shear strength of about 250 Pa was measured.[a] The second core sample was handled so as to minimize disruption and a shear strength of about 1500 Pa resulted.[b] Clearly, if shear strength measurements are to be used to make ECR predictions, care must be taken to ensure sludge disruption is kept to a minimum before measuring the shear strength.

The temperature at which the shear strength measurement is made can also be important. Figure 4.7 shows the shear strength of a sludge sample taken from Tank 101-SY as a function of temperature.[c] As the sludge temperature is increased from 32°C to 80°C, the shear strength decreases by a factor of ten or more. Whether this behavior is exhibited by other waste sludges is not known. Shear strength versus temperature testing has been conducted only on samples taken from Tank 101-SY. The data in Figure 4.7 illustrate the dramatic effect temperature can have on the sludge shear strength. In order to make accurate ECR predictions, the sludge shear strength must be measured at the waste temperature expected during retrieval. Most hot-cell shear strength measurements made on core samples have been conducted only at the hot-cell temperature, which routinely is about 30°C.

---

[a]Scheele, R. D., M. E. Peterson, and J. L. Tingey. 1989. *Characterization of the First Core Sample of Neutralized Current Acid Waste from Double-Shell Tank 101-AZ.* Pacific Northwest Laboratory, Richland, Washington.

[b]Gray, W. J., M. E. Peterson, R. D. Scheele, and J. L. Tingey. 1990. *Characterization of the Second Core Sample of Neutralized Current Acid Waste from Double-Shell Tank 101-AZ.* Pacific Northwest Laboratory, Richland, Washington.

[c]Data for Figure 4.7 were taken from *Rheological Properties of Waste from Tank 101-SY.* by J. M. Tingey. Technical report prepared for Westinghouse Hanford Company by the Pacific Northwest Laboratory, Richland, Washington. May 1992.

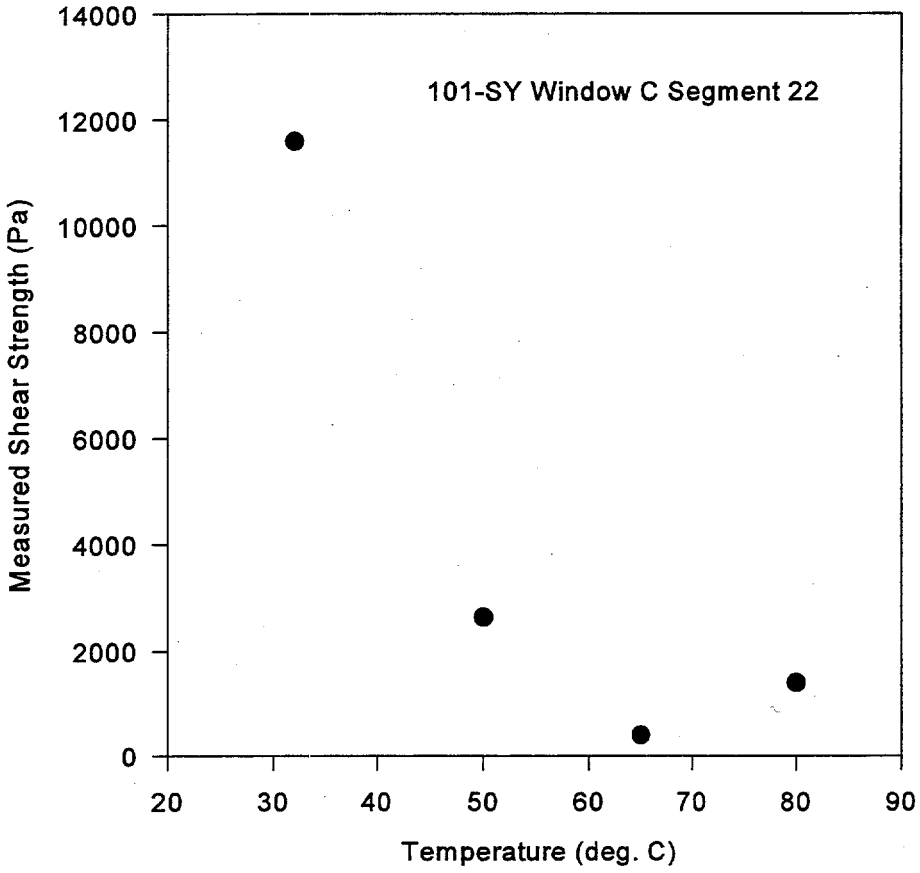

Figure 4.7. Shear Strength of Tank 101-SY Sludge versus Temperature

The difficulties associated with accurately characterizing the relevant sludge properties are considerable. Unless a reliable method can be developed to measure the in situ sludge shear strength at the appropriate temperature, the accuracy of ECR predictions is unlikely to improve significantly.

4.5.4 Non-Newtonian Fluid Jet Uncertainties

The effects of non-Newtonian slurry rheology on the behavior of submerged fluid jets was studied as part of the fiscal year 1994 sludge mobilization work. The findings are described in Section 4.3.1 of Powell et al. (1995a).

Non-Newtonian rheology appears to have two significant effects on sludge mobilization. First, the jet velocity decay rate is affected by the fluid rheology. Under highly turbulent conditions (high jet flow rates), the non-Newtonian effects are diminished and the jet behaves like a jet of Newtonian fluid. Far away from the nozzle, however, the local Reynolds numbers are low and inertial effects no longer dominate the viscous effects. In such cases, the fluid velocity may decay very quickly to zero, as in the case of a slurry with a significant yield stress (Shekarriz et al. 1996).

In general, whether the rheology of the liquid during mobilization becomes non-Newtonian depends on a number of parameters such as the particle size distribution, the total solids concentration, and the colloidal interactions between the particles. For example, it was previously shown with a sample of Tank SY-102 waste that the particles tend to aggregate and produce a non-Newtonian suspension if the zeta-potential of the particle is near the isoelectric point (Onishi et al. 1996a; Smith et al. 1997). The chemistry of the solution and surface properties of the particles during mobilization ultimately dictate to what extent aggregation is promoted. In the case of Tank SY-102 waste during mobilization, although the initial mixture (sludge) had a non-Newtonian rheology, a 1:1 dilution with an electrolyte resulted in a Newtonian mixture (Onishi et al. 1996). However, these results cannot be extrapolated to all DST wastes. Results from in-tank characterization of Tank SY-101 waste using the ball rheometer reveals that the rheology of the mixture (after mixer pump operation) is non-Newtonian (Stewart et al. 1996). The reason(s) for obtaining such non-Newtonian behavior in this tank (versus Tank SY-102) is not clear at this time. One may hypothesize that the non-Newtonian rheology is due to the high solids concentrations in the mixed slurry as well as, possibly, agglomeration of particles due to colloidal forces. Using this argument, one would expect similar behavior in other DSTs such as Tanks AN-105, AN-104, AN-103, and AW-101.

The impact of gelation on the jet and on ECR may be shown using a simple mathematical argument supported by experimental data. Figure 4.8 is a schematic diagram of a submerged jet. The jet is issued out of the nozzle with a velocity of U_o and density ρ. The decay or dissipation of momentum in the jet is governed by the time-averaged integral momentum equation in the x-direction (streamwise direction):

$$\frac{1}{2\pi}\frac{d}{dx}\int_0^{\infty} 2\pi r\, dr\, \rho u^2 = -(r\tau)\Big|_0^{\infty} \qquad (4.4)$$

From Equation 4.4, it can be shown that the momentum of a yield-pseudoplastic fluid decreases quadratically with downstream distance (see Appendix A for derivation).

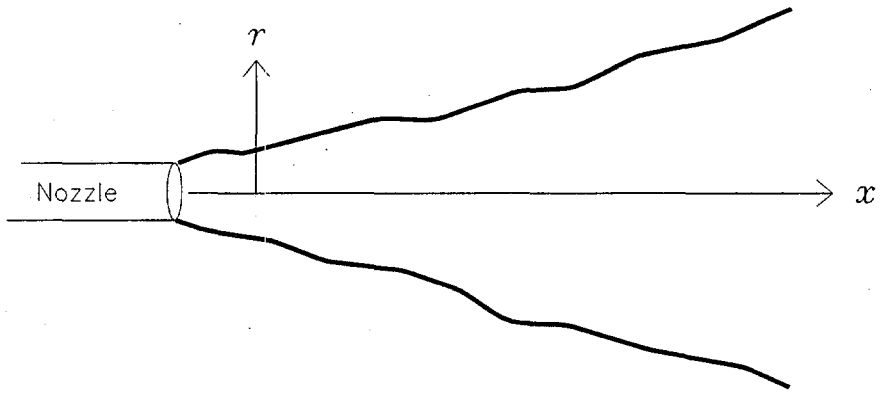

Figure 4.8. Jet Issuing from Nozzle

Figure 4.9 is the plot of total momentum of a yield-pseudoplastic jet in the axial direction. These results were obtained by measuring the radial distribution of axial velocity in the jet at several streamwise positions in the jet. The profile of velocity at each axial location, x/D, was then integrated to obtain the total momentum. As mentioned before, the theory based on Newtonian flow behavior predicts that no loss in the momentum should take place, as shown by the solid line. However, as argued previously, for a non-Newtonian mixture, a loss in the momentum occurs. Based on Figure 4.9, the 0.1% Carbopol jet has no net axial momentum at approximately 75 diameters downstream of the nozzle. Rheological characterization of this fluid revealed that the Bingham yield stress is approximately 3 Pa.

The rate of jet spread may be quantified through the mass flux within the jet. Based on empirical relations (Rajaratnam 1976) for Newtonian liquids, the mass flux in the jet (Q) at each downstream location grows as

$$\frac{Q}{Q_o} = 0.32\,\frac{x}{D} \qquad x > \approx 3D \tag{4.5}$$

where x is the streamwise position, D is the diameter of the nozzle, and Q_o is the mass flux at the nozzle. Thus, at 60 diameters downstream of the nozzle, the jet has entrained more than 20 times its initial mass flowrate. The data in Figure 4.10 show that this entrainment rate is reduced to less than 10 times for a non-Newtonian jet. In addition, a reversing effect is observed where the non-Newtonian jet suffers from loss of mass into its stagnant surroundings.

ECRs in the range of 5 to 12 m are needed in the DSTs. Using 15-cm (6-in.) nozzles, this ECR range translates to between about 30 and 80 nozzle diameters. The non-Newtonian effects shown in Figures 4.9 and 4.10 are clearly significant in this range of downstream distances.

Another possible effect of non-Newtonian slurry rheology is an increase in the mobilization resistance of the sludge surface to the impinging mixer pump jet. Based on some of the fiscal year 1994 1/25-scale test results, it is suggested that slurry with a high apparent viscosity at low shear rates will form a layer near the eroding sludge surface that resists the penetration of turbulent eddy bursts from the mixer pump jet. This effect has not been adequately studied, but it appears that the mobilization

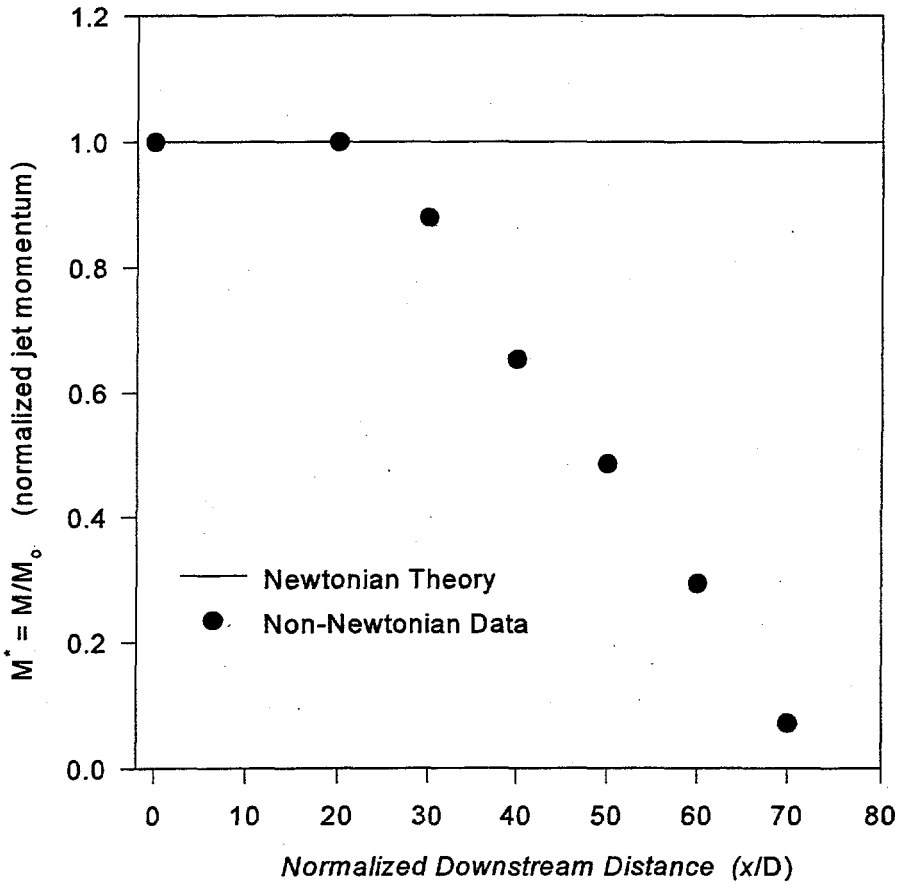

Figure 4.9. Momentum Loss in the Streamwise Direction for 0.1% Carbopol at 6 m/s

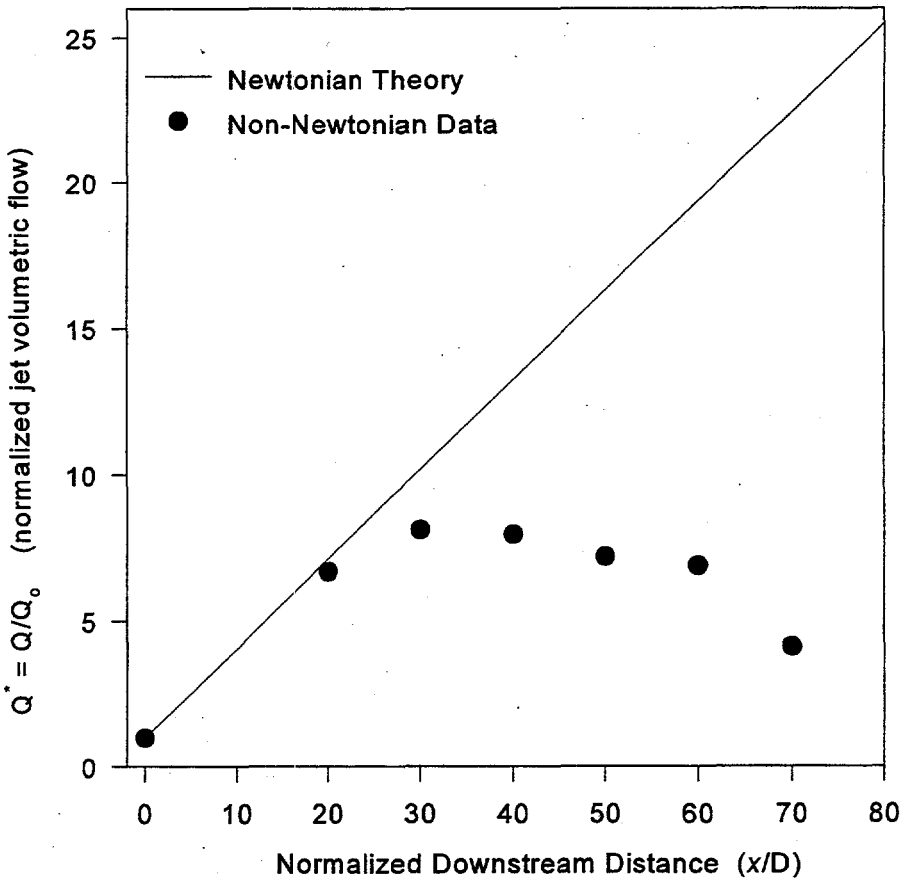

Figure 4.10. Mass Flux in the Non-Newtonian Jet (0.1% Carbopol at 6 m/s)

resistance of the sludge is increased by an amount that is on the same order of magnitude as the apparent yield stress of the slurry. For example, consider a sludge that can be eroded by a Newtonian fluid when the applied shear stress exceeds 5 Pa. When, instead of a Newtonian fluid, a non-Newtonian slurry with a yield stress of about 3 Pa is used to erode the sludge, the required applied stress for erosion may increase to about 10 Pa or more. This was observed in one of the fiscal year 1994 1/25-scale tests in which xantham gum was used to create a non-Newtonian slurry during the sludge mobilization test.

Currently, efforts are underway to characterize the turbulence in the jet as a function of rheology and to parametize the bounds within which such behavior can be expected.

5.0 Numerical Modeling of Sludge Mobilization

Computational modeling has been applied to help address many waste retrieval questions. Waste mobilization, mixing, gas retention, and chemical reactions have all been modeled to varying degrees using computer codes. The efforts that have been made to model sludge mobilization are described in this section.

5.1 Major Technical Considerations

Most of the Hanford tank wastes were generated from reprocessing of irradiated nuclear fuels to extract plutonium and recover uranium (Bunker et al. 1995). However, wastes vary from tank to tank. Solids, salt cakes, sludges, liquids, and vapors often coexist in the same tank. They are chemically and physically complex. For the waste retrieval operation, wastes in the DSTs will be retrieved by one or two 300-hp mixer pumps installed in each tank (Figure 5.1).

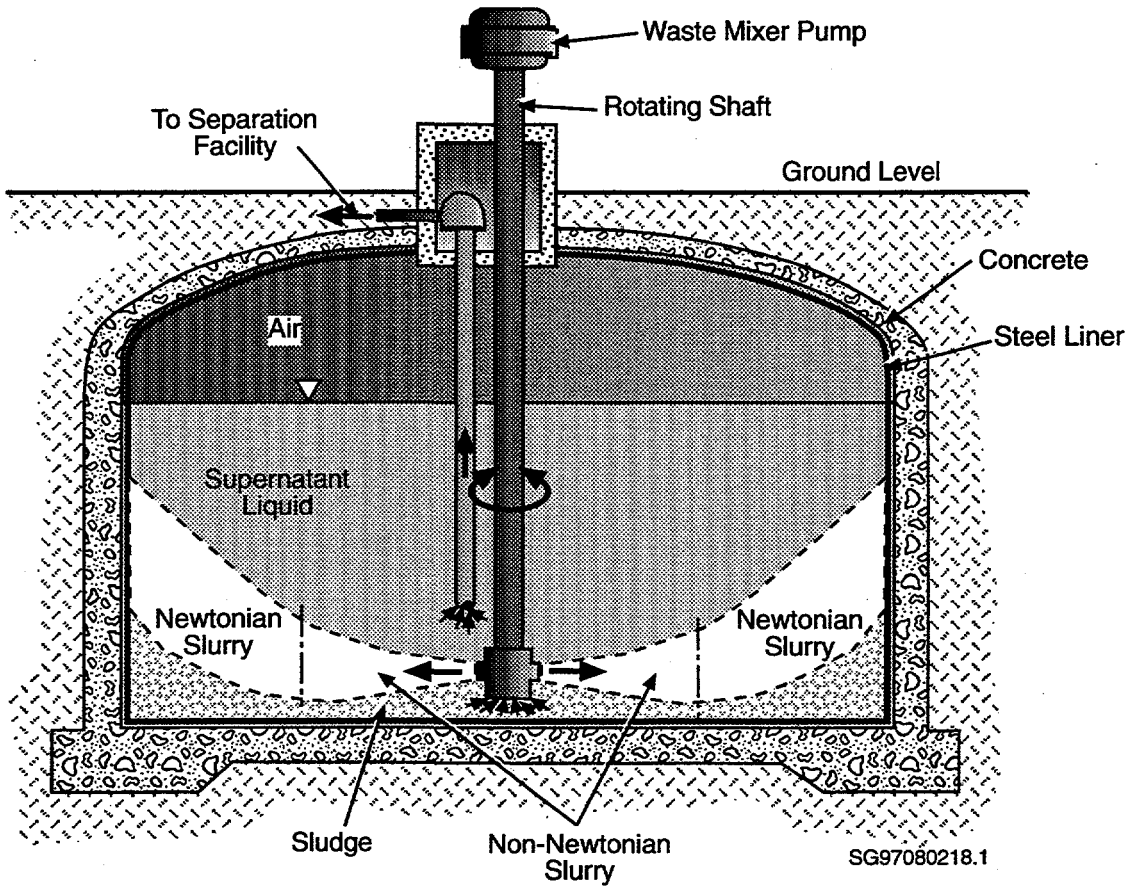

Figure 5.1. Mixer Pump Jet Mixing

When a sludge is mixed with supernate during waste retrieval, dissolution/precipitation reactions may occur. The dissolution and precipitation change solid and aqueous (and possibly gaseous) chemical compositions and thus affect physical properties (e.g., densities of supernatant liquid and sludge), rheology (e.g., viscosity and yield stress/strength), and flow conditions (e.g., drag behind air bubbles and solid particles). These changes, in turn, affect the physical behavior of tank wastes, including gas retention in the sludge layer, solids resuspension and settling, and slurry flow. Modeling of the tank waste retrieval operation, including predicting ECRs, must address the following four main technical considerations:

- Multi-component, multi-phase, high-ionic strength, dissolution/precipitation reactions
- Complex waste rheology and its changes
- Combined Newtonian and non-Newtonian jet mixing hydrodynamics
- Transport, erosion, and deposition of fine solids

We will discuss these four technical points in some detail. Significant progress has been made with the incorporation of a chemical model for the tank salt solutions, such as for the major electrolyte system of Na^+, NO_2^-, NO_3^-, OH^-, PO_4^{-3}, and $H_2SiO_4^{-2}$, including temperature-dependent standard chemical potentials for the solid phases of $NaNO_{3(s)}$, $NaNO_{2(s)}$, $Al(OH)_{3(s)}$, $AlOOH_{(s)}$, $NaAlO_2.nH_2O$, $Na_3(PO_4).nH_2O$, and silica. However, constructing equations-of-state that are valid for the highly concentrated tank brines has proven to be difficult.

The complexity of tank waste chemical reactions is illustrated by the chemical modeling results for Hanford DST SY-102, which predict the occurrence of solid dissolution and precipitation during waste retrieval (Onishi and Hudson 1996). The upper-most plot in Figure 5.2 shows the predicted chemical concentrations of dissolved species compared to the measured concentrations for a sample of the Tank SY-102 sludge interstitial solution. The middle plot in Figure 5.2 shows the solids concentrations used to perform the modeling ("prediction" was set equal to measured values) When the sludge is mixed with existing supernate in Tank SY-102, most of the sodium-containing solids are predicted to dissolve, and a small amount of gibbsite ($Al(OH)_{3(s)}$) is predicted to precipitate (Onishi and Hudson 1996). Concentrations of the solids predicted to remain after Tank SY-102 mixing are shown in the lower-most plot in Figure 5.2. Dissolution of the sodium-containing solids will change the amount of solids in the tank and affect the waste physical properties and rheology. As might be expected from such a complex mixture, there are many complex chemical reactions that occur under multi-component, multi-phase, high ionic-strength tank waste conditions. For example, potential aluminum reactions alone are:

$$Na^+ + Al(OH)_4^- \rightleftharpoons Na^+ + OH^- + Al(OH)_3(s)$$
$$Na^+ + Al(OH)_4^- \rightleftharpoons Na^+ + OH^- + H_2O + AlOOH(s)$$
$$Na^+ + Al(OH)_4^- \rightleftharpoons NaAl_2(s) + 2H_2O$$
$$Na^+ + AlO_2^- \rightleftharpoons NaAlO_{2(s)}$$

The chemical simulation predicted that gibbsite, $Al(OH)_{3(s)}$, is the solubility controlling solid for aluminum. However, if boehmite (AlOOH) is formed, instead of gibbsite, a gel may be formed preventing wastes from being removed from the tank, or easily transferred through pipelines (see Onishi and Hudson 1996).

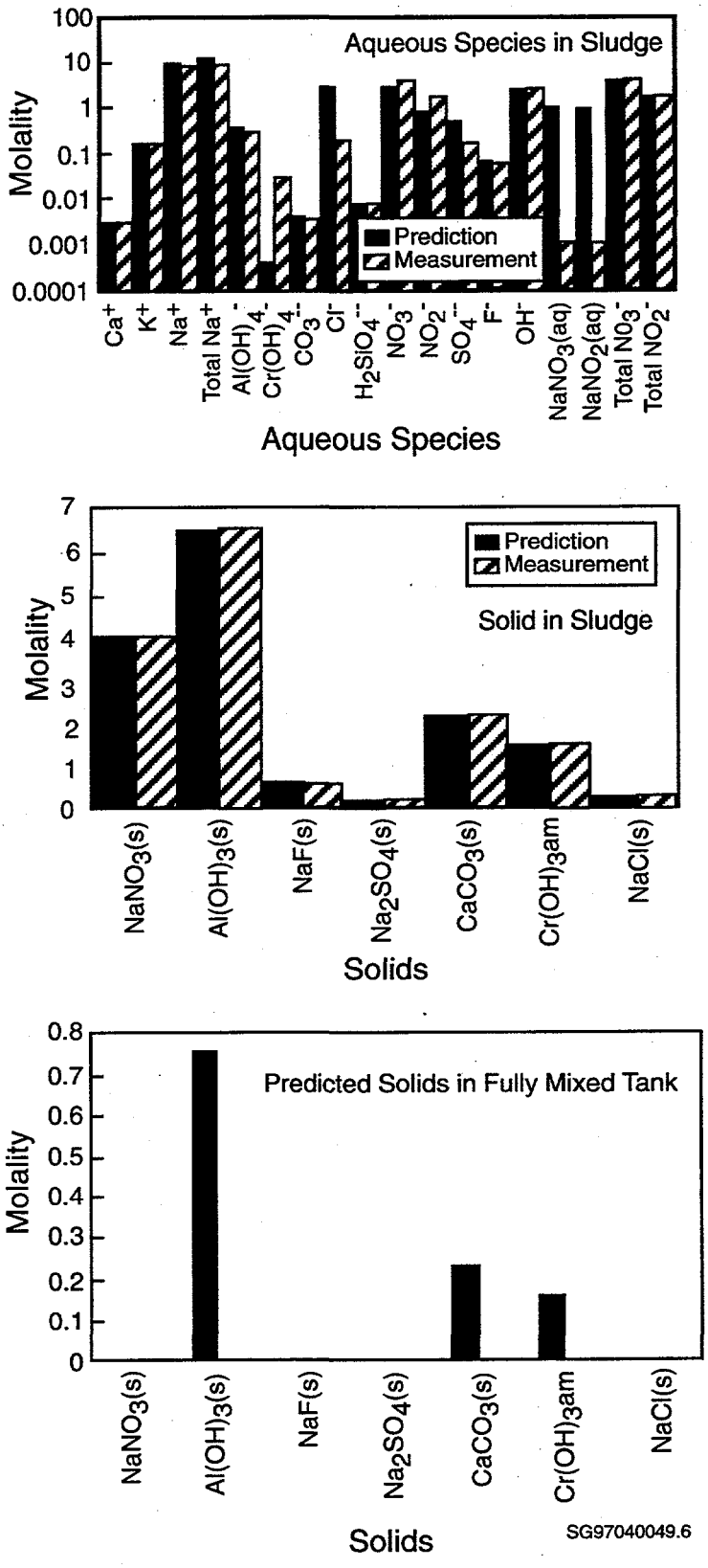

Figure 5.2. Chemical Changes before and after Hanford Tank SY-102 Waste Mixing

The second technical challenge is modeling the effects of chemical reactions and physical mixing on tank waste rheology. A key feature of sludge rheology is the effect of precipitation, dissolution, and particle surface charges on the viscosity versus shear rate relationship exhibited by the sludge. In particular, changes in ionic strength, which is coupled to the dissolution and precipitation of soluble phases such as sodium nitrate and sodium nitrite, affects the thickness of the double layer formed around insoluble aluminum hydroxide/oxyhydroxide phases.

Even in the absence of chemical reactions, tank wastes display complex rheological characteristics. For example, the viscosity measurements of the Hanford Tank SY-102 disturbed sludge revealed that the sludge is shear-thinning as shown in Figure 5.3 (Onishi et al. 1996a). Moreover, at lower shear rates, the sludge is rheopectic, while at higher shear rates it is thixotropic. Figure 5.4 shows the measured rheogram of Tank SY-102 sludge mixed with 0, 1, and 48 wt% of supernate. Figure 5.4 indicates that the sludge itself is non-Newtonian, while the 52 wt% slurry is a Newtonian fluid with significantly smaller viscosity.

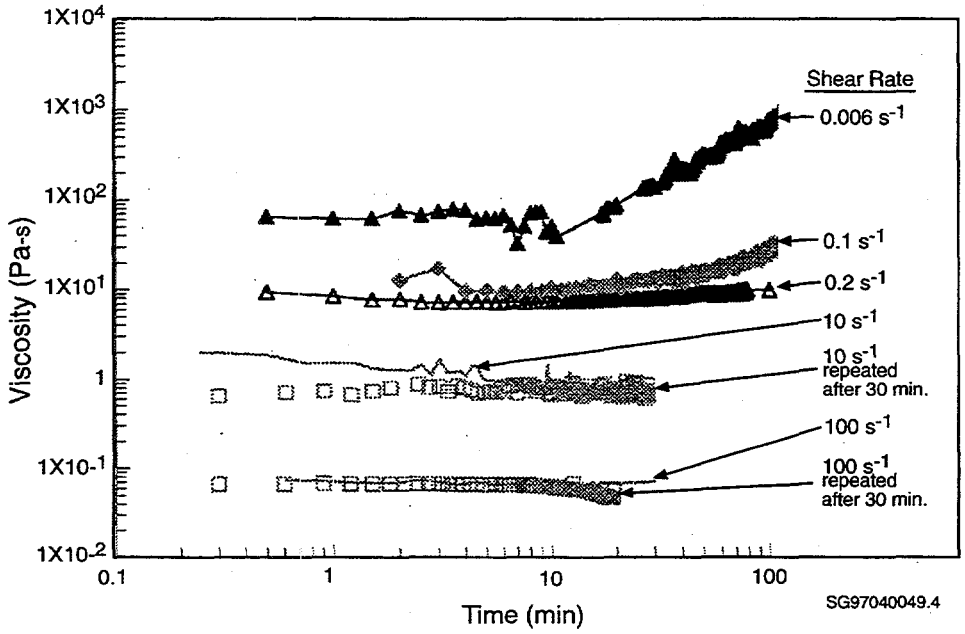

Figure 5.3. Time-varying Viscosity Variations with Shear Rates (Onishi et al. 1996a)

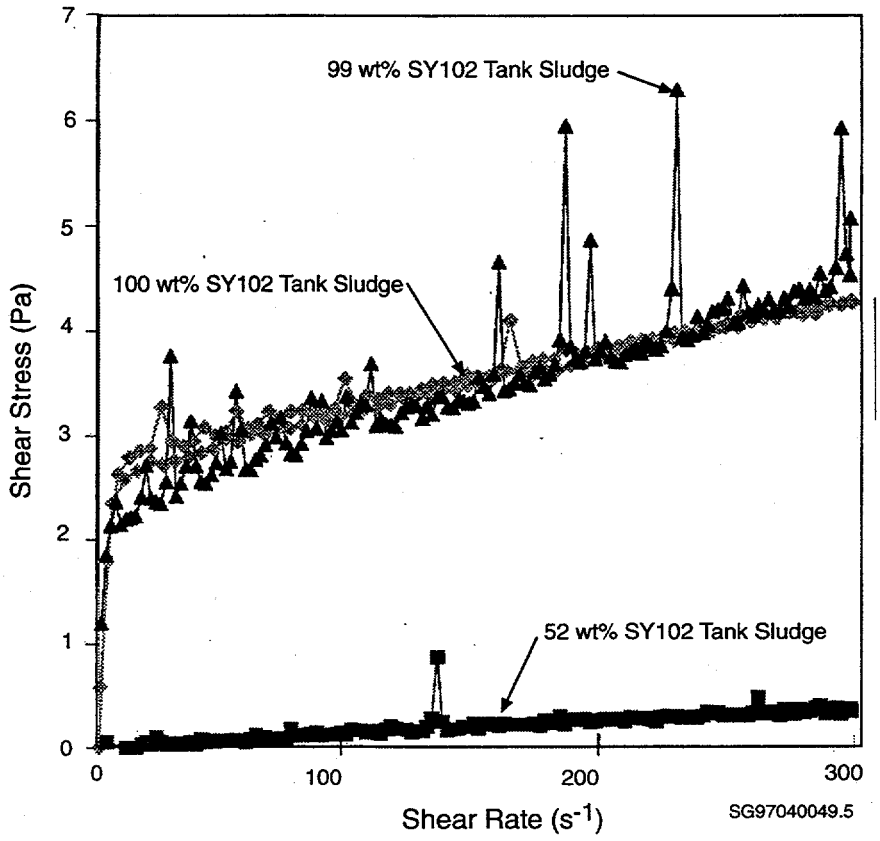

Figure 5.4. Rheogram of the Hanford SY-102 Waste (Onishi et al. 1996a)

In the early stage of pump mixing, when the sludge and some supernate are drawn into the mixer pump near the tank bottom, they are injected back into the sludge layer and the jet fluid may be non-Newtonian (Onishi and Recknagle 1997). As the jet entrains supernate, its fluid becomes more Newtonian with a significantly reduced effective viscosity (see Figure 5.1). Changes from non-Newtonian to Newtonian flows affect jet spread and sludge erosion.

Many of the tank waste solids are cohesive. Thus, the fourth technical point is related to cohesive-solid transport, erosion, and deposition, including solid agglomeration, hindered settling, and interaction between solid concentrations, waste rheology, and mixing intensity.

The commonly used, empirically derived expressions for the deposition (Partheniades 1962) and erosion (Krone 1962) of fine cohesive sediment are :

$$S_d = w_s c \left(1 - \frac{\tau_0}{\tau_{cd}}\right) \qquad \text{for } \tau_0 < \tau_{cd} \tag{5.1}$$

$$S_e = E\left(\frac{\tau_0}{\tau_{ce}} - 1\right) \qquad \text{for } \tau_0 > \tau_{ce} \tag{5.2}$$

where,

c = solid concentration
w_s = apparent particle fall velocity
E = erodibility coefficient
S_d = amount of solid deposited per unit bottom surface area per unit time
S_e = amount of solid eroded per unit bottom surface area per unit time
τ_0 = bed shear stress
τ_{cd} = critical shear stresses for deposition
τ_{ce} = critical shear stresses for erosion

When bed shear stress, τ_0, is less than the critical shear stress for deposition, τ_{cd}, fine solids will be deposited at the rate expressed by Equation 5.1. When τ_0 is greater than τ_{cd}, but is less than τ_{ce}, no fine solids will be deposited or eroded. When τ_0 exceeds τ_{ce}, fine solids will then be eroded at a rate determine by Equation 5.2.

The FLESCOT code (Onishi et al. 1993), the sediment and contaminant transport version of the TEMPEST code, has Equations 5.1 and 5.2 built in for the simulation of fine sediment erosion and deposition in natural environments (e.g., estuary and coastal water). These formulas require that estimates be supplied for the shear stress, critical shear stresses for deposition and erosion, erodibility coefficient, and apparent particle setting velocity. These parameters likely vary from waste to waste and mixing conditions and their values are not known for the tank wastes.

The apparent particle fall velocity alone, for example, is affected by fluid, flow, and solid characteristics, which require knowledge of the solid density, size, and shapes affected by solid flocculation/aggregation behavior. Solid flocculation/aggregation are in turn controlled by complex physical and chemical interactions (LaFemina 1995), as briefly stated above.

The fall velocity (w_s) of a non-interacting spherical particle in a dilute suspension can be estimated by

$$w_s^2 = \frac{4}{3}\frac{d_s g}{C_D}\left(\frac{\gamma_s - \gamma}{\gamma}\right) \tag{5.3}$$

where,

C_D = drag coefficient.
d_s = solid diameter
g = gravitational acceleration
γ_s and γ = specific weights of solid and fluid

When a particle Reynolds number (Re_p) is less than 0.1, Stokes' Law can be used to estimate the fall velocity by assigning C_D equal to $24/Re_p$ (Vanoni 1975).

At higher concentrations (e.g., above 300 mg/L), aggregation or break-up of cohesive solids affects the fall velocity. Thus, the fall velocity becomes a function of solid concentration under this condition. An example expression for this relationship, which is used in TEMPEST, is (Vanoni 1975):

$$w_s = A c^{\frac{4}{3}} \tag{5.4}$$

where, A is a constant.

At solid concentrations above approximately 10 g/L, particle settling is hindered by the close spacing of settling aggregates. In this case, the resulting fall velocity is commonly expressed by

$$w_s = w_0 (1 - kc)^n \tag{5.5}$$

where,

k = constant
n = constant
w_0 = non-hindered fall velocity.

If Krone's formula (Equation 5.2) for the erosion of fine cohesive sediment is indicative of the sludge erosion, the rate of the sludge erosion from the tank bottom is linearly proportional to the shear stress (see Figure 5.5).

Thus, in order to determine how much of the tank wastes can be retrieved, we need to know both the physical characteristics of the wastes (e.g., density, viscosity, solid concentrations) and the chemical species and their potential chemical reactions (e.g., what solids and aqueous species exist in a tank and what will happen to them during the retrieval operation). Moreover, interactions of chemical reactions, flow/transport, and rheological changes must be fully accounted for to evaluate the waste retrieval operation. Since the critical shear stresses have a direct effect on ECR determination, we will discuss their estimates and modeling in Sections 5.2 and 5.3.

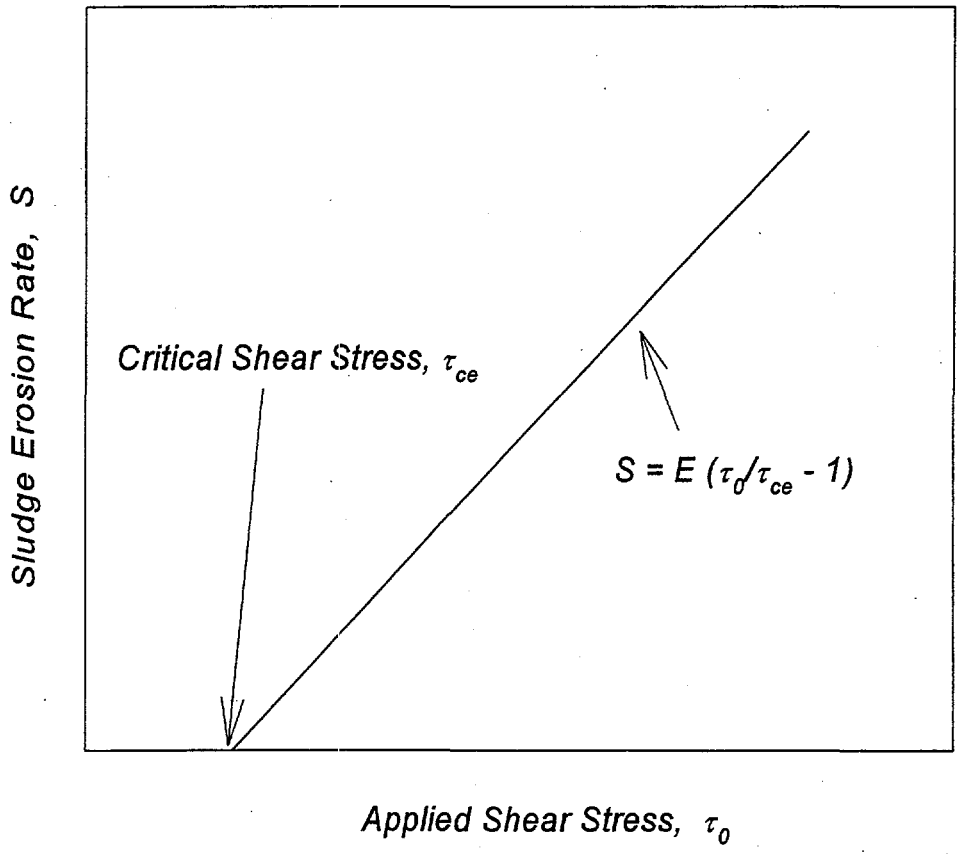

Figure 5.5. Sludge Erosion Rate versus Shear Stress

5.2 Critical Shear Stress Estimates

There have been many attempts to estimate the critical shear stress of sediments in the solid mechanics and sediment transport fields (Vanoni 1975). Some of the oldest information on the erosion resistance of sediments was obtained by engineers working on the design and operation of canals (Frontier and Scobey 1926). The minimum bed shear stress needed to move a sediment bed is generally expressed by the well known Shields diagram for the initiation of motion, as shown in Figure 5.6 (Shields 1936; Vanoni 1975). As originally derived by Shields (1936), the initiation of motion of a non-cohesive bed may be estimated by

$$\tau_* = \frac{\tau_0}{d_s(\gamma_s - \gamma)} = f_1\left[\frac{u_* d_s}{\nu}\right] = f_2\left[\frac{d_s}{\nu}\sqrt{0.1\left(\frac{\gamma_s}{\gamma} - 1\right) g d_s}\right] \quad (5.6)$$

Where,

$f_1[\ ]$ and $f_2[\ ]$= functional relationship

u_* = shear (friction) velocity = $\sqrt{\frac{\tau_0}{\rho}}$

ν = liquid viscosity
ρ = liquid density
τ_* = dimensionless shear stress
τ_o = bed shear stress
d_s = characteristic diameter of the particles
γ_s and γ = specific weight of sediment and liquid, respectively.

Shear stress that is greater than the critical shear stress shown as a line in Figure 5.6 would erode the solids from the bottom. Since the critical shear stresses for non-cohesive solids are uniquely determined by the fluid characteristics, particle size/shape, and particle density, Figure 5.6 works well for these solids. However, many Hanford sludges are believed to be fine cohesive solids, and for these, critical shear stresses are dependent on the interparticle cohesive forces, which can arise in many different ways that are not easily quantified. Thus, Figure 5.6 and Equation 5.6 do not provide a good estimate for the initiation of the motion of solids that have strong particle-particle interactions. This is evident because the very fine solids (e.g., clay in water) have much larger but unknown critical shear stresses (shown as a dotted line in the left side of Figure 5.6) than the coarser non-cohesive solids (e.g., sand in water).

Alternatively, a critical shear stress may be estimated using a soil mechanics approach. The densities of most soil particles and water are about 2.65 and 1.0 kg/L, respectively, and thus, are relatively similar to those of many tank waste solids and supernate (Onishi et al. 1996a). Since Sundborg (1956) derived the critical shear stress for cohesive soil, many studies have correlated the stress strength to plasticity index. For example, Dunn (1959) conducted measurements with sediment ranging from sand to silty clay and derived the following relationship for the sediment with a plasticity index between 5 and 16:

$$\tau_{ce} = 0.001(\tau_s + 180)\ \tan(30 + 1.73 I_p) \quad (5.7)$$

where,

I_p = plasticity index
τ_s = shearing strength.

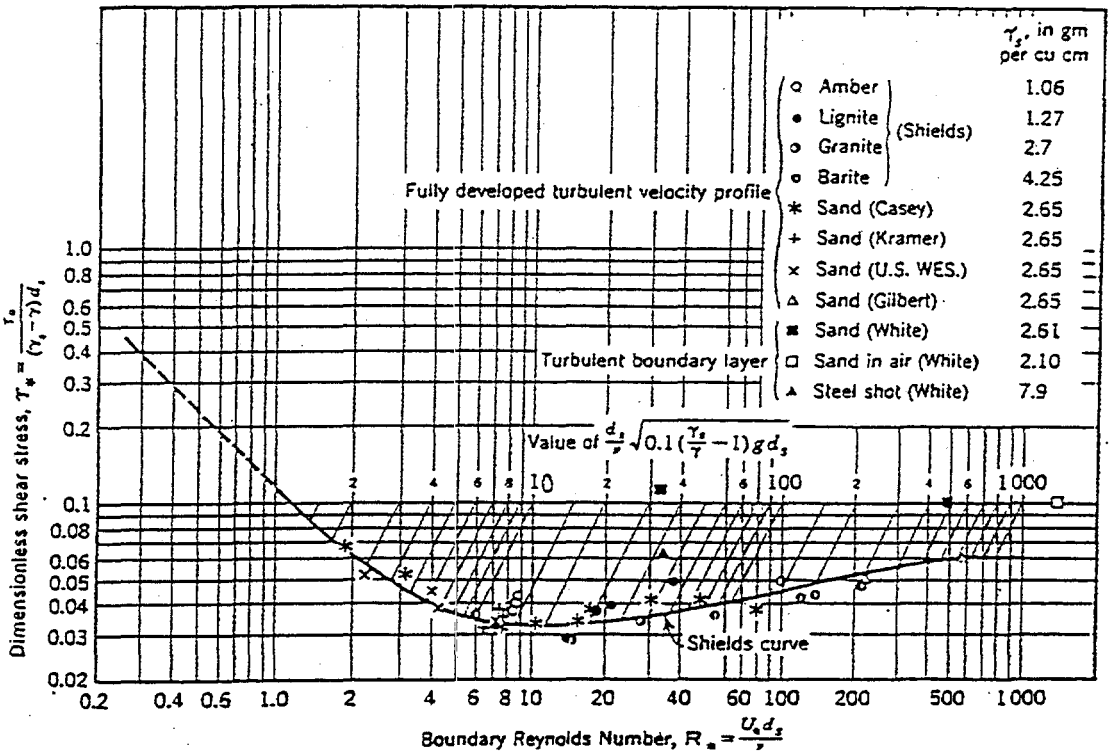

Figure 5.6. Shields Diagram (Shields 1937; Vanoni 1975)

The shearing strength of the sediment is expressed as a stress and is determined by standard soil tests. The plasticity index is the difference between the liquid limit and plastic limit. The liquid limit is the water content, in percentage by weight of sediment, at which the sediment exhibits a small shearing strength. The plastic limit is the water content, in percentage by weight of sediment at which the sediment begins to crumble when rolled into thin cylinders. These values are not known for tank wastes.

Many studies provided a wide range of critical shear stresses for soil erosion, as illustrated by the examples in Table 5.1. These values are much smaller than those expected for the tank wastes based on a comparison of the waste shear strengths with those of the soils used in the Table 5.1 studies (Stewart et al. 1996).

Table 5.1. Critical Shear Stresses for Soil Erosion

Reference	Critical Shear Stresses (N/m^2)
Dunn (1959)	0.058 ~ 0.24
Smerdon and Bearsley (1961)	0.0038 ~ 0.024
Flaxman (1963)	0.11 ~ 0.72
Abdel-Rahmann (1964)	0.0072 ~ 0.043

As stated previously, other important factors related to critical shear stress for solid erosion are the formation of agglomerates and bottom solids consolidation, which require additional information on the solid characteristics and deposition history. For example, primarily cohesive particles will flocculate to form agglomerates. These agglomerates will form larger agglomerates, and so on. In general, the larger the agglomerates, the smaller the critical shear stress for erosion, as indicated by the San Francisco Bay sediment data shown in Table 5.2 obtained by researchers at the University of California at Davis.[a]

In Table 5.2, the 0-order aggregate is made up of the primary solid particles themselves. The first order aggregate is made up of 0-order aggregates, etc. These critical shear stress values indicate the importance of solid aggregation on solid erosion, but it is unclear how this information applies to tank wastes.

Various empirical correlations can be used to estimate critical shear stresses based on soil properties (e.g., plasticity, action exchange capacity, dielectric dispersion, shear strength, particle size distribution, and clay content). However, using any single correlation to determine appropriate critical shear stress values for a wide range of solid types and histories has been unsuccessful. Further, many of the solid property measurements required by these formulas have not been made for tank wastes. Thus, laboratory experiments and/or field (in-tank) measurements most likely will be required to obtain critical shear stress values for solids erosion and deposition.

---

[a]Data obtained by personal communication from Prof. R. B. Krone to Y. Onishi.

Table 5.2. Variation of Erosion Critical Shear Stress with Solid Aggregation

Orders of Solid Aggregation	Erosion Critical Shear Stress N/m^2
0	2.2
1	0.39
2	0.14
3	0.14
4	0.082
5	0.036
6	0.020

5.3 Cohesive Solid Erosion/Deposition/Transport Modeling

As discussed in Section 5.1, Equations. 5.1 and 5.2 are widely used to predict erosion and deposition of fine solids (Onishi 1994). The critical shear stress for erosion and deposition as well as the erodibility coefficient and apparent solid settling velocity must be estimated accurately to conduct mathematical modeling of solid transport, erosion, and deposition. Since obtaining these values from empirical correlations is not successful, these values are usually obtained by 1) in-situ measurement, 2) laboratory flume experiments, or 3) model calibration efforts to select values to reproduce measured fine solid concentrations (Teeter 1988).

Teeter (1988) conducted experiments specifically to obtain the parameters used in Equations 5.1 and 5.2 for silt and clay in Buzzards Bay, Massachusetts by using sediment collected in the bay. Teeters' data are shown in Table 5.3. These values were used by TEMPEST/FLESCOT to simulate transport, deposition, and erosion of sediment (silt and clay) and sediment-sorbed contaminants (cadmium, copper, lead, and polychlorinated biphenyls) in Buzzards Bay (Onishi et al. 1993a). The predicted sediment and PCB concentrations in the water and estuarine bottom, including their fluxes, matched reasonably well with field data.

Equations 5.1 and 5.2 were also used to simulate fine sediment and ^{137}Cs attached to sediment in the Clinch and Tennessee Rivers, Tennessee (Rose et al. 1993) to estimate ^{137}Cs distributions and accumulation over the approximately 50 years of the ORNL operation. The University of California at Davis conducted a series of experiments with sediment collected from these rivers to obtain sediment erosion/deposition parameters in Equations 5.1 and 5.2. These experiments produced a wide range of values: the erodibility coefficient, E varied from 0.33 to 104 g/m^2-s, critical shear stress for erosion from 0.1 to 6.8 N/m^2, and critical shear stress for deposition from 0.33 to 3.0 N/m^2. A critical shear stress value for fine sediment deposition may be roughly assigned to be the cation exchange capacity of a solid. The PNNL-developed TODAM code (Onishi et al. 1993b) used these experimentally determined results to simulate the transport of (cohesive and non-cohesive) sediments and (dissolved and sediment-sorbed) ^{137}Cs in the Clinch and Tennessee rivers. The critical shear stress values used for the modeling are shown in Table 5.4. The model reproduced well measured overall changes in sediment and ^{137}Cs distributions

Table 5.3. Measured Solid Erosion and Deposition Parameters for the Buzzards Bay, Massachusetts

Parameters	Clay and Fine Silt	Medium Silt	Coarse Silt and Fine Sand
Sediment Diameter, d_s mm	0.002 ~ 0.014	0.014 ~ 0.030	0.030 ~ 0.072
Critical Shear Stress for Erosion, τ_{ce}, N/m^2	0.0060	0.6 ~ 0.16	> 0.6
Erodibility Coefficient, E , g/m^2-s	4.2 x 10^{-3}	- - -	- - -
Critical Shear Stress for Deposition, τ_{cd} , N/m^2	0.043	0.033	0.42
Constant, A	1.8 x 10^{-5}	3.2 x 10^{-3}	6.4 x 10^{-3}
Fall Velocity, w_s , cm/s	6.0 x 10^{-4}	0.104	0.202

over 50 years, including riverbed elevation changes resulting from sediment erosion and deposition, and radionuclide build up within the river bottoms.

Many PNNL-developed codes (including TEMPEST/FLESCOT) use Equations 5.1 and 5.2 to simulate transport, deposition, erosion/resuspension of fine sediment and the chemicals attached to those fine sediments in natural environments. These codes have been applied to wide ranges of water bodies (e.g., Columbia River in Washington, Pripyat and Dnieper Rivers in Ukraine, James and Hudson River Estuaries in Virginia and New York, Pacific Ocean Coast, and the Irish Sea) (Onishi 1994).

As discussed above, the prediction of cohesive solid erosion and deposition requires knowledge of the critical shear stresses for erosion and deposition, the erodibility coefficient, and the fall velocity. These parameters are best obtained through laboratory experiments and/or direct field measurements. Because these data are not currently available, the ability to accurately model sludge erosion and deposition is limited.

5.4 TEMPEST Description and Past Tank Applications

Waste retrieval and solidification of a large volume of these complex radioactive tank wastes is planned by DOE to start in year 2002. To address waste retrieval questions, PNNL integrated chemical reactions, hydrodynamic/transport, and changing waste rheology (Mahoney and Trent 1995) into one model by combining the time-dependent, three-dimensional computer program, TEMPEST (Trent and Eyler 1993), the equilibrium chemical reaction code, GMIN (Felmy 1995), a kinetic chemical reaction model, and formulations for tank waste physical property/rheology (Onishi et al. 1996b).

Table 5.4. Calibrated Solid Erosion and Deposition Parameters for the Clinch and Tennessee Rivers, Tennessee

River Reaches	Critical Shear Stress for Erosion for Silt τ_{ce}, N/m^2	Critical Shear Stress for Erosion for Clay τ_{ce}, N/m^2	Critical Shear Stress for Deposition for Silt, τ_{cd}, N/m^2	Critical Shear Stress for Deposition for Clay τ_{cd}, N/m^2
Upper Clinch River	3.0	5.0	1.5	1.0
Lower Clinch River	1.5	3.0	1.0	0.5
Upper Tennessee River	7.0	7.5	6.5	2.0
Lower Tennessee River	7.5	9.5	0.2	0.1

5.4.1 TEMPEST description

The integrated TEMPEST code is a time-dependent, three-dimensional, finite volume, reactive computational fluid dynamic code. Its fluid dynamic portion simulates flow, turbulent momentum, heat, and mass transport and uses the k-e turbulence model (Rodi 1984). It can accommodate non-Newtonian power-law fluids as well as fluids whose rheology depends on solids concentration. Transport modeling of multiple liquid, gas, and solid species can be performed. The thermal energy solution accommodates fully coupled heat transfer in liquids, gases, and solids.

TEMPEST uses the integral form of the fundamental conservation laws applied in the finite volume formulation and solves the equations with the modified simplified marker-in-cell numerical method. The governing equations of computational fluid dynamics used in TEMPEST are:

- Conservation of mass (continuity)

$$\frac{\partial}{\partial t}\int_{cv}\rho dV + \int_{cs}\rho U_s dA_s = 0 \qquad (5.8)$$

- Conservation of momentum (Newton's second law)

$$\frac{\partial}{\partial t}\int_{cv}\rho U_r\,dV + \int_{cs}(\rho U_r U_s + j_{\mu_s})dA_s = \dot{S}_m + F_r \tag{5.9}$$

- Conservation of energy (1st law of thermodynamics)

$$\frac{\partial}{\partial t}\int_{cv}\rho e\,dV + \int_{cs}(\rho U_s h + j_{qs})\,dA_s = \dot{S}_q \tag{5.10}$$

- Conservation of turbulent kinetic energy, k

$$\frac{\partial}{\partial t}\int_{cv}\rho k\,dV + \int_{cs}(\rho U_s k + j_{ks})\,dA_s = \dot{S}_k \tag{5.11}$$

- Conservation of turbulent kinetic energy dissipation

$$\frac{\partial}{\partial t}\int_{cv}\rho \epsilon\,dV + \int_{cs}(\rho U_s \epsilon + j_{\epsilon s})\,dA_s = \dot{S}_\epsilon \tag{5.12}$$

- Conservation of mass constituents, C_i

$$\frac{\partial}{\partial t}\int_{cv}C_i\,dV + \int_{cs}(U_s C_i + j_{C_i s})\,dA_s = \dot{S}_{C_i} \tag{5.13}$$

Nomenclature for the tensor quantities in the above conservation laws is as follows:

r = tensor coordinate index, r = 1, 2, 3
s = tensor summation index (used as a free index), s = 1, 2, 3
X_r = r^{th} space coordinate
U_r = velocity component, in the r^{th} coordinate direction
F_r = force component, in the r^{th} coordinate direction
g_r = gravitational component, in the r^{th} coordinate direction
A_s = area, in the s coordinate direction
j_{xs} = diffusive flux for conserved quantity, x, in the s coordinate direction (μ and q as x are momentum and heat).

Nomenclature for scalar quantities:

ρ = density
t = time
V = volume
e = internal energy
h = enthalpy
k = turbulent kinetic energy
ϵ = turbulent kinetic energy dissipation
C_i = mass concentration, i^{th} constituent (partial density)
$\dot{S}_m$ = source term for momentum
$\dot{S}_q$ = source term for thermal energy
$\dot{S}_k$ = source term for turbulent kinetic energy
$\dot{S}$ = source term for dissipation of turbulent kinetic energy
$\dot{S}_{C_i}$ = source term for i^{th} mass constituent

Others: cs, cv = control surface and volume, respectively.

The flux terms $\mathbf{j}_{xs}$ used in above equations are gradient functions of the conservative quantity, x. In general, the transport coefficient (e.g., diffusivity or conductivity) for each of these relationships is a tensor quantity that reflects the anisotropic behavior of the transport media. In the conservation of momentum,

$$j_{\mu_s} = - \mu \frac{\partial U_s}{\partial x_r} \tag{5.14}$$

where μ is viscosity. For mass diffusion (Fick's law), the flux, $j_{C_i s}$ is defined as

$$\mathbf{j}_{C_i s} = -D_i \left(\frac{\partial C_i}{\partial x_s} \right) \tag{5.15}$$

where D_i is the diffusion coefficient for the i^{th} constituent.

The modified TEMPEST code explicitly accounts for the temporally and spatially varying interactions of aqueous chemical reactions, dissolution/precipitation, and associated rheology changes to simulate gas retention, solid settling/resuspension, and convective motion of physical and chemical species in the tank (Onishi et al. 1996b).

5.4.2 Previous Tank Applications

TEMPEST application without chemical modeling:

The TEMPEST code has been applied to Hanford Tanks C-106, SY-101 (Trent and Michener 1993), SY-102 (Onishi and Hudson 1996, Onishi et al. 1996a), AY-102 (Whyatt et al. 1996), and AZ-101 (Onishi and Recknagle 1997).

The main objective of the SY-102 tank simulation was to determine if two submerged pumps having four rotating 18.3-m/s (60-ft/s) jets located at 43 cm (17 in.) above the tank bottom would sufficiently mix the sludge with the supernatant liquid for waste retrieval. The occurrence of solid dissolution/precipitation during waste mixing was predicted by the equilibrium chemical model, GMIN, as shown in Figure 5.2 (Onishi and Hudson 1996). The Tank SY-102 waste rheology data are shown in Figures 5.3 and 5.4. Figure 5.7 illustrates waste mixing induced by two rotating mixer pumps (located 22 ft off tank center) for Tank SY-102, depicting TEMPEST-predicted distributions of velocity and volume fraction of the coarsest solid (with a 100-175 μm particle diameter) of the seven size-fraction solids used to simulate the sludge (Onishi et al. 1996a).

The yield stress of the disturbed Tank SY-102 sludge was estimated to be 2.7 Pa based on rheological measurements made on a disturbed sludge sample (see Figure 5.4). The SY-102 modeling did not account for the sludge yield stress, predicting that most of the tank sludge will be mobilized over several hours. This is much faster than is expected based on scaled and full-scale mixer pump testing (see Sections 3.1 and 4.5.2).

One way to examine the potential sludge mobilization by incorporating the yield stress is to examine the velocity distributions, since a moving fluid exerts the force (dynamic pressure, or velocity head) equivalent to one-half the product of the density and square of velocity. If we assume that the dynamic pressure is the main force that overcomes the yield stress and initiates sludge movement, the jet flows with 0.2, 0.5, 1.0, 1.5, and 2.0 m/s velocities exert approximately 26, 160, 650, 1,500, and 2,600 Pa of the dynamic pressure on the sludge, if we assume that the density of the mixed jet is 1.3 mg/L. Thus, the velocity contours of these values may correspond to the areas where the sludge with these corresponding yield stresses will be mobilized. Figure 5.8 shows the estimated tank bottom areas for possible sludge mobilization at different velocities and yield stresses for Tank SY-102. This figure indicates that about half of the tank bottom experiences a jet velocity greater than 2 m/s (or the fluid force exceeding 2,600 Pa), and that there are only small areas with a velocity less than 0.2 m/s (and 26 Pa of force) where the solids may not mobilize or may settle down. Based on shear vane and Haake viscometer measurements, DiCenso et al. (1995) reported that the yield stress of SY-102 tank sludge was 3,900 Pa. The ECR values for this tank, estimated by the empirical formulas derived from the 1/12- and 1/25-scale models, are approximately 4 and 8.5 m, respectively, for an assumed sludge yield stress of 3,900 Pa, as plotted with dotted lines in Figure 5.8. With a sludge yield stress of 3,900 Pa, an ECR value based on the TEMPEST-predicted velocity distribution is similar to 4 m obtained from the ECR formulas based on the 1/12-scale model for the 3,900 Pa yield stress value.

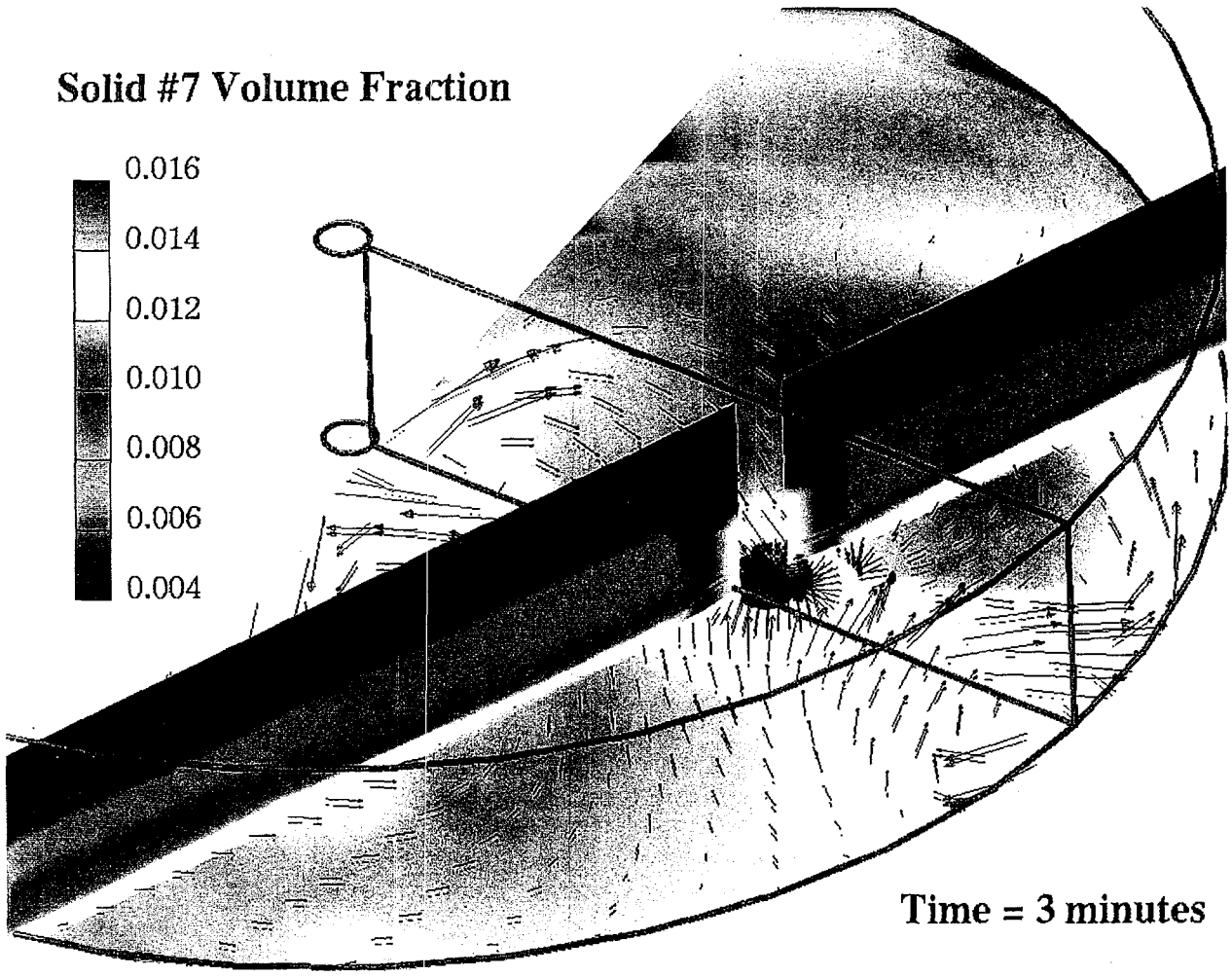

Figure 5.7. Predicted Distributions of Velocity on the SY-102 Tank Bottom and Three-Dimensional Distribution (on the Tank Bottom and in Two Vertical Plants) of the Volume Fraction of the Coarsest solid (100-175 μm Diameter) at 3 Simulation Minutes (Onishi et al. 1996a).

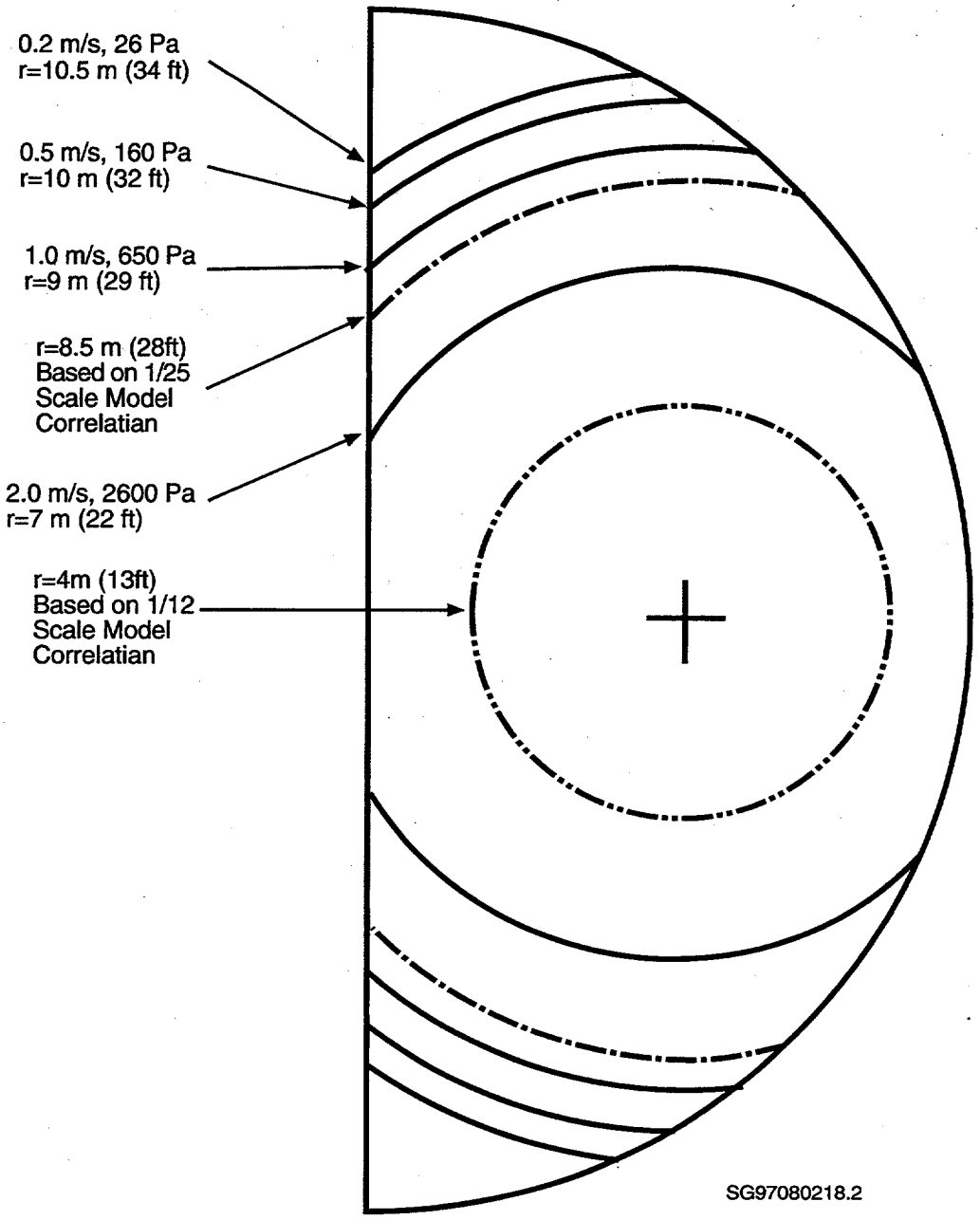

Figure 5.8. Comparison between TEMPEST and Empirical Correlations for a Newtonian Jet

The sludge mobilization force may not be the dynamic pressure head but could be the shear stress. If that is the case, the estimation of an ECR value from the TEMPEST simulation may use its predicted shear stress values since TEMPEST also internally computes shear stress at every computational cell and time step. To use these computed shear stress values, however, the critical shear stresses (τ_{ce} and τ_{cd}) must be estimated for the sludge being modeled. As stated earlier, the critical shear stresses for tank sludge are currently unknown and cannot be estimated with sufficient accuracy to allow accurate ECR predictions to be made.

The TEMPEST code was also used to determine whether two 300-hp pumps with four rotating 18.3-m/s (60-ft/s) jets in Tank 101-AZ could concentrate plutonium in pump housings during mixer pump operation, and as a result, would cause a criticality (Onishi and Recknagle 1997). The modeling assumed heterogeneous distributions of plutonium within the sludge and simulated sludge and supernate mixing and settling both within and outside of the pump housings. TEMPEST predicted that the pump jet mixing operation of Tank 101-AZ will not produce sufficiently high plutonium concentrations and mass within the pump housings to cause criticality. TEMPEST was also applied to Tank SY-101 to predict tank waste rollovers caused by the generation of gasses and to determine the usefulness of pump jet mixing as a mitigating action for waste rollovers (Trent and Michener 1993).

Tank C-106 potentially has the highest plutonium inventory among Hanford waste storage tanks (Onishi and Recknagle 1997). Tank C-106 waste is to be sluiced using Tank AY-102 supernate and the resulting slurry will be transferred to Tank AY-102. A retrieval pump will withdraw the slurry through a 3-ft deep, 5-ft diameter excavation hole (well point) in the Tank C-106 sludge from which the slurry pump will extract the slurry material and transfer it to Tank AY-102. TEMPEST simulated the three-dimensional transport, deposition, and accumulation of nine size-fractions of Tank C-106 sludge particles, whose sizes range from 5 to 55 μm within this well-point during the slurry pump-out operation for 50 minutes (Whyatt et al. 1996). The pumped-out slurry containing 30% C-106 solids will then be introduced into Tank AY-102 through a distributor consisting of four 1-in.-diameter nozzles located 6 ft off the AY-102 tank center and 13 ft above the tank bottom. A 4-in. suction pipe was placed within the AY-102 supernate to recirculate the supernate back to C-106 for sluicing C-106 waste. Tank AY-102 initially will contain 1.5 ft of the sludge and 15 ft of supernate. TEMPEST simulated three-dimensional mixing and settling of C-106 and AY-102 wastes for one simulation hour, predicting rapid descending and subsequent spreading and accumulation of the solids, as shown in Figures 5.9 and 5.10 (Whyatt et al. 1996). Although the particles settle in particular regions of the tank preferentially, the model predicted that the resulting particle segregation was not pronounced enough to cause criticality concerns.

In addition to Hanford tank modeling, TEMPEST has also been applied to tanks at INEEL and ORNL Sites. There are eleven 300,000-gallon, high-level radioactive liquid waste storage tanks at INEEL. These tanks will contain approximately 500 to 15,000 gallons of a heel (mixture of liquid and solids) after normal tank farm emptying operations. Mixer pumps were considered as a possible means to mobilize solids in some of the tanks, which contain cooling coils. TEMPEST was applied to rectangular test cases with a series of non-rotating jets over the cooling coils to obtain three-dimensional velocity distribution and shear stress on the tank bottom (Meyer 1994). A main objective of this INEEL tank modeling was to use these model results to develop a semi-empirical formula, which would then be used to determine necessary pump horsepower and jet rotating speed to achieve the required ECRs, design configurations, pump operational conditions, and required mixing times.

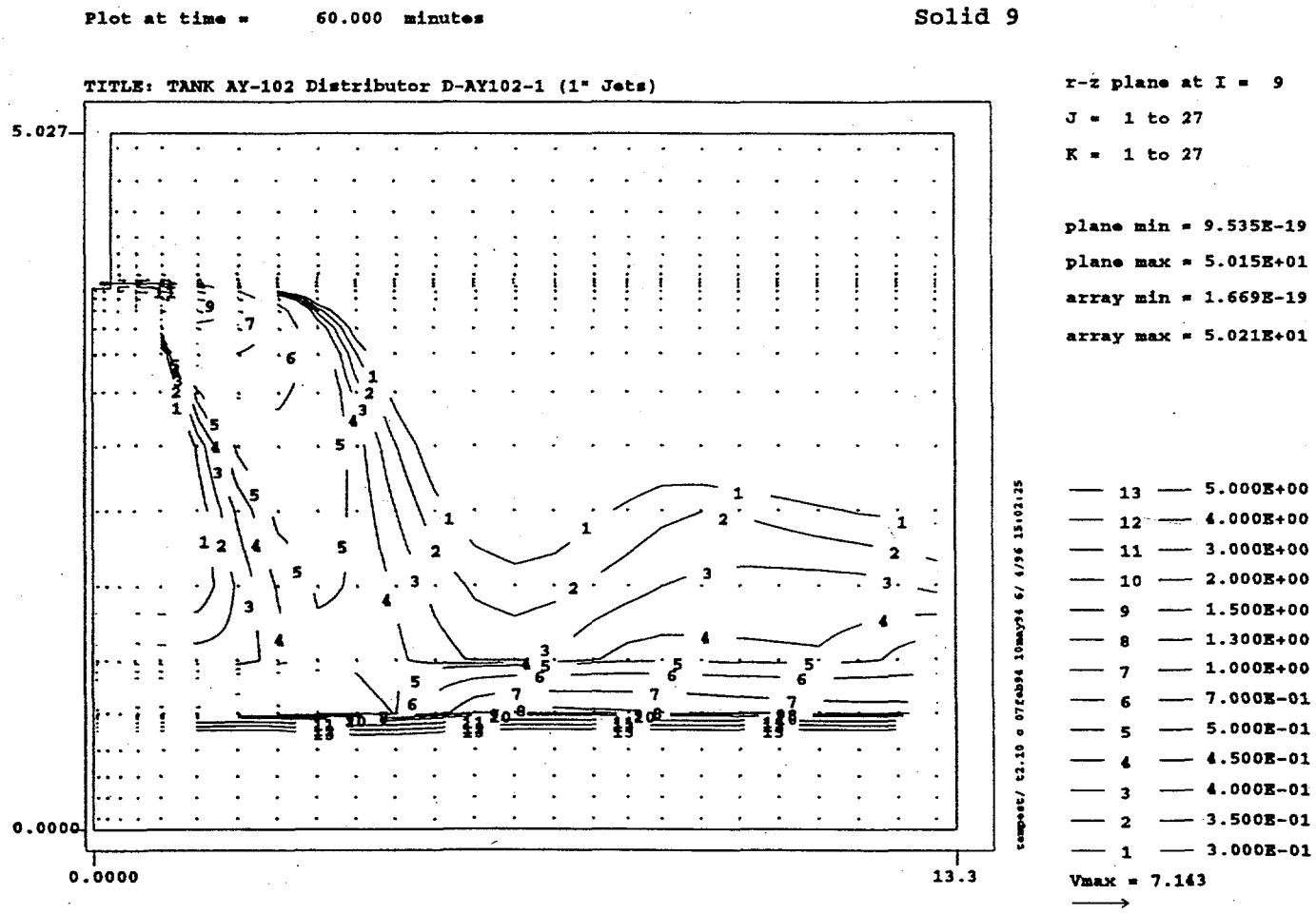

Figure 5.9. Predicted Distributions of Velocity (m/s) and Concentrations (kg/m^3) of the Coarsest Solid (50-55 μm Diameter) on a Vertical Plane Containing One of four 1-inch Nozzles in Tank AY-102 at 1 Simulation Hour (Whyatt et al. 1996).

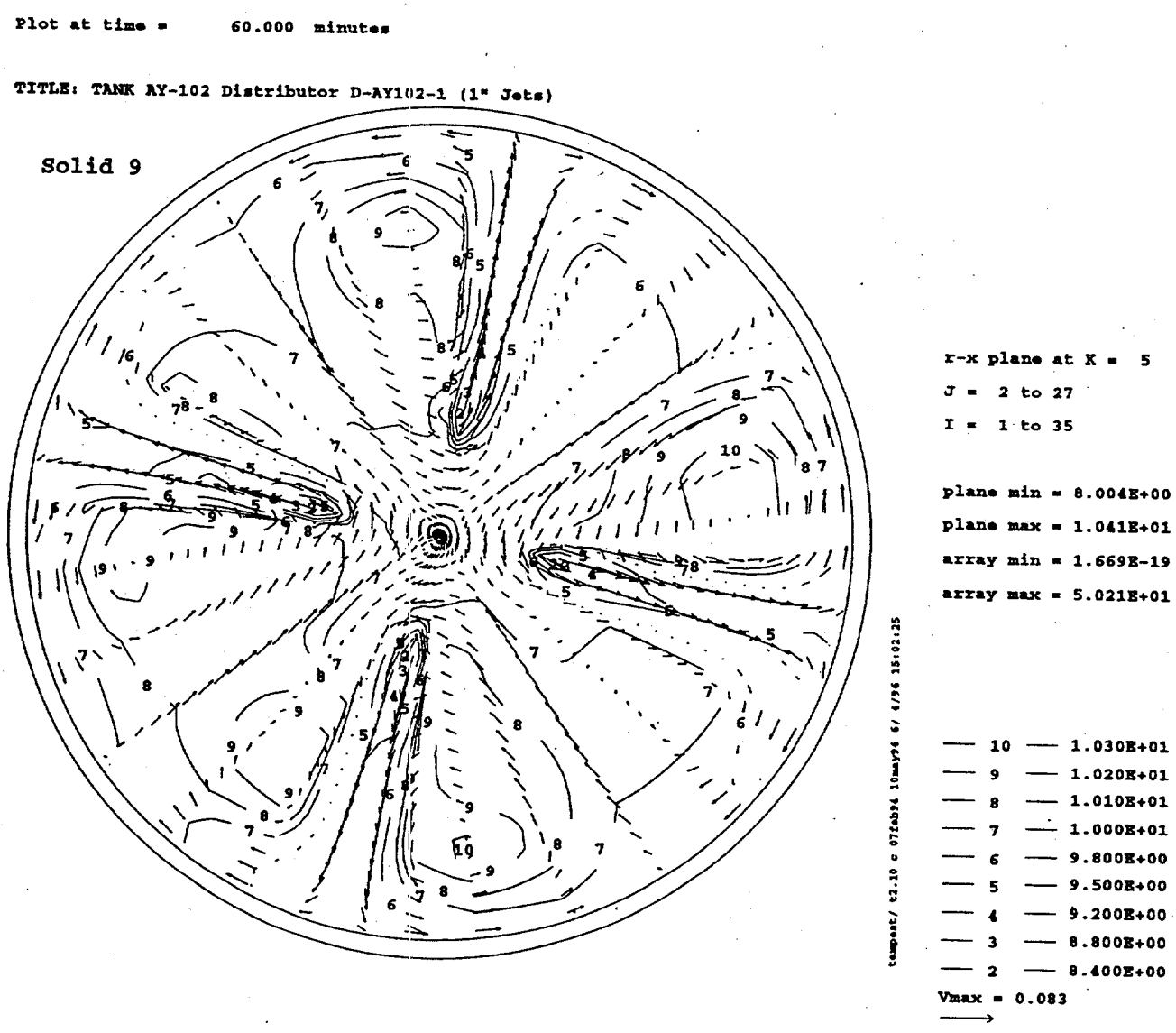

Figure 5.10. Predicted Horizontal Distributions of Velocity (m/s) and Concentrations (kg/m^3) at 23 in. above the Tank AY-102 Bottom at 1 Simulation Hour (Whyatt et al. 1996)

TEMPEST was also applied to cases resembling the Melton Valley Storage Tanks (MVST) at ORNL (Terrones and Eyler 1993). These tanks are 60-ft long, 12-ft-diameter, horizontal, cylindrical storage tanks with 50,000 gallon storage capacity. They contain both liquid and sludge, exhibiting non-homogeneous, non-Newtonian, rheological characteristics that change with changes in solids concentration. Rheological measurements of sludge in eight tanks indicate that sludge and slurry behave as viscoplastic materials with a small yield stress, and that once the yield stress is exceeded, the sludges exhibit psuedoplastic behavior (Ceo et al. 1990). Their behavior can be expressed by the Bingham plastic model or the power law (Ostward de Waele) model (Youngblood et al. 1991).

TEMPEST used the power law, non-Newtonian rheology model for MVST W-28 sludge to simulate potential mixing behavior of the sludge mobilized by the submerged jets. In these cases, the power law formula was adjusted such that its consistency factor and the behavior index vary as a function of solid concentrations. With this rheological expression, TEMPEST was applied to a 1/6-scale experimental model of MVST W-28 to determine the effectiveness of the jet mixing at various jet velocities ranging from 5 to 20 ft/s. It was also applied to the same model tank by assuming that the sludge was highly viscous, but Newtonian. The model was used to predict the mixing time required to achieve full mixing. The simulation results show a marked difference on sludge/supernate mixing patterns and time required to mix the waste between these Newtonian and non-Newtonian cases, revealing the importance of accurately determining the sludge rheology on waste mixing. Comparison of the TEMPEST predictions with the experiments conducted at ORNL showed that the mixing time predictions agreed well with the mixing times observed in salt-tracer mixing studies without sludge in the tank, but the TEMPEST predictions for mobilization of the kaolin clay sludge simulant did not agree with the experiment results (Hylton et al. 1995).

TEMPEST application with chemical modeling:

As stated above, PNNL has developed an integrated physical/chemical modeling capability by incorporating GMIN, a kinetic chemical model, and tank waste rheology into the hydrodynamic/transport code, TEMPEST. Thus, the coupled TEMPEST code is capable of predicting waste movements with simultaneous chemical reactions and associated changes in waste properties (Onishi et al. 1996b).

The modified TEMPEST code was tested for simplified axisymmetric cases, in which a jet is injected into a waste tank, resembling the processes planned for the Hanford waste tanks (Onishi et al. 1996b). The following chemical reactions were considered in these cases with various kinetic chemical reaction rates:

$$Na^+ + NO_3^- \rightleftharpoons NaNO_{3(aq)}$$
$$Na^+ + NO_2^- \rightleftharpoons NaNO_{2(aq)}$$
$$Na^+ + NO_3^- \rightleftharpoons NaNO_{3(s)}$$
$$Na^+ + NO_2^- \rightleftharpoons NaNO_{2(s)}$$

With pure water injected vertically into the tank from the tank center near the bottom, the model predicted that the solids of $NaNO_{3(s)}$ and $NaNO_{2(s)}$ reduced their concentrations due not only to dilution but also to their dissolution. The reduction of the solids will decrease slurry viscosity and sludge shear resistance (see Figure 5.4), allowing more flow to penetrate into the interior of the sludge layer. Figure 5.11 shows the predicted distributions of $NaNO_{3(s)}$ at 15 simulation minutes, depicting the effects of the rapid rise of the lighter water jet and mixing and solid dissolution near the tank bottom on $NaNO_{3(s)}$

concentrations. With these reactive solids dissolving, their concentration reductions are twice as large as those without chemical reactions. Conversely, aqueous chemical species at some locations and times could increase in concentration in response to water being injected in the tank, which would offset the effects of water-jet dilution by the solid dissolution. Table 5.5 shows predicted concentrations at Location 3 identified in Figure 5.11.

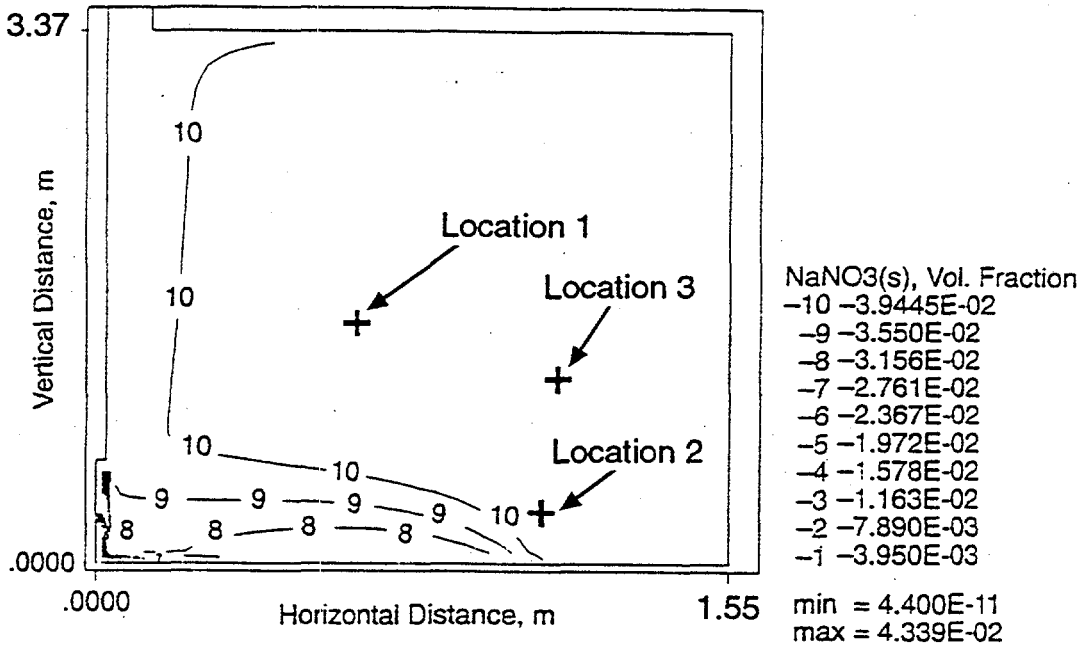

Figure 5.11. Predicted $NaNO_{3(s)}$ at 15 Minutes for the 15-Minute Kinetic Reaction Case (Onishi et al. 1996b).

Table 5.5. Predicted Concentrations of Chemical Species at 15 Minutes at Location 3 Shown in Figure 5.11 (Onishi et al. 1996b)

Chemical species	$NaNO_{3(s)}$	$NaNO_{2(s)}$	Na^+	NO^-_3	NO^-_2	$NaNO_{3(aq)}$	$NaNO_{2(aq)}$
Initial Concentration, kg/m^3	430	398	117	137	133	38	87
Concentration at 15 min., kg/m^3	94	67	139	166	155	33	71

The model results indicate that TEMPEST can, in principle, predict the distributions of reactive solids and aqueous species, while accounting for their chemical and physical interactions, to address complex tank waste operational activities more broadly and reliably. These activities include including dilution of tank wastes, mixing and retrieving various tank wastes, pipeline transfer of wastes, and some waste pretreatment processes.

5.5 TEMPEST Testing and Validation

The TEMPEST code is very versatile and can accommodate extensive engineering and natural environment applications. These applications include

- waste storage tank mixing phenomena
- nuclear reactors
- environmental assessment in natural environment (rivers, estuaries, coastal waters, oceans, and lakes)
- waste processing and storage
- energy conversion and storage
- ventilation systems.

Because TEMPEST is used for nuclear reactors, nuclear power plant environmental assessments, and the U.S. Environmental Protection Agency's Superfund project, the code has been extensively tested for basic code verification and its specific applications in these fields. For these tests, predicted TEMPEST results were compared with known analytical solutions and experimental/field measurements for a wide range of cases (Meyer and Fort 1993; Trent and Michener 1993; Onishi et al. 1993a). These tests include

- conduction heat transfer
- isothermal laminar flows
- laminar flows with heat transfer
- turbulent flow
- Newtonian jets
- buoyancy-driven flows
- estuarine and coastal water environment.

For turbulent flows, the code was tested for 1) grid generated turbulence decay, 2) turbulent flow in a channel, and 3) mixed convection in a circular tube. For Newtonian jets, it was tested for 1) momentum jets in Cartesian coordinates and 2) momentum jets with the tank coordinate system. In all these cases, comparisons between the predicted and measured experimental data show good agreements, indicating general validity of the code in these fields. However, the TEMPEST code has not been tested against measured data on non-Newtonian jet flows or tank sludge erosion/mobilization, partially because there are no readily available, accurate data required for both model parameter determination and model validation. As will be discussed later, we plan to test TEMPEST in these fields with recently obtained measured data.

Three examples of previous TEMPEST testing related to basic code verification and to momentum jets are shown below:

Test Case 1: The Morton's problem is a good case for testing the validity of TEMPEST for heat convection and the basic Navier-Stokes equations for computational fluid dynamics. This test problem deals with a pipe laminar flow with the pipe wall temperature linearly increasing along the pipe length. Comparisons between an analytical solution and the TEMPEST results are shown in Figures 5.12 and 5.13 for various Rayleigh numbers. These figures show the distributions of the longitudinal velocity, u (normalized by the cross-sectionally average velocity, u_m) and temperature below the wall temperature, Q (normalized by the product of Reynolds, Re and Prandtl numbers, Pr) along the radial direction from the pipe center to the wall. These comparisons indicate excellent agreements for all cases, confirming the basic capability of heat transfer and the implementation of the Navier Stokes equations in TEMPEST.

Test Case 2: This example deals with a fully developed turbulent flow in a circular tube. In this two-dimensional case, TEMPEST predictions for mean velocity and turbulent kinetic energy were compared with experimental data obtained by Laufer (1953) for Reynold numbers of 50,000 and 500,000. These comparison are shown in Figures 5.14, depicting radial distribution of the mean velocity, u normalized by the fully developed centerline velocity, U_c. This figure also shows the turbulent kinetic energy, k normalized by the square of the friction velocity, u_τ^2. Friction velocity is defined by

$$u_\tau = \left(-\nu \left(\frac{du}{dr} \right)\Big|_{r=a} \right)^{\frac{1}{2}} \tag{5.14}$$

where,

- a = radius of the circular tube
- r = radial direction
- u = mean velocity
- ν = kinematic viscosity.

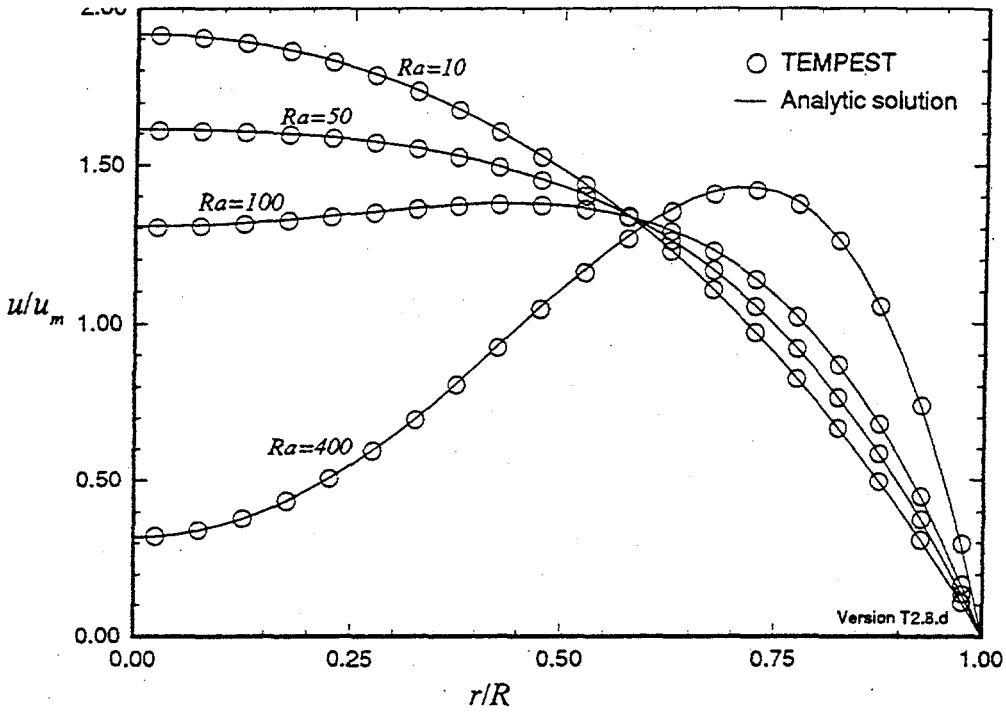

Figure 5.12. Comparison between Normalized Computed Velocity and the Analytical Solution for Morton's Problem (Meyer and Fort 1993)

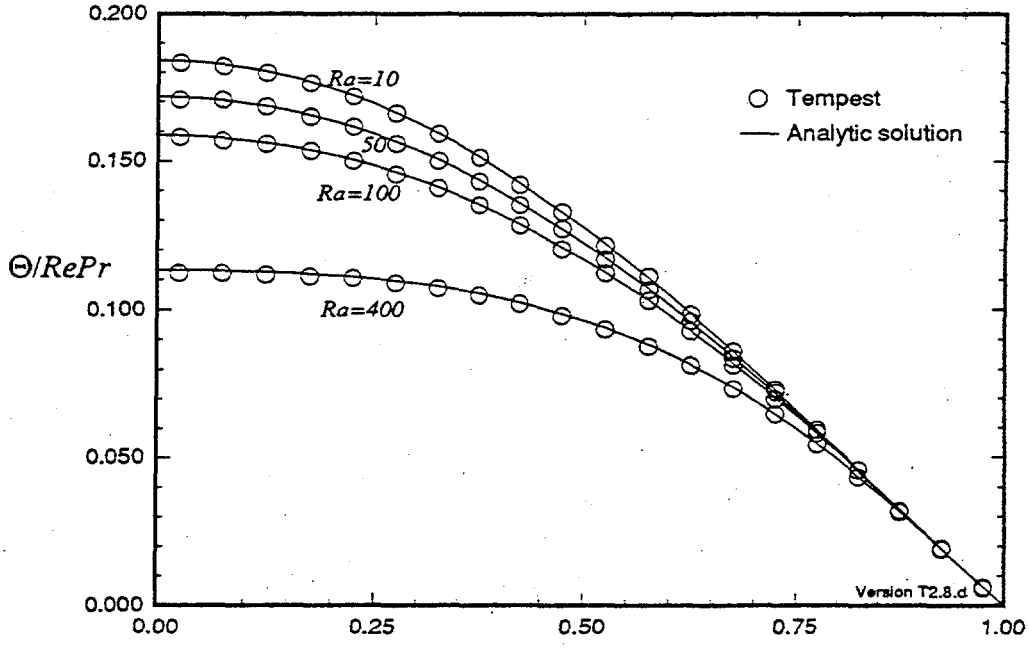

Figure 5.13. Comparison between Normalized Computed Temperature and the Analytical Solution for Morton's Problem (Meyer and Fort 1993).

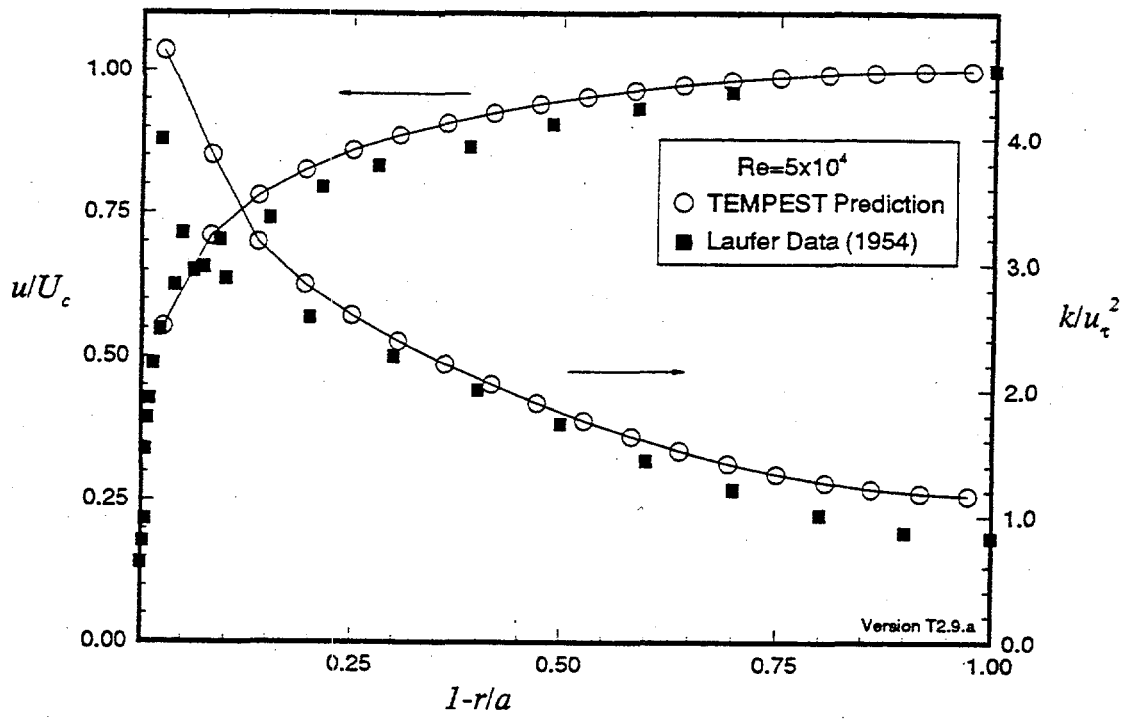

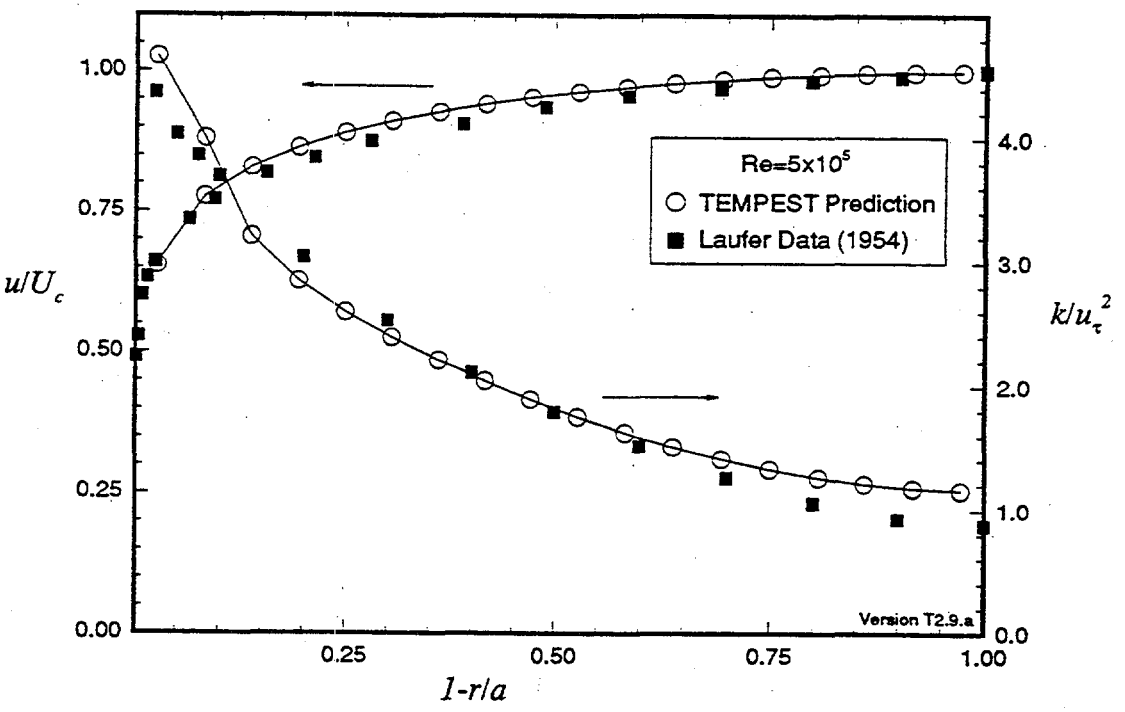

Figure 5.14. Comparison between the TEMPEST Prediction and Experimental Data for a Fully Developed Turbulence Flow in a Circular Tube for $Re = 50{,}000$ and $Re = 500{,}000$ (Meyer and Fort 1993).

The computed velocities are in fairly good agreement with measured values. The computed kinetic energy for intermediate distance of r is in good agreement with the data. TEMPEST somewhat overpredicted the turbulent kinetic energy near the wall and centerline, probably because TEMPEST uses the k-ϵ homogeneous, isotropic, turbulence model, whereas Laufer's experiment shows the presence of anisotropic turbulence. These test results support the general applicability of TEMPEST to turbulence flows, but also reveal a need to evaluate the applicability and limitations of the k-ϵ turbulence model to tank waste problems.

Test Case 3: Since Hanford tank waste retrieval plans are to use the pump jet mixing to mobilize the sludge, it is important to evaluate the validity of TEMPEST for jet mixing. The predicted results by TEMPEST with the k-ϵ turbulence model for horizontal round jet injection and the corresponding empirical correlation are shown in Figure 5.15, whose horizontal axis is the dimensionless axial distance from the nozzle, z^* (equal to z/D), normalized by the nozzle diameter and the vertical axis is the dimensionless centerline velocity, V^*, (equal to v_{cl}/v_0) normalized by the nozzle exit velocity. The figure shows an excellent agreement between them in both zones of "flow establishment" and "established flow".

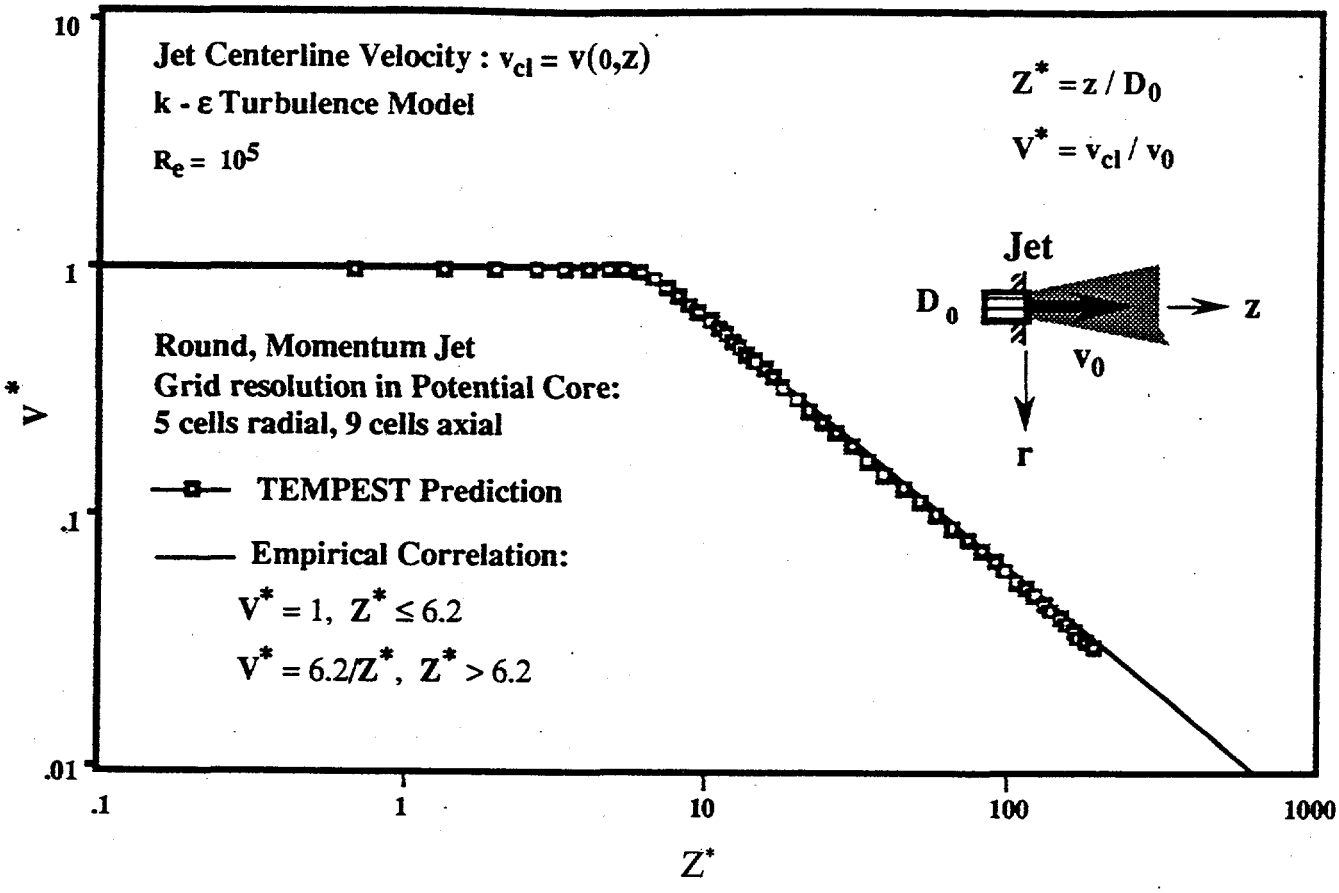

Figure 5.15. Comparison between the TEMPEST Prediction and Empirical Correlations for a Newtonian Jet (from Meyer and Fort 1993)

5.6 Expected Modeling Uses and Limitations

Waste tank remediation operations involve dilution and mixing, retrieval, pipeline transport, and pretreatment of the tank wastes. During these activities, the tank wastes undergo complex chemical and physical changes. Because of the chemical interactions that take place, an integrated modeling capability is needed to model these changes.

The overall goal of the numerical modeling efforts is to assist these operations using a high-performance, reactive, rheological flow computer program on advanced, parallel computing system. To pursue this goal, we developed the multi-phase, multi-component, coupled chemistry and physical process model in TEMPEST (Onishi et al. 1996b). For the waste retrieval operation, TEMPEST aims to help determine

- whether tank waste can be retrieved from a tank
- how much and in what physical/chemical forms the sludge can be removed
- how long the pump mixing and sludge sluicing should be performed
- under what operating conditions the retrieved wastes can be transferred through a pipeline to a separation facility.

As presented in Section 5.4.2, TEMPEST demonstrated the usefulness of addressing some of these questions. These results also indicated that in order to accurately simulate waste mixing and retrieval, the modeling needs to address fast/equilibrium and slow phase-transition (precipitation/dissolution) chemical reactions for multi-components with high ionic strengths; physical property/rheology changes due to physical movements, chemical reactions, and solid crystal formations; non-Newtonian fluid with a proper turbulence representation; and transport/deposition/resuspension of multi-phase, multi-component, constituents with fine solids having high concentrations.

This is a formidable task and there are technical and computational issues facing the tank waste modeling. As discussed in Section 5.1, the main physical and chemical aspects that still need an adequate fundamental understanding are

- many chemical (equilibrium and kinetic) reactions with high ionic strength conditions
- turbulence and mixing of non-Newtonian jet flow
- multi-phase fluid dynamics with very high solid concentration, and associated rheology
- cohesive solid transport, deposition and resuspension, including flocculation and agglomeration
- interactions between chemical reactions and physical processes, especially chemical reactions versus waste physical property/rheology changes.

The main computational problems of tank modeling associated with the current TEMPEST code are

- slowness of the simulation, especially the chemical modeling
- maintaining sharp solid/liquid interfaces (i.e., the ability to model yield stress).

Concerning the equilibrium chemical reactions, constructing equations-of-state that are valid for the highly concentrated tank brines is a difficult task. Progress has been made to incorporate some tank brines into the realistic simulation (Felmy 1995). In particular, we have an equation of state for the major electrolyte system Na^+, NO_2^-, NO_3^-, OH^-, PO_4^{-3}, and $H_2SiO_4^{-2}$ from 0 to 100° C, including

temperature-dependent standard chemical potentials for the solid phases of $NaNO_{3(s)}$, $NaNO_{2(s)}$, $Al(OH)_{3(s)}$, $AlOOH_{(s)}$, $NaAlO_2.nH_2O$, $Na_3(PO_4).nH_2O$, and silica in the Hanford Databank (Felmy and Sterner 1995).

To address the technical issues listed above, PNNL is currently

- expanding the thermodynamic database applicable to high ionic strength conditions
- conducting basic experimental research on jet-induced turbulence and mixing for Newtonian and non-Newtonian jet flows with high solid concentrations
- examining the validity of the k-ϵ turbulence model by applying TEMPEST to the above stated experimental setup
- modifying TEMPEST to better handle sludge yield stress and resuspension physics
- planning TEMPEST simulations to reproduce known pump jet mixing in an actual tank and/or its scaled physical model.

For the two computational problems listed above, TEMPEST currently requires approximately 100 times more computational time to simulate equilibrium and kinetic chemical reactions than to model the flow and transport. This slowness may make it difficult to simulate some slow solid dissolution and precipitation processes. For example, as discussed above, the formation of boehmite adversely affects the waste physical properties and may make the waste very difficult to retrieve from the tank and subsequently transfer. These kinetic reactions, however, could take days and weeks, depending on the waste conditions and temperature. To solve this problem, the chemistry was simulated once for every 100 flow/mixing simulation time steps, since the flow computational time step was approximately 1 millisecond (Onishi et al. 1996b). The other computation problem is that TEMPEST has difficulty maintaining a sharp front of sludge and supernate interface for a long time. Since the mixing of the sludge and supernate converts a non-Newtonian sludge to a Newtonian slurry, artificial (numerical) mixing may produce a Newtonian flow prematurely, thus potentially affecting the jet spread and the sludge erosion. To minimize this problem, the diffusion coefficients were assigned zero for all recent TEMPEST tank applications.

To address these two computational problems, PNNL has submitted proposals on TEMPEST to

- develop robust numerical schemes under parallel process architecture for the transport equations to maintain a sharp solid/liquid interface during the mixing process

- implement efficient numerical schemes for the chemical model coupled with the hydrodynamic/transport equations.

In summary, the overall objective of tank waste modeling is to predict jet mixing, sludge erosion, and solid precipitation/dissolution during the waste retrieval operation to provide better estimates of the amount of sludge to be removed from the tank bottom. It is a very difficult task in light of the many technical and computational difficulties that remain to be solved. Current and proposed fundamental studies address some of the above shortcomings of the current coupled chemistry-physics tank waste simulation. Currently, mathematical modeling can reproduce the overall waste mixing pattern and behavior. The accuracy of a model prediction, especially of ECR and its variation with time, depends most strongly on how accurately critical shear stress for erosion and deposition, erodibility coefficient, and fall velocity can be estimated for the tank waste. With the current state of the knowledge on

cohesive solids, these parameters are best obtained by direct laboratory experiments and/or in-tank measurements.

6.0 Conclusions and Recommendations

Mixer pump testing at Hanford, SRS, and WVDP, has resulted in correlations between waste properties, mixer pump parameters, and the ECR. This represents a substantial advancement in the understanding of mixer pump performance compared to that before the testing was performed. ECRs can now be conservatively predicted based on the sludge shear strength, assuming that the mixed slurry rheology is not strongly non-Newtonian.

In addition to their use in making ECR predictions, scaled testing along with parametric studies using computational models can be used to help resolve mixer pump design and operation issues. For example, the importance of nozzle design was illustrated by a series of 1/25-scale tests in which the ECR was found to be reduced by 50% when a poorly designed nozzle was used (Powell et al. 1994a). Similarly, computational modeling has been successfully employed to address questions of the effects of waste dilution and mixing (Onishi and Hudson 1996).

The accuracy of ECR predictions depends not only on the accuracy of the ECR correlation but also on the accuracy of the sludge shear strength data. Obtaining accurate sludge shear strength data is challenging for three reasons.

First, the effect of temperature on the shear strength must be considered. Shear strength is likely to decrease as temperature is increased, so testing the sludge at the appropriate temperature will yield more accurate ECR predictions. If shear strength measurements are made at a temperature lower than that expected during mixer pump operation, then the actual ECRs are expected to exceed those predicted by the correlation. Thus, this effect need be quantified only for those wastes, if any, where mixer pump performance is predicted to be insufficient based on low-temperature shear strength measurements.

The second issue is that of waste uniformity. Variations in waste composition throughout the tank will result in variations in the shear strength. A sufficient number of strength measurements must be made in different regions of the tank (or on samples taken from different regions) to ensure that the these variations are adequately quantified.

The third issue is that of the sludge's sensitivity to disruption. Shear strength measurements made in the hot cell may result in shear strengths that are biased low because of disruption during core sampling and extrusion.

The sludge uniformity and sensitivity to disruption issues can be addressed using either an in situ shear vane or the cone penetrometer. Multiple measurements would need to be made in differing regions of the tank. It is unlikely that the temperature dependence of shear strength could be measured in situ, so hot cell measurements may be required.

The effect of disruption on sludge shear strength could potentially be estimated by subjecting a variety of sludge simulants to a process analogous to core sampling and extrusion. If the sludge simulants that are most sensitive to disruption show only minor decreases in shear strength, then we have improved confidence that the hot cell shear strength data can be used to make conservative predictions of the ECR. The effect of temperature on shear strength does not necessarily need to be addressed because the increased temperatures during retrieval are expected to decrease the shear strength, which renders the

ECR predictions based on hot cell shear strength measurements conservative. The only practical way to address the temperature effect is to perform shear strength measurements on waste samples at various temperatures.

Yet another potential method for extracting waste strength data is to study the slumping behavior of waste core samples as they are extruded horizontally in the hot cell. Recent work by Gauglitz and Aikin (1997) demonstrated the feasibility of correlating sludge shear strength with the photographs taken during horizontal extrusion. Refinement and subsequent application of this technique will help to decrease the uncertainty in the sludge shear strength data.

7.0 References

Abdel-Rahmann, N. M. 1964. "The Effect of Flowing Water on Cohesive Beds." Contribution No. 56, *Versuchsanstalt fur Wasserbau und Erdbau an der Eidgenossischen Technischen Hochschule*. Zurich Switzerland. pp. 1-114.

Abdelhamid, M. S., P. C. Newsom, and L. E. Rykken. 1984. "In Situ Characterization of the High-Level Waste Sludge at West Valley." *Advances in Ceramics, Volume 8: Nuclear Waste Management.* Edited by G. G. Hicks and W. A. Ross. American Chemical Society.

Bradley, R. F., F. A. Parsons, C. B. Goodlett, and R. M. Mobley. 1977. *A Low-Pressure Hydraulic Technique for Slurrying Radioactive Sludges in Waste Tanks.* DP-1468, Savannah River Laboratory, Aiken, South Carolina.

Brooks, K. P., R. L. Myers, and K. G. Rappe. 1997. *Bench-Scale Enhanced Sludge Washing and Gravity Settling of Hanford Tank C-106 Sludge.* PNNL-11432. Pacific Northwest National Laboratory, Richland, Washington.

Bunker, B., J. Virden, B. Kurn, and R. Quinn. 1995. "Nuclear Materials, Radioactive Tank Wastes," In: *Encyclopedia of Energy Technology and the Environment*, John Wiley & Sons, Inc., New York. pp. 2023 - 2032.

Ceo, R. N., M. B. Sears, and J. T. Shor. 1990. *Physical Characterization of Radioactive Waste Tank Sludges*, ORNL/TM-11653, Martin Marrietta Energy Systems, Oak Ridge National Laboratory, Oak Ridge, Tennessee.

Churnetski, B. V. 1982. "Prediction of Centrifugal Pump Cleaning Ability in Waste Sludge." *Nuclear and Chemical Waste Management.* 3:199-203.

Cleaver, J. W. and B. Yates. 1973. "Mechanism of Detachment of Colloidal Particles from a Flat Substrate in a Turbulent Flow." *J. Colloid and Interface Science.* v. 44, n. 3, pp. 464-474.

DiCenso AT, LC Amato, and WI Winters. 1995. *Tank Characterization Report for Double-Shell Tank 241-SY-102*. WHC-SD-WM-ER-366 Rev. 0, Westinghouse Hanford Company, Richland, Washington.

Dickey, D. S. 1976. "Fundamentals of Agitation," *Chemical Engineering.* Feb. 2, 1976, pp. 93-100.

Dunn, I. S. 1959. "Tractive Resistance of Cohesive Channels," *Journal of the Soil mechanics and Foundations Division*, American Society of Civil Engineers, No. SMC, Proc. Paper 2062, pp. 1-24.

Elder, H. H. 1979. "Demonstration of Radioactive Sludge Removal from a Savannah River Plant Storage Tank." *Proceedings of 27th Conference on Remote Systems Technology.*

Flaxman, E. M. 1963. "Channel Stability in Undisturbed Cohesive Sediment," *Journal of Hydraulics Division*, American Society of Civil Engineers, Vol. 89, No. HY2, Proc. Paper 2462, pp. 87-96.

Felmy, A.R. 1995. "GMIN, A Computerized Chemical Equilibrium Program Using A Constrained Minimization of the Gibbs Energy: Summary Report", In: *Chemical Equilibrium and Reaction Models*, Soil Science Society of America, Special Publication 42.

Felmy, A.R. and S.M. Sterner . 1995. *Solubility Experiments with the Hydroxides, Carbonates, and Phosphates of Magnesium, Calcium, and Strontium in Sodium Hydroxide and Sodium Carbonate Solutions*, PNNL Technical Report TWRSPP-95-039, Pacific Northwest National Laboratory, Richland, Washington.

Frontier, S., and Scobey, F. C. 1926. "Permissible Canal velocities," *Transactions*, ASCE, Vol. 89, Paper No. 1588, pp. 940-984.

Gauglitz, P. A., and J. A. Aikin. 1997. *Waste Behavior During Horizontal Extrusion: Effect of Waste Strength for Bentonite and Kaolin/Ludox Simulants and Strength Estimates for Wastes from Hanford Tanks 241-SY-103, 241-AW-101, 241-AN-103, and 241-S-102.* PNNL-11706. Pacific Northwest National Laboratory, Richland, Washington.

Gephart, R. E., and R. E., Lundgren. 1997. "Hanford Tank Clean up: A guide to Understanding the Technical Issues," PNNL-10773. Pacific Northwest National Laboratory, Richland, Washington.

Hamm, B. A., W. L. West, and G. B. Tatterson. 1989. "Sludge Suspension in Waste Storage Tanks." *AIChE Journal.* **35**(8):1391-1394.

Haji, G. H., B. Hussain, and O. N. Wakhlu. 1988. "Soil Erosion - A Function of Shear Resistance." *Indian Geotechnical Conference (IGC-88).* Allahabad. 1:455-459.

Hylton, T. D., R. L. Cummins, E. L. Youngblood, and J. J. Perona. 1995. *Sludge Mobilization with Submerged Nozzles in Horizontal Cylindrical Tanks.* ORNL/TM-13036. Oak Ridge National Laboratory, Oak Ridge, Tennessee.

Johnstone, R. E. and M. W. Thring. 1957. *Pilot Plants, Models, and Scaleup Methods in Chemical Engineering.* McGraw-Hill Book Company. New York.

Krone, R. B. 1962. *Flume Studies of the Transport of Sediment in Estuarial Shoaling Processes*, Hydraulic Engineering Laboratory and Sanitary Engineering Research Laboratory, University of California, Berkeley, California.

LaFemina, J. P. 1995. *Tank Waste Treatment Science Task Quarterly Report for January - March 1995.* PNL-10763. Pacific Northwest Laboratory, Richland, Washington.

Laufer, J. 1953. *The Structure of Turbulence in Fully Developed Pipe Flow*, NACA technical Note 2954.

Leavell, D. A. and J. F. Peters. 1987. *Uniaxial Tensile Test for Soil.* Dept. of the Army, Waterways Experiment Station, Vicksburg, Mississippi. Geotechnical Laboratory. Final Report GL-87-10. April 1987.

Mahoney, L. A., and D. S. Trent. 1995. *Correlation Models for Waste Tank Sludge and Slurries.* PNL-10695, Pacific Northwest Laboratory, Richland, Washington.

Martin, R. T. 1962. "Discussion of Paper by Walter L. Moore and Frank D. Masch, Jr., 'Experiments on the Scour Resistance of Cohesive Sediments.'" *J. Geophysical Research.* 67(4):1447-1449.

McMahon, C. L. 1990. *Design Characteristics of the Sludge Mobilization System.* DOE/NE/44139-63. NTIS Report No. DE93014680. West Valley Nuclear Services Company, Inc. West Valley, New York.

Meyer, P. A. 1994. *Computer Modeling of Jet Mixing in INEL Waste Tanks.* PNL-9063. Pacific Northwest Laboratory, Richland, Washington.

Meyer, P. A., and J. A. Fort. 1993. *A Computer Program for Three-Dimensional Time-Dependent Computational Fluid Dynamics: Volume 3 Validation and Verification*, PNL-8857, Vol. 3, Pacific Northwest Laboratory, Richland, Washington.

Moore, W. L. and F. D. Masch. 1962. "Experiments on the Scour Resistance of Cohesive Sediments." *J. Geophysical Research.* 67(4):1437-1446.

Nearing, M. A., S. C. Parker, J. M. Bradford, and W. J. Elliot. 1991. "Tensile Strength of Thirty-Three Saturated Repacked Soils." *Soil Sci. Am. J.* 55:1546-1551.

Onishi, Y., 1994. "Contaminant Transport Models in Surface waters," Chapter 11, in: *Computer Modeling of Free Surface and Pressurized Flows,* pp. 313-341, M.H., Chaudrey and L. W. Mays edi., NATO ASI Series E, Applied Sciences- Vol. 274, Klumer Academic Publisher, Dordrecht, The Netherlands.

Onishi, Y., H. C. Graber and D. S. Trent. 1993a. "Preliminary Modeling of Wave-Enhanced Sediment and Contaminant Transport in New Bedford Harbor." In Book Series 42 of *Estuarine and Coastal Water Cohesive Sediment Transport*, pp. 541-557, A. J. Mehta ed., American Geophysical Union.

Onishi, Y., G. M. Petrie, L. W. Vail, O. V. Voitscekhovitch, M.J. Zheleznyak, V. M. Shershakov, and A.V. Konoplov. 1993b. "USA/CIS Coordinating Committee and Its Hydrologic Studies." In *Proceedings of the United Nations UNESCO Workshop on Hydrologic Impact of Nuclear Power Plant System*, September 23-25, 1992, Paris, France.

Onishi, Y. and J. D. Hudson. 1996. *Waste Mixing and Diluent Selection for the Planned Retrieval of Hanford Tank 241-SY-102: A Preliminary Assessment.* PNNL-10927. Pacific Northwest National Laboratory, Richland, Washington.

Onishi, Y., H. C. Reid, D. S. Trent, and J. D. Hudson. 1996b "Tank Waste Modeling with Coupled Chemistry and Hydrothermal Dynamics." In: *Proceedings of 1996 National Heat Transfer Conference,he American Nuclear Society,* Houston, Texas, August 3-6, 1996, Vol. 9, pp. 262-269.

Onishi, Y., R. Shekarriz, K. P. Recknagle, P. A. Smith, J. Liu, Y. L. Chen, D. R. Rector, and J. D. Hudson. 1996a. *Tank SY-102 Waste Retrieval Assessment: Rheological Measurements and Pump Jet Mixing Simulations.* PNNL-11352. Pacific Northwest National Laboratory. Richland, Washington.

Onishi, Y., and K. P. Recknagle. 1997. *Tank AZ-101 Criticality Assessment Resulting from Pump Jet Mixing: Sludge Mixing Simulations*. PNNL-11486, Pacific Northwest National Laboratory, Richland, Washington.

Partheniades, E. 1962. *A Study of Erosion and Deposition of Cohesive Soils in Salt Water*, Ph.D. Thesis, University of California, Berkeley, California.

Perigaud, C. 1984. "Erosion of Cohesive Sediments by a Turbulent Flow Part II: High Mud Concentration." *Journal de Mecanique Theorique et appliquee.* v. 3, n. 4, pp. 505-519.

Poirier, M. R. 1995. *Slurry Pump Opertation in Tank 48 (U).* WSRC-RP-94-01223, Rev. 1. Savannah River Laboratory, Aiken, South Carolina.

Powell, M. R. 1996. "Prediction of Mixer Pump Effectiveness for Sludge Mixing." *Proc. of the International Topical Meeting on Nuclear and Hazardous Waste Management: Spectrum '96.* American Nuclear Society, Inc. La Grange Park, IL 60526. pp. 2355-2362.

Powell, M. R., C. M. Gates, C. R. Hymas, M. A. Sprecher, and N. J. Morter. 1995a. *Fiscal Year 1994 1/25-Scale Sludge Mobilization Testing.* PNL-10582. Pacific Northwest Laboratory, Richland, Washington.

Powell, M. R., G. R. Golcar, C. R. Hymas, and R. L. McKay. 1995b. *Fiscal Year 1993 1/25-Scale Sludge Mobilization Testing.* PNL-10464. Pacific Northwest Laboratory, Richland, Washington.

Rajaratnam, N. 1976. *Turbulent Jets.* Elsevier Scientific Publishing Co., New York.

Rodi, W. 1984. *Turbulence Models and their Application in Hydraulics.* Institute of Hydromechanics, University of Karlsrule, Karlsrule, Federated German Republic.

Rose, K.A., A. L. Brenkert, G. A. Schohl, Y. Onishi, J. S. Hayworth, F. Holly, W. Perkins, L. Beard, R. B. Cook, and W. Waldrop. 1993, "Multiple Model Analysis of Sediment and Contaminant Distributions in the Clinch River/Watts Bar Reservoir, Tennessee," In *Proceeding of the Contaminate Aquatic Sediment: Historical Records, Environmental Impacts, and Remediation*, on July 14-16, 1993, Milwaukee, Wisconsin.

Sabersky, R. H., A. J. Acosta, and E. G. Hauptmann. 1971. *Fluid Flow.* MacMillian Publishing Co., Inc., New York, Chapter 5.

Sundborg, A. 1956. "The River Klaralven, A Study of Fluvial Processes," *Geografiska Annaler*, pp. 127-316.

Scales, P. J., P. C. Kapur, S. B. Johnson, and T. W. Healy. 1997. "The Shear Yield Stress of Partially Flocculated Suspensions with Size Distributed Particles." (In Press) *J. Colloid and Interface Sci.*

Schiffhauer, M. A., J. T. Groth, and D. W. Scott. 1985. "The Status of the Waste Removal System for the West Valley Demonstration Project." *Proc. Symposium on Waste Management '85.* Volume 2, R. G. Post, ed., pp. 611-619.

Schiffhauer, M. A., and R. E. Inzana. 1987. *Scale Model Equipment Testing: Final Report for the Period FY 1985 to FY 1987.* DOE/NE/44139-36. June 1987. West Valley Nuclear Services Co., Inc., West Valley, New York.

Searle, A. B., and R. W. Grimshaw. 1959. *The Chemistry and Physics of Clays and Other Ceramic Materials.* 3rd ed. Interscience Publishers, Inc., New York.

Selby, C. L. 1981. *Rheological Properties of Kaolin and Chemically Simulated Waste.* DP-1589. Savannah River Laboratory, Aiken, South Carolina.

Shekarriz, A., J. R. Phillips, and T. D. Weir. 1994. "Experimental Study of a Pseudoplastic Jet Using Particle Image Velocimetry." *ASME-FED: Laser Anemometry - 1994 Advances and Applications.* v. 191, pp. 191-202.

Shekarriz, A., J. R. Phillips, and T. D. Weir. 1995. "Quantitative Visualization of a Submerged Pseudoplastic Jet Using Particle Image Velocimetry." *Journal of Fluids Engineering.* 117(3):369-373.

Shekarriz, A., G. Douillard, and C.D. Richards, 1996, "Velocity Measurements in a Turbulent Non-Newtonian Jet," Journal of Fluids Eng., Vol. 118, pp. 872-874.

Shields, A. 1936. "Anwendung der Aenlichkeitsmechanik und der Turbulenzforschung auf die Geschiebebewegung," *Mitteilungen der Preussischen Versuchsanstalt fur Wasserbau und Schiffbau,* Berlin, Germany, Translated to English (*Application of Similitude Mechanics and the Research on Turbulence to Bed-load Movement.*) by W. P. Ott and J. C. van Uchelen, California Institute of Technology, Pasadena, California.

Smalley, I. J. 1970. "Cohesion of Soil Particles and the Intrinsic Resistance of Simple Soil Systems to Wind Erosion." *J. Soil Science.* 21(1):154-161.

Smerdon, E. T., and R. P. Beasley. 1961. "Critical Tractive Forces in Cohesive Soil," *Agricultural Engineering*, St. Joseph, Michigan, pp. 26-29.

Smith, P. A., D. R. Rector and A. Shekarriz. 1997. (In Press) "Microstructural and Rheological Characterization of Colloidal Aggregates of Nuclear Waste Slurries." *Int. J. Mineral Processing.*

Stewart, C.W., J.M. Alzheimer, M.E. Brewster, G. Chen, R.E. Mendoza, H.C. Reid, C.L. Shepard, G. Terrones, 1996. *In Situ Rheology and Gas Volume in Hanford Double-Shell Waste Tanks.* PNNL-11296, Pacific Northwest National Laboratory.

Tatterson, G. B. 1994. *Scaleup and Design of Industrial Mixing Processes.* McGraw-Hill, Inc., New York.

Teeter, A. M. 1988. *New Bedford Harbor Project -- Acushnet River Estuary Engineering Feasibility Study of Dredging and Dredged Material Disposal Alternatives - - Report 2, Sediment and Contaminant Hydraulic Transport Investigations*, U. S. Army Corps of Engineers Waterways Experiment Station, Vicksburg, Mississippi.

Terrones, G., and L. L. Eyler. 1993. *Computer Modeling of ORNL Storage Tank Sludge Mobilization and Mixing*, PNL-8855, Pacific Northwest Laboratory, Richland, Washington.

Trent, D.S., and L.L. Eyler. 1993. *TEMPEST: A Computer Program for Three-Dimensional Time Dependent Computational Fluid Dynamics*. PNL-8857 Vol. 1, Version T, Mod 2, Pacific Northwest Laboratory, Richland, Washington.

Trent, D. S., and T. E. Michener. 1993. *Numerical Simulation of Jet Mixing Concepts in Tank 241-SY-101*, PNL-8559, Pacific Northwest Laboratory, Richland, Washington.

Vanoni, V. A., ed. 1975. *Sedimentation Engineering*. ASCE Manuals and Reports on Engineering Practice. American Society of Civil Engineers, New York.

Whyatt, G. A., R. J. Serne, S. V. Mattigold, Y. Onishi, M. R. Powell, J. H. Westik, Jr., L. M. Liljegren, G. R. Golcar, K. P. Recknagle, P. M. Doctor, V. G. Zhirnov, and J. Dixon. 1996. *Potential for Criticality in Hanford Tanks Resulting from Retrieval of Tank Waste.* PNNL-11304, Pacific Northwest National Laboratory, Richland, Washington.

Wyganski, I. and H. Fielder. 1969. "Some Measurements in the Self-Preserving Jet." *J. Fluid Mech.* 38(3):577-612.

Young, R. 1991. *Surface Erosion of Compacted Cohesive Soil: A Dimensional Analysis.* U.S. Department of the Interior, Bureau of Reclamation, Denver Office. R-91-05.

Youngblood, E. L., J. B. Berry, and J. R. De Vore. 1991. "Predicting Transport Behavior for Radioactive Sludges at Oak Ridge National Laboratory," Presented at the *AIChE Summer Meeting*, August 18-21, 1991, Pittsburgh, Pennsylvania. Martin Marrietta Energy Division, Oak Ridge National Laboratory, Oak Ridge, Tennessee.

Appendix

Effect of Non-Newtonian Rheology on Jet Propagation

Appendix: Effect of Non-Newtonian Rheology on Jet Propagation

The time-averaged integral momentum equation in the x-direction for a submerged, turbulent fluid jet is:

$$\frac{d}{dx}\int_0^\infty (2\pi r\, dr)\, \rho u^2 = -(2\pi r\tau)\Big|_0^\infty \qquad \text{(A.1)}$$

where x is the axial direction, r is the radial direction (see Figure 4.8), ρ is the fluid density, u is the fluid velocity, and τ is the shear stress. The left-hand side of Equation A.1 describes the rate of change in the jet axial momentum. The right-hand side is the rate of dissipation of momentum at the jet boundaries. For a Newtonian jet in a free-shear geometry (infinite domain), the right-hand side vanishes since both the gradient of velocity and the shear stresses at the limits where r approaches zero and r approaches infinity. The preservation of jet momentum in Newtonian fluids can be shown to result in the prediction that the jet centerline velocity will decay according to the equation (Rajaratnam 1976):

$$U_{\max} = C\,\frac{U_o D}{x} \qquad \text{(A.2)}$$

where Uo is the nozzle exit velocity, D is the nozzle diameter, x is the downstream distance from the virtual origin of the jet, which is near the nozzle, and C is a constant.

For a non-Newtonian fluid, however, the predicted velocity decay is more complicated. The jet momentum is not preserved in the case of a yield-pseudoplastic fluid, and this can significantly affect the velocity profile. This effect is important because many of the tank waste slurries have been shown to possess yield-pseudoplastic rheology under conditions of relatively high solids loadings. The ECR depends on the downstream jet velocities, so determining where these non-Newtonian effects are significant is essential.

The shear stress (τ) experienced by a yield-pseudoplastic fluid with yield stress τ_o, consistency index K, and flow behavior index n is given by:

$$\tau = \tau_o + K\left(\frac{\partial u}{\partial r}\right)^n \quad \text{where } n\le 1,\ \tau_o > 0 \qquad \text{(A.3)}$$

Substituting Equation A.3 into Equation A.1 gives:

$$\begin{aligned}\frac{d}{dx}\int_0^\infty (2\pi r\, dr)\, \rho u^2 &= -2\pi r\left[\tau_0 + K\left(\frac{\partial u}{\partial r}\right)^n\right]_0^\infty \\ &= -2\pi R\left[\tau_o + K\left(\frac{\partial u}{\partial r}\right)^n_{r=R}\right] - 0\end{aligned} \qquad \text{(A.4)}$$

Let the dependence of u on r be represented by a series expansion of the form:

$$u = u(0) + \left(\frac{\partial u}{\partial r}\right)_0 \Delta r + \left(\frac{\partial^2 u}{\partial r^2}\right)_0 \frac{\Delta r^2}{2!} + O(\Delta r^3) \tag{A.5}$$

As a first order approximation, the partial derivative of u with respect to r can be taken to be:

$$\left(\frac{\partial u}{\partial r}\right)_0 = C\frac{u_{\max}}{R} + O(\Delta r) \tag{A.6}$$

where C is a constant of proportionality, which may be empirically determined. Substituting this relationship into Equation A.4 gives:

$$\frac{d}{dx}\int_0^\infty (2\pi r\, dr)\,\rho u^2 = -2\pi R\left[\tau_0 + K\left(C\frac{u_c}{R}\right)^n\right] \tag{A.7}$$

At the minimum,

$$\left(\frac{\partial u}{\partial r}\right)_R \to 0 \quad \Rightarrow \quad \frac{d}{dx}(M_{axial}) \geq -2\pi R\tau_o \tag{A.8}$$

For a Newtonian Jet,

$$R_{FWHM} \approx 0.1x \tag{A.9}$$

$$\text{or} \quad R_{0.05} \approx 0.2x \quad \text{where } u < 0.05u_c \tag{A.10}$$

Using $R_{0.05}$ in Equation A.7 yields

$$\frac{d}{dx}\int_0^\infty (2\pi r\, dr)\,\rho u^2 \geq -2\pi(0.2x)\tau_0 \tag{A.11}$$

Integrating both sides with respect to x gives:

$$\int_0^\infty (2\pi r\, dr)\,\rho u^2 \geq -0.4\pi\frac{x^2}{2}\tau_0 \tag{A.12}$$

Therefore, based on a linear growth of the jet, the momentum in the jet drops quadratically.

In dimensionless form,

$$\frac{d}{dx^*}\int_0^\infty r^* dr^* (u^*)^2 = -0.2x^* \frac{\tau_0}{\rho u_0^2} \tag{A.13}$$

where $r^* = r/D$, $x^* = x/D$, and $u^* = u/u_o$. Equation A.13 integrates to:

$$\left[\int_0^\infty r^* dr^* (u^*)^2\right]_x = -0.1 (x^*)^2 \frac{\tau_0}{\rho u_0^2} + \text{constant} \tag{A.14}$$

The left-hand side of Equation A.14 can be expressed in terms of the dimensionless jet momentum ($\dot{M} = M/M_o$) as

$$M^* = -0.1 x^{*^2} \frac{\tau_0}{\rho u_0^2} + 1 \tag{A.15}$$

To illustrate the effect of yield-pseudoplastic rheology, Equation A.15 is plotted in Figure A.1 using $\tau_o = 10$ Pa, $\rho = 1000$ kg/m^3, and $u_o = 10$ m/s. It is evident from the plot that all of the jet momentum for this hypothetical fluid is lost by 100 nozzle diameters downstream. Results shown in this figure are in qualitative agreement with the experimental data presented in Figure 4.9.

References

Rajaratnam, N. 1976. *Turbulent Jets.* Elsevier Scientific Publishing Co., New York.

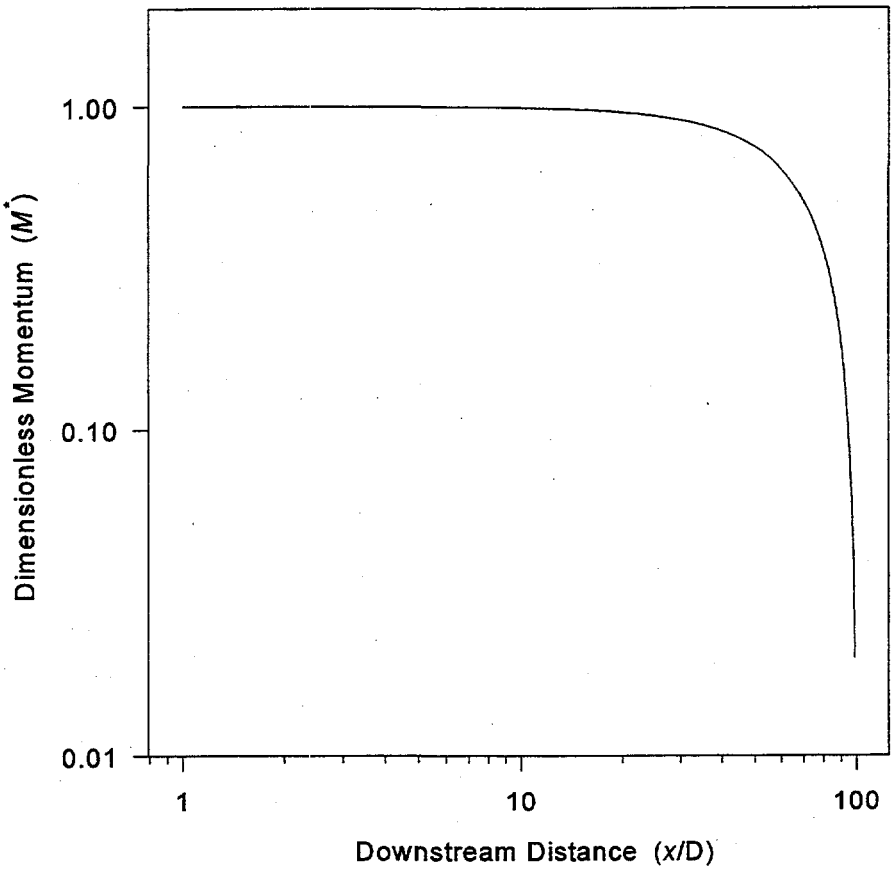

Figure A.1. Jet Momentum Decay for Non-Newtonian Jet

PNNL-11686
UC-721

Distribution

No. of
Copies

Offsite

2 DOE/Office of Scientific and
Technical Information

Onsite

2 **DOE Richland Operations Office**

J. J. Davis, S7-53 (2)

9 **Numatec Hanford**

R. E. Bauer, S7-14
P. W. Gibbons, H6-12
J. W. Lentsch, S2-48
C. A. Rieck, S2-48 (3)
J. E. Van Beek, S2-48 (3)

46 **Pacific Northwest National Laboratory**

J. A. Bamberger, K7-15
W. F. Bonner, K9-14
B. C. Bunker, K8-93
E. A. Daymo, P7-19 (5)
C. W. Enderlin, K7-15
J. A. Fort, K7-15
G. R. Golcar, P7-20
J. P. LaFemina, K9-91
O. D. Mullen, K5-22
Y. Onishi, K7-15 (5)
M. R. Powell, P7-19 (10)
D. R. Rector, K7-15
M. W. Rinker, K5-22 (2)
R. Shekarriz, K7-15 (5)
C. W. Stewart, K7-15
D. S. Trent, K7-15
J.A. Yount, K5-22
Information Release Office, K1-11 (7)